More than protamines: Identification of further sperm proteins from which Prtl99C is essential for male fertility and full chromatin compaction in *Drosophila melanogaster*

Dissertation

for the award of the degree

"Doctor rerum naturalium" (Dr. rer. nat.)

Division of Developmental Biology

Faculty of Biology

Philipps Universität Marburg

Submitted by

MSc. Zeynep Eren Ghiani

from Gönen

Marburg/ Lahn 2015

Vom Fachbereich Biologie der Philipps-Universität Marburg (Hochschulkennziffer: 1180)

als Dissertation am 25.01.2016 angenommen.

Erstgutachter: Prof. Dr. Renate Renkawitz-Pohl

Zweitgutachter: Prof.Dr. Alexander Brehm

Tag der mündlichen Prüfung am: 15.02.2016

To my grandmother

Refiye Yaşar Onay

Table of Contents

Zusammenfassung....1

1 Summary....2

2 Introduction....3

2.1 *Drosophila melanogaster* as a model organism to study male infertility....3

2.2 Spermatogenesis of *Drosophila melanogaster*....3

2.3 Chromatin organization during spermiogenesis....5

2.3.1 Conservation of the common features between mammalian and fly spermatogenesis....6

2.3.2 HMG-box proteins during spermiogenesis....11

2.3.3 Molecular chaperons and CTCF in *Drosophila* spermiogenesis....12

2.4 What do *Drosophila* testis and sperm proteomes tell us?....14

2.5 Prtl99C as a candidate basic chromosomal protein....15

2.6 Aims....17

3 Materials....18

3.1 Equipment....18

3.2 Media and chemicals....19

3.3 Culture media....22

3.4 Enzymes....22

3.5 Antibodies and antiserums....22

3.6 Molecular reagents and kits....23

3.7 Buffers and solutions....24

3.8 Bacterial strains....24

3.9 Fly strains....25

3.10 Plasmids....28

3.11 Oligonucleotides....28

3.12 Sequencing DNA 30
3.13 Other materials 30
3.14 Software and websites 30
4 Methods 31
4.1 Handling *Drosophila melanogaster* 31
4.1.1 Strain Maintenance 31
4.1.2 *Drosophila* Crossings 31
4.1.3 Generation of transgenic flies (Spradling and Rubin, 1982) 32
4.1.4 Chromosomal localization of the P-element 34
4.2 Molecular Biological Methods 35
4.2.1 Preparation and Analysis of DNA from *Drosophilae* 35
4.2.2 Preparation of single-Fly DNA (Gloor et al., 1993) 35
4.2.3 Polymerase Chain Reaction (PCR) (Saiki et al., 1988) 36
4.2.4 Agarose gel electrophoresis of DNA/RNA (Sambrook, 1989) 37
4.2.5 DNA extraction from agarose gel 38
4.2.6 Ligation of PCR products to TOPO® vectors (Invitrogen) 38
4.2.7 Ligation using T4 Ligase 39
4.2.8 Preparation of chemically competent *Escherichia coli* (Sambrook, 1989) 39
4.2.9 Transformation of chemically competent *Escherichia coli* 40
4.2.10 Plasmid preparation from *E.coli* on an analytical scale (mini-prep) (Birnboim and Doly, 1979) 41
4.2.11 Plasmid preparation from *E.coli* in preparative scale (midi-prep) (JETSTAR 2.0 Plasmid Kit, Genomed) 41
4.2.12 DNA restriction with endonucleases 42
4.2.13 Determination of plasmid DNA concentration 43
4.3 Preparation and experiments with RNA 43

4.3.1 RNA isolation from *Drosophilae*, testes and larvae 43
4.3.2 cDNA synthesis 44
4.3.3 Reverse Transcription Polymerase Chain Reaction (RT-PCR) 44
4.3.4 Quantitative PCR (qPCR) 45
4.4 Histological Methodologies 46
4.4.1 Determination of gene expression patterns using *in situ* hybridization in *Drosophila* testes 46
4.4.2 Immunostaining protocol for testes squash preparations 49
4.4.3 Blocking with immunizing peptide 50
4.4.4 Decondensation of *Drosophila* spermatids 51
4.5 Preparation and experiments with proteins 51
4.5.1 Protein extraction from *Drosophila* testes and seminal vesicles 51
4.5.2 Western blot Analysis (Bio-Rad) 51
4.6 Experimental approaches to separate head and tail from *Drosophila* sperm 54
4.6.1 Sonication of *Drosophila* sperm 54
4.6.2 Percoll and sucrose gradient ultracentrifugation 54
4.6.3 Chemical treatment of *Drosophila* sperm 55
5 Results 57
5.1 Functional analysis of Prtl99C during spermiogenesis 57
5.1.1 Prtl99C as a candidate for sperm protein of *Drosophila* 58
5.1.2 *Prtl99C* encodes a protein of the sperm chromatin 59
5.1.3 Prtl99C is essential for male fertility 64
5.1.4 Different *Prtl99C* mutants cause elongation of the chromatin region in sperm 72
5.1.5 Sperm nuclei of homozygous protΔ and Prtl99C mutants are longer than sperm nuclei of Prtl99C mutants 82
5.1.6 The removal of histones and loading of Mst77F and Protamines are independent of Prtl99C 84

5.1.7 Majority of the sperm chromatin relevant proteins seem to localize in different chromatin regions....85
5.1.8 Prtl99C cannot rescue *protΔ* phenotype....87
5.2 *Drosophila* sperm head enrichment assays....87
5.2.1 Sonication power effect on *Drosophila* sperm....88
5.2.2 Tests for *Drosophila* sperm head fractionation using gradient centrifugations....90
5.3 Conclusions....92
5.4 Outlook....93
5.4.1 Potential loading factors for Prtl99C....95
6 Discussion....98
6.1 Protamine-like proteins in sperm....99
6.2 Chromatin condensation during *Drosophila* spermiogenesis....100
6.3 Role of Prtl99C....102
6.3.1 Role of Prtl99C in male fertility....102
6.3.2 Role of Prtl99C in chromatin compaction....103
6.4 Mst77F and Protamines are deposited to the sperm chromatin independent of Prtl99C 106
6.5 Model for additive chromatin compaction by independent loading of different proteins to condense the sperm chromatin....107
6.6 Further candidate proteins for sperm chromatin....109
7 Supplemental Information....112
8 References....116
9 Abbreviations....124
10 Curriculum vitae....127
11 Acknowledgements....130
12 Declaration....131

Zusammenfassung

Bei der Spermatogenese handelt es sich um den konservierten Prozess der männlichen Keimzellentwicklung, welcher im Wesentlichen aus drei Stadien besteht: prae-meiotische, meiotische und post-meiotische Stadien.,Nach der Meiose entwickelt sich aus einer Histon-reichen runden haploiden Spermatidenkern der Protamin-haltige Kern des nadelförmiger Spermium-.In dieser Phase wird das Chromatin neu organisiert und das Volumen des Nukleus dramatisch reduziert. Die Kompaktierung der DNA durch spezielle Chromatinkomponenten dient dem Schutz des väterlichen Erbguts gegen chemische und physikalische Schäden, um Mutationen und Fertilitätsdefekte zu verhindern. In Drosophila, wird der Austausch von Histonen zu Protaminen von der Expression weiterer HMG (high mobility group)-Box haltiger Proteine begleitet. Im Gegensatz zu Maus, führt ein Verlust der Protamine in Drosophila nicht zu Sterilität. Trotz Mutationen in den Protamin-Genen, findet jedoch in beiden Organismen eine effiziente Kompaktierung des väterlichen Genoms statt. Aufgrund dieser Kenntnisse wurde angenommen, dass neben den Protaminen noch weitere HMG-box-haltige Proteine an der Chromatin Kondensation beteiligt sein müssen. Im Rahmen dieser Arbeit wurde das Protein Prtl99C identifiziert und charakterisiert, welches eine HMG-Box Domäne besitzt und spezifisch im späten Spermatiden exprimiert wird. Mittels einem GFP-gekoppelten Fusionsprotein, sowie einem Prtl99C-spezifischen Antikörper konnte das Protein in den reifen Spermienkernen detektiert werden. Analysen homozygoter Prtl99C-ΔC Mutanten zeigen verlängerte Spermienkerne und reduzierte Fertilität, demnach scheint der C-terminale Bereich von Prtl99C notwendig für die Chromatin_Kompaktierung zu sein. RNAi vermittelter Knock-down von Prtl99C führt ebenfalls zu einer Verlängerung der Spermienkerne bis zu 35% und einer reduzierten Fertilität. Während der Verlust der Protamine nur zu um 8% längeren Kernen führt, elongieren die Kerne bei Verlust von Protaminen und Prtl99C um bis zu 47%. Aufgrund dieser Ergebnisse wird postuliert, das während der Spermatogenese viele Chromatin-assoziierende Proteine eine Funktion in der Chromatin-Reorganisation ausüben, um ein kompaktes männliches Genom zu bilden. Im Rahmen dieser Arbeit wurde zum ersten Mal eine Chromatinkomponente des reifen Drosophila Spermiums beschrieben, welche essentiell für die männliche Fertilität ist. Die hier erzielten Erkenntnisse helfen, den Prozess der Kondensation des Spermiengenoms durch verschiedene in additiver Weise wirkende basische Proteine besser zu verstehen. Zusätzlich wurde durch Analysen vorhandener Testis Proteom Daten ein weiteres basisches Protein identifiziert, welches ein Homolog zu dem Mammalia THEG Protein darstellt und ebenso essentiell für die Fertilität von Drosophila sein könnte.

1 Summary

Spermatogenesis is a highly conserved process that can be divided into three stages: pre-meiosis, meiosis and post-meiosis. At the end of the post-meiotic stage of spermatogenesis, a protamine rich spermatozoon is formed from a histone rich spermatid with round nucleus. During this stage, the chromatin is highly packed and the volume of the nucleus is remarkably reduced. Therefore, it is expectable that the poor packed chromatin within the sperm nuclei cannot protect the DNA properly against chemical and physical damage, potentially leading to mutations and infertility problems. In *Drosophila*, during the replacement process of histones by protamines several high mobility group-box (HMG-box) containing proteins are expressed. Our group previously identified *Drosophila* protamines being not essential for fertility in contrast to those of mice which cause sterility already in haplo-insufficiency. In both organisms, the compaction of the genome is very efficient despite of the mutated protamine genes.

On the basis of these findings, we hypothesized that other proteins may act in functional redundancy or in an additive manner with protamines. For this reason, we searched for additional HMG-box-containing proteins which might play a role during chromatin condensation. We identified Prtl99C specifically expressed in male germ cells. We demonstrated with transgenic flies and with an antibody against Prtl99C that the protein persists until the mature sperm. Analysis of homozygous *Prtl99C-ΔC* sperm showed longer nuclei, indicating that the C-terminal region is required for chromatin compaction moreover affects male fertility. Knockdown of *Prtl99C* via RNA interference (RNAi) led also to elongation of the sperm nucleus region by about 35% yet the fertility was highly reduced. Whereas loss of protamines led to an 8% longer nucleus, deletion of both protamines and Prtl99C, led to an elongation of the sperm nucleus by 47%. Based on these findings, we proposed that many chromatin-binding proteins have a function in chromatin reorganization during spermatogenesis in favor of building a compacted male genome.

The actual work presents for the first time a *Drosophila* sperm chromatin component that is essential for male fertility. The insights obtained from this study can help to understand in particular the condensation of the sperm genome carried out by several basic proteins. Lastly, we analyzed a comparative proteome approach to find more basic protein and identified a homolog to mammalian THEG as likely being essential for male fertility *Drosophila*.

2 Introduction

2.1 *Drosophila melanogaster* as a model organism to study male infertility

Drosophila melanogaster has a small genome of 201 Mb, which full sequence was published in the year 2000 (Adams et al., 2000; Bosco et al., 2007). Availability of extensive genetic and physical maps of its 4 chromosomes, its rapid life cycle, large number of mutant lines and genomic resources make *Drosophila* an excellent model organism for research studies on any field.

Adult *Drosophila* testes contain the same kind of germ cells that exist in mammalian testes such as: spermatogonia, spermatocytes, spermatids and sperm. Also, on the molecular site, many features are conserved (Rathke et al., 2014). For this reason, *Drosophila* has also become a preeminent model to screen genes related to male infertility.

2.2 Spermatogenesis of *Drosophila melanogaster*

To clarify the reasons of infertility, the initial step seems to better understand the key steps involved in spermatogenesis, which is the differentiation of sperm from primordial germ cells.

Spermatogenesis can be divided into three stages: pre-meiosis, meiosis and post-meiosis. It begins when a diploid spermatogonium encapsulated by two cyst cells is produced from the testis stem cell niche. These two cyst cells evolve and remain associated to the germ cells. Spermatogonium enters four mitotic divisions in which 16 primary spermatocytes surrounded by two cyst cells are formed. Cells within each cyst remain interconnected by cytoplasmic bridges. The spermatocyte or 16 cell stage in which cells go through cellular growth and differentiation lasts 3.5 days (Fuller, 1998). This phase is characterized by high levels of transcription and a cell volume increase of 25 times. Primary spermatocytes produce

transcripts that are used at three different time points in spermatogenesis. These transcripts are either directly translated during the expansive growth, or later for meiosis, or during post-meiotic differentiation (for review see Renkawitz-Pohl 2005).

At the end of this highly transcriptionally active phase, mature primary spermatocytes exit the cell growth program and undergo meiosis to form a cyst of 64 inter-connected primary spermatids. During meiotic divisions the nucleus becomes smaller, the chromosomes condense and the size of the round spermatid is much smaller compared to primary spermatocyte.

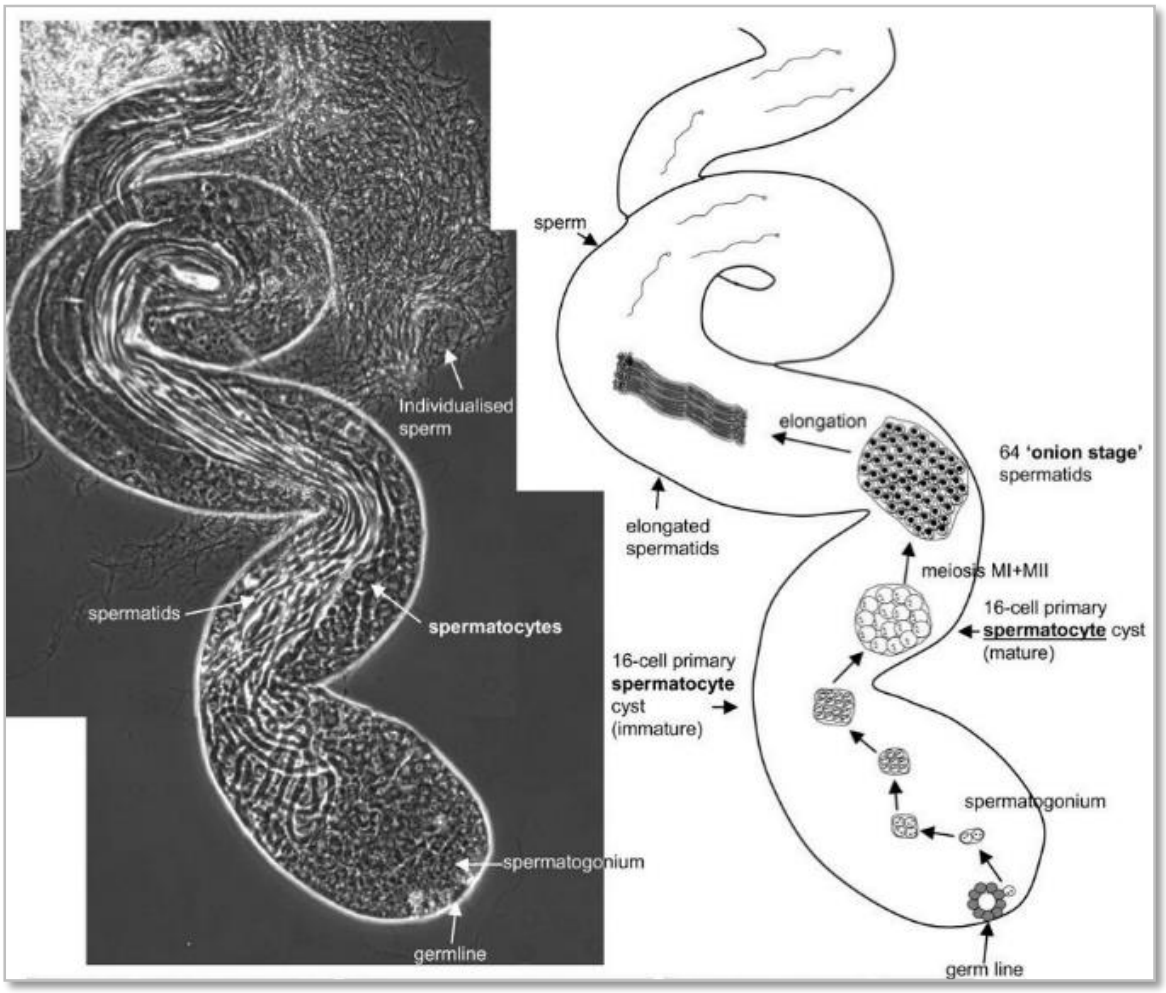

Figure 1 An overview of *Drosophila* spermatogenesis. Spermatogenesis begins at the apical tip of the testes with continuous asymmetric division of stem cells. The germ line cells spermatogonium in a cyst go through four mitotic divisions and then enter the primary spermatocyte stage in cysts of 16 primary spermatocytes. The mature spermatocytes complete their cell growth and undergo meiosis I and II to form a cyst of 64 inter-connected spermatids. Onion stage spermatid is typical that each nucleus flanked by a nebenkern (mitochondrial aggregate) which morphology resembles an onion. These inter-connected haploid spermatids undergo cellular remodeling and nuclear elongation. The final step of spermatogenesis is individualization. After this step, each individualized spermatids are released to seminal vesicles for storing. Reprinted from Hirst and Carmichael, 2011.

The last phase of spermatogenesis is called spermiogenesis. At the end of meiosis II, mitochondria aggregate together and fuse to form two mitochondrial derivatives that wrap around each other in an onion-shaped structure called the nebenkern. The nebenkern elongates down the axoneme which will become part of the tail. During this event, the chromatin condenses at the periphery of the nucleus. While developing in synchrony within a cyst, the 64 spermatid nuclei become closely aligned.

During elongation, enormous morphological changes occur that transform a 15 μm diameter round spermatid into a 0.3 μm diameter needle-like shaped mature sperm with a length of nearly 2mm. The main features during this phase are chromatin remodeling, formation of the flagellum, selective release of translationally repressed genes required for spermiogenesis and finally individualization. Spermiogenesis can be divided into six stages according to nuclear morphology of spermatids: round spermatid stage, young elongating stage, early canoe stage, late canoe stage, individualization stage and mature sperm. Following elongation and nuclear shaping, mature sperm become individualized by a process called individualization. The individualization complex (IC), composed of 64 aligned actin cones, moves progressively down the length of the cyst and stripes away unneeded organelles and cytoplasm components in a caspase-dependent process. Individual sperm cells are shortly later transferred and stored in the seminal vesicles until they are needed for copulation (Reviewed by Fuller, 1993, Figure 1).

2.3 Chromatin organization during spermiogenesis

During the post-meiotic phase of male germ cell development, chromatin reorganization is essential. Although differences are apparent between species (e.g., humans, mice, *Drosophila*) the journey of a round spermatid to become a motile sperm is quite similar in particular with respect to packaging of the paternal genome. Through development, histones are gradually replaced by sperm-specific nuclear basic proteins. This is a process in which first testis-specific histone variants are incorporated, followed by the expression of small and basic transition proteins, and finally protamines or protamine-like proteins are expressed to pack the sperm chromatin (Rathke et al., 2014). According to the evolution of

species, three sperm chromatin organization scenarios have been observed; 1) somatic histones may persist or sperm-specific histones may appear, 2) histones may be replaced directly by sperm-specific nuclear basic proteins or 3) histones may be replaced first by intermediate basic proteins which are themselves replaced by one or several protamines (Wouters-Tyrou et al., 1998). Protamines are small, very basic arginine- and cysteine-rich proteins which belong to a diverse family. They are expressed from plants to animals. They are best characterized in mammals and have been proposed to serve a role in 1) the capability to bind to DNA with their small "anchoring" domains containing multiple arginine or lysine amino acids , 2) enabling the inactivation of temporal transcription from the haploid male genome, 3) protecting the paternal DNA against damage for example by radiation and 4) giving indirectly the final hydrodynamic shape to the sperm head (Balhorn, 2007; Rathke et al., 2014).

Fully packed sperm chromatin can protect DNA against chemical and physical damage more efficiently than a poorly packed chromatin, preventing mutations and leading to healthy offspring (Kanippayoor et al., 2013). Thus, the existence of this particular chromatin packaging has important influences in the medical infertility field (Ward, 2010). Interestingly, it is unclear why condensation patterns of different species with different spermiogenic nuclear proteins may be similar or different. Understanding the epigenetics of sperm is therefore pivotal for male infertility studies. In this chapter, I summarize the recent advances in the field, highlight the conservation of common features between mammals and *Drosophila*, and point out the relevance of our focus in *Drosophila* spermatogenesis.

2.3.1 Conservation of the common features between mammalian and fly spermatogenesis

Although differences such as sperm size and shape, time line of spermatogenesis etc. are apparent between *Drosophila* and mammals, the process of sperm development is highly conserved. This makes *Drosophila* a good model system (Fabian and Brill, 2012; Rathke et al., 2014).

Drosophila and mammalian spermatogenesis are divided into similar stages. Even if the species are so different, the working mechanisms are very similar (Figure 2). *Drosophila* cyst cells, known to surround developing germ cells, are comparable to the Sertoli cells in mammals which act as a physical barrier as well as a source for nutrients and regulatory molecules (Zoller and Schulz, 2012). As shown in Figure 1, *Drosophila*'s germ cells develop from the apical tip of the testis through the basal end and finally mature sperm are released to the seminal vesicles for storing. Differently, mammalian germ cells move from the periphery to the lumen and mature sperm are afterwards stored in the epididymis. For genetic recombination and crossover formation, meiotic DNA double-strand breaks are induced in mammals whereas *Drosophila* males interestingly do not have any synaptonemal complex, thus, recombination does not occur in male germ cells (Vazquez et al., 2002). With the length of 1.8 mm *Drosophila melanogaster*'s sperm is approximately 300 time longer than human spermatozoa and one of the longest sperm among all organisms (Scott Pitnick, 1995). In contrast to flattened pear shape mammalian sperm head, the *Drosophila* sperm head is needle-like shaped, almost indistinguishable from its tail by light microscopy (Kanippayoor et al., 2013) (Figure 3).

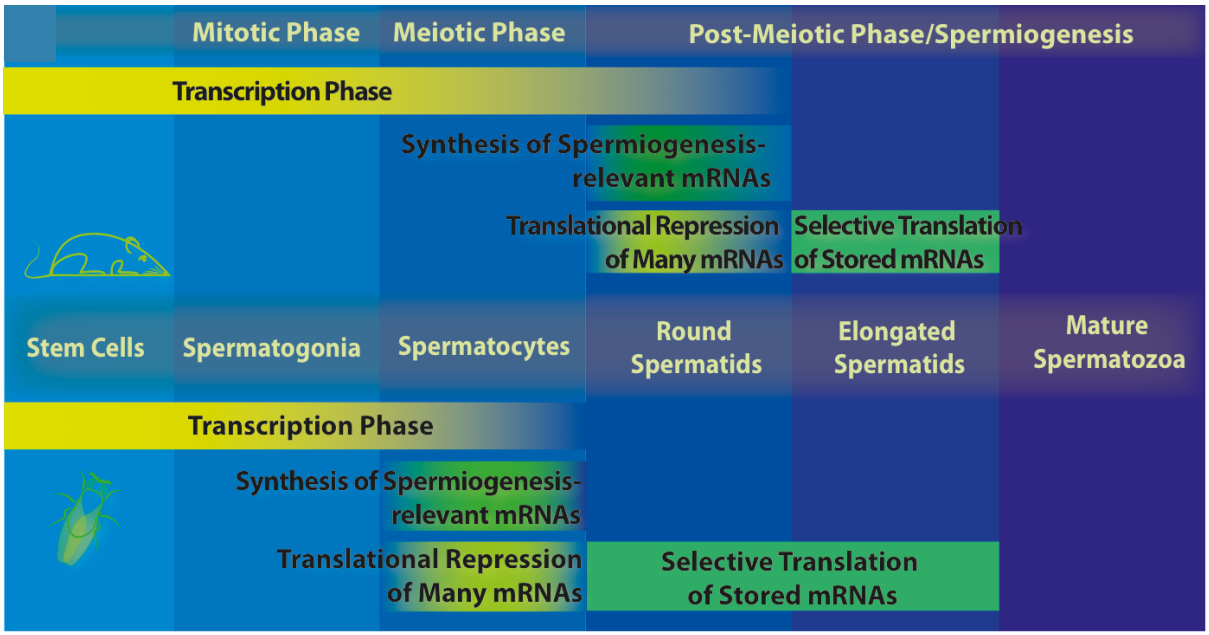

Figure 2 Scheme comparing spermatogenesis of mice and flies. Spermatogenesis consists of different stages defined by a mitotic proliferation phase, a meiotic phase, and a post-meiotic phase known as spermiogenesis both in mice and flies. Global transcription is repressed by the time round spermatids start to elongate in mice, whether in *Drosophila* there is almost no active transcription during post-meiotic phase. So, spermiogenesis is programmed by translationally repressed mRNAs synthesized in spermatocytes (in flies) or in round spermatids (in mice). During post-meiotic phase, translationally repressed mRNAs are continuously released and specific post-meiotic proteins are expressed. Reprinted from Rathke et al., 2014.

During spermiogenesis, due to chromatin compaction and nucleoplasm removal, the volume of the nucleus is reduced by 20 fold in mammals (Braun, 2001) and after meiosis by 200 fold in *Drosophila* (Fuller, 1993). This serious reduction in volume is naturally desired for the favor of fully functional motile sperm. During this process, both in flies and mammals most of the histones are gradually replaced, initially by intermediate basic proteins which are themselves replaced by one or several protamines as mentioned earlier in Chapter 2.3. This process is accompanied first by histone variants which destabilize nucleosomes and followed by stage specific post-translational modifications and transient DNA breaks (Govin et al., 2004; Rathke et al., 2014) (Figure 3). A very well studied post-translational modification is a high H4 hyperacetylation which indicates histone disassembly and correlates with H3K79 methylation (Figure 3). Indeed, altered H4 acetylation or H3K79 methylation affects spermatogenesis, therefore reduces male fertility of *Drosophila*, mice and humans (Dottermusch-Heidel et al., 2014). Acetylation, methylation, phosphorylation, ubiquitination, sumoylation and crotonylation are the known post-translational histone modifications which occur during spermatogenesis. However, their working mechanisms and target roles in chromatin reorganization are not completely understood (Rousseaux and Khochbin, 2015). Importantly, these post-translational modifications are suggested to provide binding sites for specific protein interactions and are best studied for acetylated histones. For example, testis specific bromodomain-containing proteins of flies and mammals bind to acetylated residues of histones and other proteins which are in transcriptionally active stages or during histone-to-protamine transition. Testis specific bromodomain-containing proteins of mice (Brdt) and flies (tBRD-1 and tBRD-2) are shown to be essential for spermatogenesis (Kimura and Loppin, 2015; Theofel et al., 2014; Leser et al., 2012; Shang et al., 2007). These proteins act in transcriptional regulation, chromocentre organization and 3′ UTR-truncation which are also studied in somatic cells. All these data make the mammalian BRDTs more interesting and acknowledge that they recognize and remove hyper acetylated histones before protamines are loaded. Moreover, they contribute to genome compaction during spermiogenesis as chromatin compaction function is difficult to investigate through mutants which may affect already transcription (Gaucher et al., 2012). Furthermore, both in mice and flies transient DNA breaks are concurring at the same time with histone H4 hyperacetylation. These transient DNA breaks are thought to be necessary to get rid of free DNA supercoils formed during histone eviction (Laberge and Boissonneault, 2005) (Figure 3).

While most of the histones are being removed, transition proteins are expressed both in mammals and in flies. Mice have two transition proteins: TP1 and TP2. Mutation of each single protein does not lead to full male sterility whereas deletion of both transition proteins leads to male infertility. This might be due to a functional redundancy between TP1 and TP2. Mice spermatids lacking both TPs show defects in chromatin condensation, high level of DNA breaks and misprocessing of protamine 2. Thus, transition proteins of mice likely are necessary for normal chromatin condensation and genomic integrity (Yu et al., 2000; Zhao et al., 2004). *Drosophila*'s transition protein Tpl94D (Transition protein like 94D) is not a true homolog to mammalian transition proteins, moreover, it shows no sequence similarity to TP1 or TP2 (Rathke et al., 2007). Nevertheless, it has high arginine (11.6%) and serine (13.4%) contents, suggesting a functional homology to mammalian transition proteins. Its HMG-box suggest DNA binding properties. Very recently *tpl94D-ΔC* mutants were analyzed but neither morphological defects nor an alteration in histone-to-protamine switch were observed. Accordingly, similar to mice, additional proteins may act redundantly with Tpl94D in *Drosophila* (Gärtner et al., 2015). tHMG1 and tHMG2 which translocate to the nucleus after meiosis may have a role in histone-to-protamine transition (Gärtner et al., 2015). Identification of more transition proteins in *Drosophila* or a null mutant of Tpl94D will help to elucidate this situation.

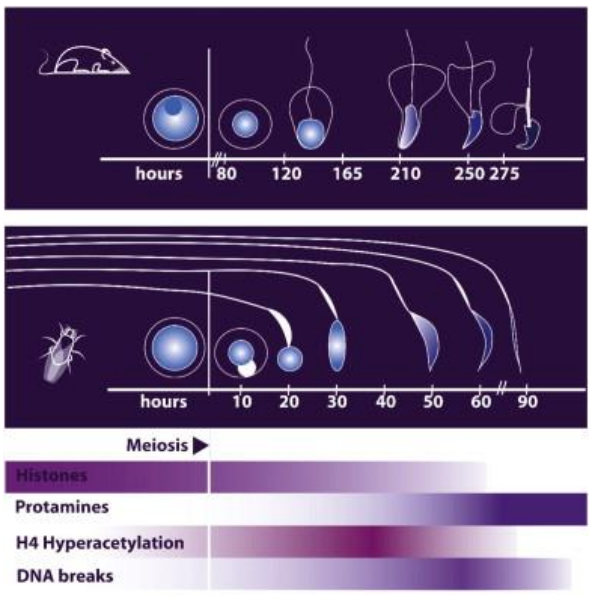

Figure 3 Chromatin remodeling events in post-meiotic phase of mice and flies are highly conserved. After meiosis round spermatid nuclei elongate and via chromatin remodeling the final shape of the mature sperm nuclei are given. During this process, histones are gradually replaced by protamines. H4 hyperacetylation and DNA breaks accompany to this event. Reprinted from Rathke et al., 2014.

Protamines form more stable complexes with DNA than histones and transition proteins do. In all primates and most of the rodents two protamine genes, P1 (*Prm1)* and P2 (*Prm2),* are transcribed and translated (Figure 3). However, some species, like bull and boar, contain only P1. The P2 gene is present but dysfunctional (Balhorn, 2007). In humans, reduced protamine levels correlate with male infertility (Jodar and Oliva, 2014). In mice, both protamines seem essential for male fertility as *Prm1* or *Prm2* haploinsufficient males are sterile. This effect also might lead to an arrest of spermatogenesis, and thus indirectly cause infertility. Protamine deficiency in mice leads to several distortions such as abnormal sperm morphology, less resistance to chemical disruptions, higher immotility and less compaction of the chromatin (Cho et al., 2003; Cho et al., 2001). Nevertheless, transmission electron microscopy images still show the presence of partially compacted sperm chromatin, and the nuclei are not spread out (Cho et al., 2003). Over and above, pharmacological studies in adult male rats reveal the existence of an endocrine-regulated molecular mechanism for histone-to-protamine transition and maintenance of chromatin integrity (Gill-Sharma et al., 2011). More experiments related to endocrinology of sperm chromatin condensation during spermiogenesis should be carried out in order to support and develop this finding.

As in mammals, *Drosophila* genes *Mst35Ba* and *Mst35Bb* encodes for two protamine-like proteins: ProtA and ProtB respectively (Jayaramaiah Raja and Renkawitz-Pohl, 2005; Russell, 1993) (Figure 3). Surprisingly, deletion of both fly protamines does not lead to sterility, however, 20% of the sperm nuclei display abnormal morphology while the chromatin remains compacted and seminal vesicles are full of morphologically wild-type sperm (Rathke et al., 2010; Tirmarche et al., 2014). This is a strong indication that in flies other sperm chromatin components act in redundancy or additively with protamines. One possible candidate is the protein Mst77F, which has been identified as a component of chromatin in *Drosophila* sperm (Jayaramaiah Raja and Renkawitz-Pohl, 2005) and is associated with microtubules during nuclear shaping (Fuller et al., 1989; Rathke et al., 2010). Mst77F shows some similarity to mammalian histone H1-like protein (HILS1) and is essential for male fertility, likely because of its second function in nuclear shaping defects as chromatin appears condensed in these mutants (Jayaramaiah Raja and Renkawitz-Pohl, 2005). Accordingly, a dual function of Mst77F in nuclear shaping and chromatin compaction has been proposed (Rathke et al., 2010). Recently the analysis of protein domains made it unlikely that Mst77F is a histone variant (Kost et al., 2015). Indeed, *in vitro* studies indicate

that Mst77F can condense naked DNA and chromatin (DNA-based oligonucleosomal arrays), thus it may play an important role in the initiation of chromatin condensation during sperm maturation. Actually, the expression of C-terminal truncated versions of Mst77F leads to very similar phenotype with bent nuclei as the protamine deletions (Kost et al., 2015).

2.3.2 HMG-box proteins during spermiogenesis

As previously mentioned in Chapter 2.3.1, many sperm chromatin proteins are expressed during *Drosophila* spermatogenesis in an overlapping or differential pattern. Various HMG-box containing proteins are found both in mammals and *Drosophila*, suggesting that they are commonly expressed during sperm development.

The HMG-box domain of 75-amino acids residue exists in all eukaryotic organisms and mediates among others DNA binding primarily through the minor groove of DNA. HMG-box containing proteins can interact with non-sequence specific or sequence-specific DNA motifs so they may be associated to many DNA-dependent processes such as transcription, modulation of DNA recombination/repair, DNA bending and unwinding, etc. HMG-box proteins are generally involved in different nuclear functions, moreover, they are also found in mitochondria of animals and yeast, where they serve as transcriptional regulators and contribute to the organization of the mitochondrial DNA (Antosch et al., 2012; Stros et al., 2007).

So far in *Drosophila* seven HMG-box containing proteins have been studied during histone-to-protamine transition. They are either expressed transiently, e.g., Tpl94D (Rathke et al., 2007), tHMG1, tHMG2, CG12104, CG30356 (Gärtner et al., 2015), or remain as sperm chromatin components, e.g., ProtA and ProtB (Jayaramaiah Raja and Renkawitz-Pohl, 2005). Besides their association with DNA, their precise function is still unclear. In flies, post-meiotic transcription occurs only for a few genes whereas in mammals transcriptional activity is very high at round spermatids and afterwards gradually decreases (Braun, 2001; Kierszenbaum and Tres, 1975) (Figure 2). Therefore, in flies these post-meiotically expressed HMG-box containing proteins are not likely acting in transcriptional activity. It has been hypothesized that these proteins may facilitate the loosening of chromatin structure and/or

DNA bending at the late stage of spermiogenesis. Surprisingly, lack of tHMG-1/tHMG-2 or Tpl94D showed no defect in spermiogenesis suggesting that HMG-box containing proteins act within a network in which each member can partially compensate for the others (Gärtner et al., 2015). In addition, lack of the *Drosophila* protamines leads also to slight defects in chromatin condensation and a higher mutation rate after radiation (Rathke et al., 2010).

In mammals three HMG-box containing proteins (Hmgb1, Hmgb2 and Hmgb4) are expressed during spermatogenesis. Hmgb1 acts as an architectural factor that bends DNA and promotes protein assembly on specific DNA targets. Hmgb2 deficient mice have reduced fertility that correlates with Sertoli germ cell degeneration and immotile sperm. Hmgb2's role has been linked to transcriptional regulation (Ronfani et al., 2001). Hmgb4 associates with chromatin, and in contrast to Hmgb1, it acts as a transcriptional repressor (Catena et al., 2009). As transcription shut down time line is different between mammals and flies (Figure 2), the role of HMG-box-containing proteins may vary among species. Indeed, the generation of Hmgb4 mutants in the future may clarify whether these proteins act only in transcriptional repression or they are also interact with remodelling proteins.

In conclusion, identification and examination of more HMG-box-containing proteins, their architectural capability to interact with DNA and/or other proteins will help to unravel the chromatin dynamics during spermiogenesis.

2.3.3 Molecular chaperons and CTCF in *Drosophila* spermiogenesis

Histone chaperones serve as prominent players in histone removal and exchange, and in addition to nucleosome assembly, they help to maintain the correct chromatin structure and dynamics (Park and Luger, 2008). Very few studies have been performed on the identification of histone chaperones and ATP-utilizing motor proteins during *Drosophila* sperm chromatin assembly. From those proteins Hanabi and nucleosome assembly protein 1 (Nap1) are studied. Hanabi functions as a chaperone for acidic proteins in nucleosome assembly *in vitro*. However, it is still not clear whether it influences histones-to-protamine

transition. *nap1* mutant shows disruption of nuclear bundles, however, nuclear condensation and shaping is normal. Thus, it has been postulated that Nap family proteins also contribute to cytoskeleton organization, nevertheless, this hypothesis needs to be investigated in more detail in the future (Kimura, 2013). Very recently, Nap-1 together with Nucleoplasmin-like protein (NLP) and nucleophosmin were described as ProtA evictors during fertilization in flies (Emelyanov et al., 2014). If indeed Nap1 plays a role also in histone-to-protamine transition during spermiogenesis, it would be a histone chaperone acting before and after fertilization. Future work should advance to investigate the molecular role of Nap1 during histone-to-protamine transition.

Drosophila chromatin assembly factor 1 (CAF1) is a canonical histone H3/H4 chaperone which plays a crucial role during the histone-to-protamine transition. Its subunit CAF1-p75 acts as a protamine-loading factor showing us that histones are not the only substrate of histone chaperons (Doyen et al., 2013).

CCCTC-binding factor (CTCF) is a zinc-finger protein involved in insulator activity in vertebrates and *Drosophila*. It is involved in many processes related to global chromatin organization, remodeling, epigenetic reprogramming, etc. With respect to the chromatin insulation activity, CTCF is required for proper development (Franco et al., 2014; Herold et al., 2012). Since the DNA-binding domain of CTCF in human and *Drosophila* shows approximately 60 % similarity, *Drosophila* is a very good model organism to study the role of CTCF, especially in sperm development. *Drosophila* CTCF is expressed during pre-meiotic and meiotic stages. Moreover, shortly after meiosis, CTCF is visible from young elongating until the late canoe stage nuclei (Rathke et al., 2007). As no tissue-specific CTCF loss-of-function mutants have been published so far, there is no evidence about the function of CTCF during *Drosophila* spermatogenesis. Regarding to its expression pattern, there are few speculations about its potential roles: 1) the earlier chromatin-associated CTCF localization may indicate an early role in chromatin, 2) CTCF may be associated primarily with loosen chromatin during pre-meiotic stages, 3) CTCF may maintain chromatin accessibility to RNA polymerase II (RNAP II), and in addition, RNAP II may require CTCF to insulate active genes from inactive ones at the late canoe stage, and 4) CTCF may set borders in the chromatin for the histone modifications (Rathke et al., 2007).

All in all, there is a big gap in the knowledge of the mechanisms which incorporate histone variants, transition proteins and protamine-like proteins into the *Drosophila* sperm. It is surprising that the studies performed until now have revealed the presence of different independent incorporation mechanisms. Histone degradation and CTCF removal seem to be regulated independently of the synthesis of protamines (Rathke et al., 2007), and similarly, histone removal and incorporation of Mst77F into sperm chromatin is not affected by the loss of CAF1 (Doyen et al., 2013). Thus, the identification of more histone chaperons and ATP-utilizing proteins needs to be done in order to understand the true mechanism of histone-to-protamine transition.

2.4 What do *Drosophila* testis and sperm proteomes tell us?

There is limited knowledge about the molecular genetic basis of male fertility and causes of infertility in human, mouse and fly. *In Drosophila*, over 9,000 genes are annotated (Chintapalli et al., 2007), however, it is not always practical to correlate the transcription levels of mRNAs with the protein expressions, and moreover it is unfeasible to detect post-translational modifications from gene expression studies (Yamamoto and Takemori, 2010). Spermatogenesis is a very complex process both in mammals and flies where spermiogenesis relevant mRNAs are synthesized and translationally repressed until their expression is required (Rathke et al., 2014) (Figure 2). Therefore, it is essential for researchers to identify proteins produced in specific tissues or organs to examine their exact role in biological processes.

So far three proteomics studies have been performed on *Drosophila*'s reproductive system. By analyzing each organ separately, a total of 440 proteins were identified from male reproductive system, from which 232 and 168 proteins correspond to testes and seminal vesicles respectively (Takemori and Yamamoto, 2009). In 2006, the first *Drosophila melanogaster* sperm proteome (DmSP) identified 381 proteins using whole-sperm mass spectrometry (Dorus et al., 2006). This approach identified mitochondrial, metabolic and cytoskeletal proteins and some chromatin components like protamines. In 2010, the DmSP-

II used “shotgun” proteomic approach and revealed 766 new proteins and an updated sperm proteome containing a total of 1108 proteins (Wasbrough et al., 2010). Although the number of the identified sperm proteins increased so much in just four years, only minor subsets of the identified proteins were nuclear proteins. For instance, a well-known sperm chromatin component, Mst77F, was not found. Very recently a former PhD student from our lab, Dr. Stefanie M. K. Gärtner, performed a *Drosophila melanogaster* stage-specific testis proteome (DmTP) with the aim to identify proteins of mitotic, meiotic and post-meiotic stages of germ-cell development. Her data revealed the presence of 6641 *Drosophila* testes proteins from which 355 were specific for adult testes (Gärtner PhD Thesis, 2014; Gärtner et al., in preparation). This new data set would be very informative in order to detect proteins encoded by translationally repressed mRNAs. Moreover, clarification of proteins that expression start at late stage of spermiogenesis is an important step towards understanding the function of paternal chromatin.

In order to obtain a more complete characterization of human sperm proteome, subcellular proteomics was performed allowing the identification of less concentrated proteins in tail or head (Amaral et al., 2013; Castillo et al., 2014). If we consider the difficulties that DmSP and DmSP-II faced in identifying sperm nuclear proteins, researchers should develop new strategies in order to detect less abundant, very basic or acidic proteins of *Drosophila* sperm. In the future, it would be convenient to perform a subcellular proteomics from *Drosophila* sperm to identify more transcription factors, zinc finger-containing proteins, chromatin associated proteins, chromatin-modifying enzymes, etc.

2.5 Prtl99C as a candidate basic chromosomal protein

So far I summarized how and why *Drosophila* melanogaster is an excellent model organism to study spermatogenesis and the gap-of-knowledge in sperm chromatin field. Researchers working on either mammalian or *Drosophila* spermatogenesis have a long way to completely understand the structural formation of the sperm cell. Identification and examination of more sperm proteins, development of new methods for the detection of unrepresented sperm proteins are essential.

While looking for functional homologues of transition protein Tpl94D in *Drosophila*; Rathke et al. identified five predicted genes (*CG4691*, *CG15510*, *CG32308*, *CG31861*, *CG31281*) encoding very basic proteins expressed in testes. The analysis of their expression pattern using *eGFP* fusion genes revealed that CG15510 is not expressed during the time spanning the histone-to-protamine transition (Rathke et al., 2007), therefore, at that time it was not their interest.

After confirming the expression pattern of CG15510-eGFP as a component of the sperm nucleus, we wanted to evaluate if indeed CG15510 is a sperm protein like protamines. CG15510 is later on named as "Prtl99C" and is further analyzed as the main topic of this thesis in particular by genetic means to elucidate its function with respect to chromatin compaction.

2.6 Aims

Spermatogenesis is a highly conserved process also in the context of DNA condensation and structural reorganization. So far, many HMG-box containing proteins have been identified. Some of these proteins are expressed during the histone-to-protamine transition and a few remain until the mature sperm. The exact mechanism of molecular actions of these proteins is poorly understood.

In *Drosophila* another HMG-box containing protein, Prtl99C, was put forward as a protamine-like protein. The expression pattern in the nucleus of late spermatids and sperm has been described using transgenic flies expressing Prtl99C-eGFP fusion protein under control of the *Prtl99C* (CG15510) gene regulatory region (Rathke et al., 2007). So far the molecular function is still unknown. The main aim of this work is to study the role of Prtl99C during chromatin reorganization in *Drosophila* spermiogenesis and to identify additional sperm proteins. To achieve this goal the following questions were addressed:

1. What is the expression pattern of Prtl99C during spermatogenesis?
2. What is the role of Prtl99C in spermiogenesis?
3. Is Prtl99C essential for male fertility?
4. What happens if *Prtl99C* is knockdown or knockout?
5. What happens in *Prtl99C-ΔC* flies?
6. What is the function of the C-terminal of Prtl99C?
7. What is the function of the N-terminal of Prtl99C?
8. Is the histone-to-protamine transition normal in Prtl99C mutants?
9. Do Prtl99C, Mst77F and protamine co-localize?
10. Can Prtl99C substitute protamines?
11. What happens when both Protamines and Prtl99C are missing?
12. Are there new sperm protein candidates from comparative proteomics analysis?

3 Materials

3.1 Equipment

Binocular	Stemi SV6/ Stemi DV4, Zeiss, Jena
Centrifuges	Biofuge fresco, Heraeus, Hanau Biofuge pico, Heraeus, Hanau Megafuge 1.0 R, Heraeus, Hanau
Developer machine Optimax Typ TR	MS-L GmbH, Diehlheim
Gel electrophoresis apparatus	University of Marburg
Ice maker machine	AF-20, Scotsman
Magnetic stirrer	Combimac RCT, IKA, Staufen
Microscope	Axioplan with ApoTome, Zeiss, Göttingen
Microscope camera	AxioCam MRm, Zeiss, Göttingen
Microwave	Dimension 4, Panasonic
Mini Trans-Blot® electrophoretic apparatus	Bio-Rad
PCR machine	Personal Cycler, Biometra, Göttingen
pH-meter	GPRT 1400A, Greisinger Electron
Photometer	GeneQuant 1300, GE Healthcare, München
Shaker	Rexa 2000, Heidolph, Schwabach; Rocky 3D, Fröbel Labortechnik, Lindau; WT-12, Biometra, GFL 3005/3033, Burgwedel
Sonicator	Bandelin Sonoplus GM70, Berlin
Spectrophotometer	Nanodrop 2000, Thermo Scientific, Waltham, Massachusetts
Thermal printer	P93, Biometra
Thermoblock	Rotilabo®-Block-Heater H250, Roth, Karlsruhe
Ultracentrifuge	Optima™ MAX-XP Benchtop Ultracentrifuge TLS-55

UV-cross-linker	UV Stratalinker™ 2400, Stratagene, La Jolla, USA
UV-Trans illuminator	Ultralum, Electronic Dual-Light-Trans illuminator
UV-Gel documenter	CCD-Camera Ultralum, Carson California
Voltage source	Bio-Rad Power Pack 300
Vortex machine	M51 Minishaker
Water-bath	C10, C1, Haake, Karlsruhe GFL 1002, Biometra, Burgwedel

3.2 Media and chemicals

Acetic acid	Roth, Karlsruhe
Acrylamide	Fluka, Neu-Ulm
Albumin Fraction V	Roth, Karlsruhe
Agarose Basic	PanReac AppliChem, Gatersleben
Ammonium persulfate (APS)	Merck, Darmstadt
Ampicillin	Fluka, Neu-Ulm and Appligene, Heidelberg
Bacto-Trypton	Difco, Eggenstein/Becton & Dickinson, Heidelberg
Bacto Yeast Extract	Difco, Eggenstein or Roth, Karlsruhe
Bleacher Detergent	Colgate Palmolive GmbH, Hamburg
Boric acid	Fluka, Neu-Ulm or Roth, Karlsruhe
α-D-thio-galactosid (X-α-Gal)	Clontech, Göttingen
β-D-thio-galactosid (X-Gal)	Roth, Karlsruhe
5-Bromo-4-chloro-3-indolyl-phosphat (X-Phosphat)	Boehringer, Mannheim
Bromphenolblue	Merck, Darmstadt
Calcium acetate	Roth, Karlsruhe
Calcium chloride	Roth, Karlsruhe

Chloroform	Riedel-de Haën AG, Hannover
Chloramphenicol	Sigma-Aldrich, Steinheim
Coomassie Brillant Blue R250	Serva, Heidelberg
Deoxynucleotide (dNTP) Solution	Amersham Pharmacia Biotech, Freiburg
Dibucaine hydrochloride	Sigma-Aldrich, Steinheim
Diethyl ether	Roth, Karlsruhe
Disodium phosphate	Roth, Karlsruhe
Epon 812	Sigma-Aldrich, Steinheim
Ethanol	Roth, Karlsruhe
Ethidium bromide	Sigma-Aldrich, Steinheim
Ethylenediaminetetraacetic acid (EDTA)	Roth, Karlsruhe
Dibucaine hydrochloride	Sigma-Aldrich, Steinheim
Digoxygenin	Roche, Mannheim
Dithiothreitol (DTT)	Fluka, Neu-Ulm
Fluoromount GTM	Southern Biotech, Birmingham, England
Formaldehyde (37% solution)	Merck, Darmstadt
Formamide	Merck, Darmstadt
Glucose	Merck, Darmstadt
Glycerine	Roth, Karlsruhe
Glycine	Roth, Karlsruhe
Heparin	Roth, Karlsruhe
Hydrogen peroxide	Merck, Darmstadt
4-Hydroxybenzoesäuremethylesther (Nipagin)	Sigma-Aldrich, Steinheim
Hoechst 33258	Sigma-Aldrich, Steinheim
Isopropanol	Roth, Karlsruhe
Kanamycin	Sigma-Aldrich, Steinheim
Levamisole	Sigma-Aldrich, Steinheim
10X Ligation buffer	MBI Fermentas, St. Leon-Rot
Lithium acetate	Sigma-Aldrich, Steinheim
Magnesium chloride	Roth, Karlsruhe
Magnesium sulfate	Roth, Karlsruhe

Manganese (II) chloride	Fluka, Neu-Ulm
β-Mercaptoethanol	Roth, Karlsruhe
Methanol	Roth, Karlsruhe
Monosodium phosphate	Roth, Karlsruhe
3-morpholinopropane-1-sulfonic acid (MOPS)	Roth, Karlsruhe
Octylphenol Polyethylene Glycol Ether (Triton X-100)	Roth, Karlsruhe
Sodium acetate	Roth, Karlsruhe
Sodium chloride	Roth, Karlsruhe
Sodium deoxycholate	Merck, Darmstadt
Sodium dodecyl sulfate (SDS)	Roth, Karlsruhe
Sodium hydroxide	Roth, Karlsruhe
Sucrose	Roth, Karlsruhe
Nitrotetrazolium Blue chloride (NBT)	Roche, Mannheim
Nocodazole	Sigma-Aldrich, Steinheim
PEG	Sigma-Aldrich, Steinheim
Penicillin/Streptomycin	GE-Healthcare Life Sciences, München
Percoll® (P1644-100ML)	Sigma-Aldrich, Steinheim
Phalloidin-TRITC	Sigma-Aldrich, Steinheim
Poly-L-Lysine	Sigma-Aldrich, Steinheim
Polysorbate 20 (Tween 20)	Roth, Karlsruhe
Propionic acid	Sigma-Aldrich, Steinheim
Rubidium chloride	Sigma-Aldrich, Steinheim
Schneider's *Drosophila* Medium	Gibco® - Life Technologies GmbH, Darmstadt
Tetramethylethylenediamine (TEMED)	Serva, Heidelberg
Tris	Roth, Karlsruhe
UltraPure™ Agarose	Invitrogen, Karlsruhe
Xylene cyanol	Merck, Darmstadt

3.3 Culture media

Escherichia coli culture medium	1% (w / v) Bacto tryptone
LB medium (Luria-Bertani)	0.5% (w/v) yeast extract 0.5% (w/v) NaCl in ddH_2O For solid media: 1.5% agar
Selection on	ampicillin 100 µg/ml chloramphenicol 23 µg/ml kanamycin 50 µg/ml

3.4 Enzymes

Proteinase K	Roche, Mannheim
Restriction endonucleases	Fermentas, Heidelberg NEB, Frankfurt am Main
RNase A	Roche, Mannheim
RnaseOut	Invitrogen, Karlsruhe
Taq DNA polymerase	Axon, Kaiserslautern
VELOCITY DNA polymerase	Bioline, Luckenwalde
T4-DNA Ligase	Thermo Fisher Scientific, Karlsruhe

3.5 Antibodies and antiserums

Primary Antibodies

Antibody	Origin	Dilution	References
α-actin	mouse	1:1000 (WB)	Biomeda
α-all histones	mouse (monoclonal)	1:1200 (IF)	Millipore MABE71
α-Mst77F	rabbit (monoclonal)	1:1000 (IF)	Rathke et al., 2010

α-Prtl99C	rabbit (monoclonal)	1:500 (IF) 1:100 (WB)	Eren-Ghiani et al, 2015
α-ProtA/B	guinea pig (monoclonal)	1:500 (IF)	Doyen et al., 2013
α-CID	rabbit	1:200 (IF)	Active Motif (No: 39720)

Secondary Antibodies

Antibody	**Dilution**	**References**
Anti-Digoxigenin-AP, Fab fragments	1:1200 (*in situ*)	Roche, Mannheim
α-rabbit, Cyanin2-conjugated	1:100 (IF)	Dianova, Hamburg
α-rabbit, Cyanin3-conjugated	1:100 (IF)	Dianova, Hamburg
α-guinea pig, Cyanin3-conjugated	1:100 (IF)	Dianova, Hamburg
α-mouse, Cyanin5-conjugated	1:100 (IF)	Dianova, Hamburg
α-rabbit peroxidase-coupled	1:5000 (WB)	Jackson Immunology, England, Newmarket
α-mouse peroxidase-coupled	1:5000 (WB)	Jackson Immunology, England, Newmarket

3.6 Molecular reagents and kits

Color Protein Standard Broad Range (P7712)	New England Biolabs, Massachusetts
DIG RNA Labeling Kit	Roche, Mannheim
ECL Novex® Chemiluminescent Reagent Kit	Invitrogen, Karlsruhe
Genomed Jetstar Midi Kit 2.0.	Genomed, Bad Oeynhausen
NucleoSpin® Gel and PCR Clean-up	Macherey-Nagel, Düren
OneStep RT-PCR Kit	Qiagen, Hilden
Oligotex®mRNA Mini Kit	Qiagen, Hilden
PCR Solutions	5x HiFi Buffer (Bioline, Luckenwalde)
	10x Puffer BD (Axon, Kaiserslautern)
	25 mM $MgCl_2$ (Axon, Kaiserslautern)
pCR®II-TOPO® Cloning Kit	Invitrogen, Karlsruhe
Penicillin/Streptomycin	Gibco, Karlsruhe
RQ1 RNase-free DNase	Promega, Madison, Wisconsin
T4 DNA Ligase Buffer	Thermo Fisher Scientific, Schwerte
Transcriptor First Strand cDNA Synthesis Kit	Roche, Mannheim
TRIzol®	Invitrogen, Karlsruhe

Zero Blunt®TOPO®PCR Cloning Kit	Invitrogen, Karlsruhe
100 bp DNA Ladder	New England Biolabs, Massachusetts
2-Log DNA Ladder (0.1-10.0 kb)	New England Biolabs, Massachusetts

3.7 Buffers and solutions

F-PBS	4% (w/v) Formaldehyde in 1x PBS
10xPBS (phosphate buffered saline)	1.3 M NaCl 7 mM Na_2HPO_4 3 mM NaH_2PO_4 in H_2O pH 7.4 autoclaved
PBSTD	1x PBS 0.3 % Triton X-100 and 0.3 % Sodium deoxycholate
PBT	0.1 % Tween-20 in 1x PBS
PBT/3% BSA	PBT 3% (w/v) Albumin Fraction V

3.8 Bacterial strains

Escherichia coli DH5α	chemically competent cells *sup*E44, *Δlac*U169, F-, Φ80 *lacZ*, ΔM15, Lambda-, *hsd*R17, *rec*A1, *end*A1, *gyr*A96, *thi*-1, *rel*A1 (Renkawitz-Pohl Lab, PUM)
One Shot® *ccdB*	chemically competent cells

3.9 Fly strains

GAL4-Driver Lines

bam-GAL4 (*Bag of marbles-Gal4*)	GAL4 driver line under the control of the bam regulatory region. Expression is restricted to 2-to 16-cell spermatogonia. (Chen and McKearin, 2003)
Bam-Gal4-VP16	(Caporilli et al., 2013)
C135-Gal4 (*6978*, Bloomington)	*w[1118]; P{w[+mW.hs]=GawB}c135*, GAL4 driver line which drive expression of UAS constructs in male reproductive tract (Hrdlicka et al., 2002).

Transgenic Fly Lines

942-Prtl99C-eGFP	P-element-bearing fly strain based on the transformation vector *pChabΔSal*. Expression of Prtl99C ORF tagged with C-terminal eGFP under the control of its own promoter and its 5 'UTR (Rathke PhD Thesis, 2007 as *CG15510-eGFP*).
ProtB-mCherry	P-element-bearing fly strain based on the transformation vector p*ChabΔSalΔLacZ.* (Dottermusch-Heidel et al., 2014)
ProtΔ2	Deletion fly line based on FLP-FRT recombinase which deletes the protamine genes *Mst35Ba* and *Mst35Bb* located at the second chromosome. (Rathke et al., 2010)

ProtB-DsRed, dj-GFP	Recombined lines to yield a strain expressing both fluorescent proteins on the same third chromosome (Köttgen et al., 2011).
v106856	*P{KK109686}VIE-260B;* RNAi line against *Prtl99C*
v6208	*w[1118]; P{GD1467}v6208;* RNAi line against *ISWI*
v20270	*w[1118]; P{GD7858}v20270;* RNAi line against *CAF1-p75*
v108857	*P{KK100986}VIE-260B;* RNAi line against *CTCF*
28918 (Bloomington)	*y[1] v[1]; P{y[+t7.7] v[+t1.8]= TRiP. HM05129} attP2;* RNAi line against *CAF1-p180*
$Cad99C^{248A}$	*Cad99C* mutant allele removes *Cad99C,Atg16*, *CG42592* and *Prtl99C* (Schlichting et al., 2006).
$Cad99C^{57A}$	*Cad99C* mutant allele (Schlichting et al., 2005).
P-Element-Insertions	
53232 (Bloomington)	*y[1] w[*]; Mi{y[+mDint2]= MIC} CG15510 [MI10224]*; Insertion at position 99C2, within the ORF of *Prtl99C*

30114 (Bloomington)	*w[1118]; P{w[+mC]=EP} Atg16[G5082]*; Insertion at position 99C2, within the 5'UTR of *Atg16*
30656 (Bloomington)	*y[1] w[*]; Mi{y[+mDint2] =MIC} Atg16[MI00187]*; Insertion at position 99C2, within the ORF of *Atg16*
23364 (Bloomington)	*y[1] w[67c23]; Mi{ET1} CG6332[MB01798];* Insertion at position 93F14, within the ORF of *CG6332*
22919 (Bloomington)	*y[1] w[67c23]; Mi{ET1} CG4691[MB00873]*; Insertion at position 35B5, within the ORF of *CG4691*
18237 (Bloomington)	*w[1118]; PBac {w[+mC]=RB} CG31542[e04201]*; Insertion at position 83A1, within the 5'UTR of *CG31542*
21782 (Bloomington)	*y[1] w[67c23]; P{y[+t7.7] w[+mC]=wHy}CG12860[DG39411]*; Insertion at position 51B9, within the 3'UTR of *CG12860*
14525 (Bloomington)	*y[1] w[67c23]; P{y[+mDint2] w[BR.E.BR]=SUPor-P} CG17377[KG07328]*; Insertion at position 27B3, within the 5'UTR of *CG17377*

General lines

w^{1118} (*6326*, Bloomington)	Transformation strain, used as wild-type strain
CSTM	w^{-}*; Sp/CyO; MKRS/TM2*; Multiple balancer used for the localization of the P-element.
TM6B	w^{-}*; Sp/CyO*^{bb}*; TM6*^{bb}*/TM2*; Multiple balancer used for the localization of the P-element.

3.10 Plasmids

pChabΔSalΔlacZ-eGFP	P-element transformation vector for *Drosophila melanogaster* originally described in Thummel et al., 1988 with a length of 9405 bp was modified, the lacZ was removed and an eGFP inserted instead. The vector has ampicillin resistance. (Kindly provided by Dr. Stephan Awe)
PCR®-Blunt II-TOPO®	(Invitrogen, Karlsruhe)
pCR®II-TOPO®	(Invitrogen, Karlsruhe)

3.11 Oligonucleotides

The oligonucleotides were synthesized by MWG Biotech (Ebersberg).

Oligonucleotide	Sequence 5'→3'
CG15510-ISH-Fw	CGACGATTACTTTGAAGAGTCCAGC
CG15510-ISH-Rv	CAAAGTGGCCTCTCAAACGCATG
CG31033-f	GATTGACCATGTGGCGCAACT
CG31033-r	CCAATTGAAGCGCCGTATGTTC
CG42592-f	GGCTTCTTATCAAGCGGTTTGC
CG42592-r	GTATAGAAAAGTGCTGGCCACAG
RTpcrMst99C-Fw	GAAAAAGGGGTCGAAAGGAG
Mst99C-r	CTCTTCAAAGTAATCGTCGATGG
Cad99C-f	GGTTCTACCTCATCGATCCCAAGA
Cad99C-r	GTTAACGATCACGGGATCGTAGC
β3-tubulin-fw (B3aa23)	ATCATTTCCGAGGAGCACGGC
β3-tubulin-rv (B3aa140)	GCCCAGCGAGTGCGTCAATTG
Rpl32-fwd (Czech et al., 2008)	ATGACCATCCGCCCAGCATAC
Rpl32-rev	CTGCATGAGCAGGACCTCCAG
Mst99C-qRv	GCTTGGAGACTGTCTTTGGCA
Mst99C-qFw	CAGCAAAGTTCTTGCCAAAGAC
RTpcrMst99CRv	TGATCTGCACAAGGTCTTCG
Mst99C-RT3-Fw	CTTCCTGCGCAAGTTCCAAA
Mst99C-RT3-Rv	CATACTGCTTACTCCTAGCC
MI10224-3Rv	CTAGTAACGTTTTCCGCACGA
MIMIC5-1	GTG TGT TAA ACA TTG CGC ACT G
CG15510_sen	GATGGTACCCTAAAATACTGATTCGC
CG15510_as	GATTCTAGAGGATTTTCCTATTGTAAC
CG42592-Fw2	GATGAATTCCATACTGCTTACTCC
CG42592-Rv2	GATACTAGTGTAGGGTATAATGGC
6332-5Fw	GGGGAGTCCATACTGAACAGAT
6332-3Rv	GATATGCGTGTTCTCGAACTC
Mst99C-TG-Fw	GGGGGTACCCTTCAAAAATCTTTT
Mst99C-TG-Rv	GGGACTAGTGGATTTTCCTATTGT
Mst99C-Nterm-Rv	GATACTAGTTGCCACTGCCGAGCC

3.12 Sequencing DNA

The sequencing was carried out by the company LGC Genomics GmbH (Berlin).

3.13 Other materials

Amersham Hyper film ECL	GE Healthcare Life Sciences, Munich
Cover slips (18x18 mm; 24x32 mm)	Roth, Karlsruhe
Dumont forceps (Inox 5)	Mercateo, Köthen
Hybond N-Membrane	Amersham, Braunschweig
Microscope slide	Roth, Karlsruhe
Nitrocellulose Membrane Optitran BA-S 83	GE Healthcare Life Sciences, Munich
Petri dish (92x16 m)	Sarstedt, Nümbrecht
Whatman paper	Schleicher and Schüll, Dassel

3.14 Software and websites

Word Processing	Microsoft Word 2013
Imaging	Adobe® Photoshop® CS2 9.0
	Axiovision Rel. 4.8
Database analysis	
ApE-A plasmid Editor (v1.17)	
cNLS Mapper (NLS)	(Kosugi et al., 2009)
Ensemble Genome Browser	(Cunningham et al., 2015)
FlyAtlas: the *Drosophila*	(Chintapalli et al., 2007)
gene expression atlas	
FlyBase	(St Pierre et al., 2014)
InterPro	(Mitchell et al., 2015)

OligoCalc (v. 3.26)	(Kibbe, 2007)
PubMed – NCBI	
SMART	(Letunic et al., 2015)
SpermPress	(Vibranovski et al., 2009)

4 Methods

4.1 Handling *Drosophila melanogaster*

4.1.1 Strain Maintenance

Food medium	90 g Agar-Agar
	1 kg Corn flour
	180 g Dry yeast
	1 kg Fructose
	120 ml 20% Nipagin in 70% Ethanol
	360 ml 20% Propionic acid
	up to 12 l H_2O

The breeding of *Drosophila melanogaster* is done in plastic culture tubes. The tubes are closed with a mite proof plug. Depending on the number of flies small (2.5 cm diameter), medium (3 cm diameter) or large (4 cm diameter) tubes can be used. The flies are kept at 25 °C or 18 °C and can be analyzed by anesthesia with diethyl ether and/or CO_2 to perform any crossing experiments. The flies are transferred to new culture tube with fresh culture medium at a time of approximately 2 to 3 weeks at 25 °C and about 4 to 5 weeks at 18 °C.

4.1.2 *Drosophila* Crossings

For crossing experiments virgin females are mated with males. For single pair crosses an animal with 2-3 animals of the opposite sex is crossed over.

4.1.3 Generation of transgenic flies **(Spradling and Rubin, 1982)**

For the production of transgenic fly lines, transformation vectors are used, which are based on naturally occurring P elements, but encode for no functional transposase. For the integration of the desired gene, transformation vectors are injected in conjunction with helper plasmid (pπ25.7wc) which provides the available transposase. The desired PCR fragment was inserted into *pChabΔsalΔlacZ-eGFP* in-frame with *eGFP*. Transgenic fly strains were established in w^{1118} background.

Collection of embryos (performed by technicians)

About 200 to 300 w^{1118} flies of 3-5 days old were collected and transferred to the apple juice agar plates coated with yeast to stimulate egg laying. The embryos for injection were collected every 30 min at 18 °C with 1-2 rounds of precollection on apple juice agar plates. The eggs were transferred with a brush carefully into a fine-mesh metal filter, and washed with 0.7 % NaCI solution. The embryos were then bleached with 1:1 ratio of Bleaching solution (Colgate Palmolive, Hamburg) and water for approximately one min to dechorionate. After thorough rinsing with 0.7 % NaCl the embryos were transferred with a brush onto a rectangular apple juice agar block and oriented in such a manner that would facilitate the injection. The lined up embryos were attached now onto the glass slide with adhesive (10 ml heptane dissolved adhesive for 10 cm adhesive tape) by giving a slight pressure on the embryos. The embryos were then dried a little bit depending upon air humidity and ambience temperature for 8 to 12 min in a desiccator over silica gel, in order to reduce the internal pressure of the embryos. Afterwards the embryos were laminated with mineral oil, in order to prevent further drying.

Microinjection of Embryos

10xInjection Buffer
150mM NaHPO4 (pH 7.4) mM KCl
10 µg of DNA
10x injection buffer (2.5 µl)
Helper plasmid pπ25.7wc (0.5 µg/µl concentration) (2.5 µl)
up to 25 µl with ddH_2O

The mixture is centrifuged (13,000 rpm, 30 min and 4°C) in order to sediment the disturbing floating particles. One µl of this DNA mixture is filled from the rear end of the injection needle with the help of Borosilicate glass capillary of internal diameter 1.2 mm. The liquid flowed up into the needle through the capillary action. This capillary was connected with the pressure system of the micro injection equipment and was fastened to the micromanipulator. To open the capillary, the front part of the capillary was broken off under the microscope (20x objective) by touching to the edge of the glass slide. After introducing the needle to the posterior end of the embryos, the DNA solution was injected. To prevent the emergence of non-transgenic flies, embryos in which the formation of the pole cells had already taken place and/or in which the germ cells were inaccessible for transformation were killed passing through the whole embryo an injection needle. After the injection, few more drops of mineral oil were added over the embryos and the glass slide was transferred onto apple juice agar Petri plate. The injected embryos were incubated at 25°C for approximately 24 hours. The embryos which survived the stress of microinjection developed into larvae and crawled around in the Petri plate. The larvae were collected with the help of a needle and transferred into fly bottles with breading medium. Each larva which developed into adult flies was collected and crossed against w^{1118} flies.

Selection of transformed flies (Klemenz et al., 1987)

The selection of transformed flies is made possible by the use of the *white+* gene (red eye color) as a dominant selection marker. Since the insertion of the P-element-construct takes place in the germ line of the injected embryos, the insertion event can be observed only in the G1-Generation. The injected animals (G0-generation) that eclose were immediately crossed with w^{1118} flies. In the G1-generation the transformed individuals can be recognized by the appearance of eye color, ranging from orange to red. Each transgenic animal was crossed again with white flies and the developing heterozygote descendants were further crossed among themselves. The homozygote descendants, usually recognized by the darker eye color, were then further-bred for the establishment of a stable transgenic line.

4.1.4 Chromosomal localization of the P-element

The chromosomal localization of the P-insertion can be possible with the help of the multi-marker-fly strain CSTM. CSTM flies bear on the second chromosome the balancer *Curly of the Oster (CyO)* and the marker *Sternopleura (Sp)*, and on the third chromosome the balancer TM2 with the marker *Ultrabithorax (Ubx)* and the MKRS with the marker *Stubble (Sb)*. Balancer chromosomes are specific to *Drosophila melanogaster* and allow for stable maintenance of recessive , lethal mutations, since in these flies homologous recombination between chromatids of homologous chromosomes by crossover is prevented due to multiple inversions. The balancer chromosomes are additionally provided with dominant markers and allow the identification of the flies in the heterozygous state. Balancer chromosomes also carry a number of mutations that lead, in the homozygous state, to lethality.

First, transgenic red-eyed males are crossed with females of the CSTM strain. Subsequently, red-eyed males of the F1 generation carrying the markers CyO and Sb are crossed with females of the CSTM strain. With the help of the F2 generation, the chromosomal localization of the P-element may then be determined whether it is on the chromosomes II, III or IV. If there is an insertion on the second chromosome, all red-eyed offspring have the marker Sb and Ubx and CyO or Sp, all white-eyed offspring have the marker CyO and Sp and Ubx or Sb. In contrast, all red-eyed flies with a P insertion on the third chromosome will have the markers CyO and Sp and Sb or Ubx. White-eyed animals posse the marker Ubx/Sb and Sb and Ubx. If a red-eyed animal from the F2 generation bear all four markers, this indicates an insertion on the fourth or X chromosome. If already the F1 generation is only red-eyed females and only white-eyed males, this indicates a localization of the P element on the X chromosome.

The same strategy is applicable also using the TM6B balancer. For facility, during the development, the non-tubby (Tb) larvae may be removed from the culture tube so the hatched flies will all carry the Tb balancer on the third chromosome.

4.2 Molecular Biological Methods

4.2.1 Preparation and Analysis of DNA from *Drosophilae*

Extraction Buffer	100 mM Tris/HCl (pH 9.0)
	100 mM EDTA
	1% (w/v) SDS

About a hundred fifty anesthetized flies were homogenized in 500 µl extraction buffer with a pestle in a 1.5 ml Eppendorf reaction tube and incubated for 20 minutes at 65°C. After addition of 180 µl of 8 M KAc, the mixture was incubated on ice for 30 minutes and centrifuged twice at 13,000 rpm at 4°C for 15 minutes. The supernatant which contained the genomic DNA was transferred to a new reaction tube which and 0.5 V of isopropanol was added. This mixture was centrifuged for 30 minutes at 13,000 rpm at 4°C. The pellet was washed twice with 70% ethanol, centrifuged and air dried. Finally the genomic DNA was dissolved in 30µl of ddH_2O and stored at -20°C for further experiments.

4.2.2 Preparation of single-Fly DNA **(Gloor et al., 1993)**

Squishing Buffer (SB)	10mM Tris pH 8.2
	1mM EDTA
	25mM NaCl

One single anesthetized fly was homogenized in 50 µl of SB buffer with a pestle in a 1.5 ml Eppendorf reaction tube and 1 µl of Proteinase K (200 µg/ml) was added and mixed gently. The following program was set in the thermocycler: 30 min at 37°C and 2 min at 85°C. Finally the single-fly DNA was stored at -20°C.

4.2.3 Polymerase Chain Reaction (PCR) (Saiki et al., 1988)

For the amplification of specific DNA fragments, polymerase chain reaction (PCR) is used. To amplify the DNA of interest we use synthetically manufactured oligonucleotides. A heat-resistant polymerase binds to the primers and synthesizes the desired DNA fragment. The polymerase chain reaction is carried out in several cycles and thus leads to an exponential amplification of the DNA fragment. The reaction conditions vary with the length of the DNA fragment to be amplified, as well as with the melting temperature of the primers.

Reaction and PCR program using Taq polymerase (Axon)

….. µl Template DNA (10-100 ng)
1 µl Forward Primer (25 pmol/µl)
1 µl Reverse Primer (25 pmol/µl)
1 µl dNTP Mix (10 mM pro dNTP)
5 µl 10x BD Buffer
5 µl $MgCl_2$ (25 mM)
0.5 µl *Taq* DNA Polymerase (5 U/µl)
Make up the volume to 50 µl with ddH_2O

Step	Temperature	Time	C
Initial Denaturation	95°C	5 min	1
Denaturation	95°C	1 min	26-35
Annealing	50-68°C	1 min	
Extension	72°C	1 min/kb	
Final Extension	72°C	10 min	1

Reaction and PCR program using VELOCITY DNA polymerase (Bioline)

….. µl Template DNA (5-500 ng)
1 µl Forward Primer (25 pmol/µl)
1 µl Reverse Primer (25 pmol/µl)
1.5 µl dNTP Mix (10 mM pro dNTP)
5 µl 5x Hi-Fi Buffer
0.5 µl Velocity DNA Polymerase (2 U/µl)

Make up the volume to 50 µl with ddH_2O

Step	Temperature	Time	Repeat
Initial Denaturation	98°C	2 min	1
Denaturation	98°C	30 s	25-35
Annealing	50-68°C	30 s	
Extension	72°C	15-30 s/kb	
Final Extension	72°C	4-10 min	1

After the completion, the reactions are stored at 4°C.

4.2.4 Agarose gel electrophoresis of DNA/RNA (Sambrook, 1989)

TAE (50x)	2 M Tris
	100 mM EDTA, pH 8
	5.71% (v/v) pure acetic acid
MOPS (1x)	20 mM MOPS, pH 7
	1 mM EDTA
	8 mM sodium acetate
Loading Buffer (10x)	0.1 % Bromphenolblue
	0.1 % Xylene Cyanol
	0.9 % Boric acid
	40 % Glycerin
	in TAE or MOPS

Using gel electrophoresis, DNA/RNA fragments can be separated according to their size. The DNA/RNA was detected by the use of ethidium bromide, a dye that intercalates into the DNA/RNA and makes the individual fragments visible under UV light. Agarose was dissolved in 1x TAE (or 1x MOPS gels for RNA) buffer at the appropriate concentration (0.5-2% agarose). The mixture was boiled and cooled to 60°C, then, the ethidium bromide (10 µg/ml) was added. The solution was poured into a horizontal gel chamber stuffed with a comb. Once the gel had solidify, 1x TAE or 1x MOPS was supplied as a running buffer. DNA samples were mix with 1/10 volume of 10x loading buffer. Samples were electrophoresed

between 60 and 100 V. DNA was detected by the means of UV irradiation and the picture was printed out.

4.2.5 DNA extraction from agarose gel

DNA fragments are purified from PCR, as well as from agarose gels using NucleoSpin® Gel and PCR Clean-up Macherey-Nagel Düren, kit according to the given instruction in the manual. The desired DNA band is cut out using a sterile scalpel from the agarose gel and transferred to a 1.5 ml reaction tube. 200 µl NTI buffer is then added for 100 mg gel and completely dissolved in 5-10 minutes at 50°C. Meanwhile, the suspension is vortexed every 2-3 minutes. Then a NucleoSpin Gel and PCR Clean-up column is placed in a receptacle and the suspension is loaded to the column. After a centrifugation for 30 seconds at 11,000 rpm, the collecting vessel is emptied and is washed twice with 700 µl wash buffer NT3 (11,000 rpm for 30 seconds). To completely remove any residual ethanol, it is then followed by a further centrifugation for one minute at 11,000 rpm. The column is placed in a fresh 1.5 ml reaction tube and 20 µl of ddH_2O is added to the column membrane. After incubation of five minutes at 65°C, the mixture is centrifuged (11,000 rpm for 30 seconds). The DNA is stored at 4 °C.

4.2.6 Ligation of PCR products to TOPO® vectors (Invitrogen)

After an incubation of about 5-20 minutes at room temperature (RT), in accordance with the size of the PCR product, the entire ligation mixture is added to 50 µl of competent cells and transformation protocol is followed. According to manual the vector has an ampicillin pCR®II-TOPO®-cassette, and thus is used for the transformation on LB agar plates with ampicillin (1 µg / µl). The vectors PCR®-Blunt II-TOPO® and pENTR ™ / D TOPO® have a kanamycin cassette and the cells are plated on LB agar plates with kanamycin (1 µg / µl). To perform in a 20 µl final volume for 2 hours at RT or overnight at 16°C.

4.2.7 Ligation using T4 Ligase

Before the ligation of an insert to a plasmid, both plasmid and the insert are cut with the appropriate restriction enzymes. For the ligation, the insert is used in a triple or fivefold molar excess. The amount of vector DNA in the ligation mix is about 80 ng on vector quantities of ~ 8 kb and about 100 ng in vector quantities of ~ 10 kb. The ligation is performed in a 20 µl final volume and for 2 hours at RT or overnight at 16 °C.

DNA vector	100 ng
DNA insert	3x and 5x molar amount
10x T4 ligation buffer	2 µl
T4 ligase	1µl
ddH2O	ddH_2O up to 20 µl

4.2.8 Preparation of chemically competent *Escherichia coli* (Sambrook, 1989)

Tfb I	30 mM Potassium acetate 100 mM Rubidium chloride 10 mM Calcium chloride 15% (v/v) Glycerin (sterile) pH of 5.8 (dilute Acetic acid) Autoclaved 50 mM Manganese (II) chloride (Sterilized)
Tfb II	10 mM MOPS 75 mM Calcium chloride 10 mM Rubidium chloride 15% (v/v) Glycerin

pH 6.5 adjust with NaOH

Autoclaved

50 ml of LB medium were inoculated with a colony of *Escherichia coli* DH5α and the culture was incubated overnight in a shaker at 37 °C. In the morning, this culture was diluted back into 500 µl fresh Erlenmeyer flask containing 500 ml Psi broth/LB and the culture was incubated again up to an OD550 of 0.5 to 0.6 at 37 °C. Subsequently, the cells were kept for 15 minutes on ice, then distributed to 50 ml Falcons, and centrifuged for 5 minutes at 3,000 rpm at 4°C. After discarding the supernatant, the cells were suspended in 1/3 volume TfbI and again incubated for 15 minutes on ice. After a further centrifugation (5 minutes, 3,000 rpm, 4 °C), the cells were suspended in 1/12 volume TfbII and incubated for 15 minutes on ice. Lastly, 50 µl cells were aliquoted into Eppendorf tubes and frozen immediately in liquid nitrogen. The *Escherichia coli* DH5a was stored at -80°C for further experiments.

4.2.9 Transformation of chemically competent *Escherichia coli*

The competent cells were taken from -80 °C and kept on ice for 10-15 minutes, then, 10 µl of ligation mixture or 0.5 µl of plasmid DNA (transformation of plasmids) were added to 50 µl chemically competent cells and incubated on ice for 30 minutes. Subsequently, the cells were exposed for 30 seconds to a heat shock at 42°C, and incubated again on ice for 2 minutes. Afterwards, 250 µl warmed LB medium were added to the cells and the mixture was incubated for 45 minutes at 37°C in a shaker. The cells were seeded on LB-agar plates with the appropriate antibiotic and incubated overnight at 37°C. As antibiotics ampicillin (100 µg/ml), chloramphenicol (23 µg/ml) or kanamycin (50 µg/ml) were used.

4.2.10 Plasmid preparation from *E.coli* on an analytical scale (mini-prep) (Birnboim and Doly, 1979)

3 ml of LB medium with the appropriate antibiotic was inoculated with an *E.coli* colony. After an overnight incubation at 37°C in a shaker, 1.5 ml culture was centrifuged (1 min, 13,000 rpm) and the supernatant was discarded. Subsequently, the pellet was suspended in 100 µl E1 to disrupt the cells and afterwards 200 µl E2 were added and the mixture was incubated for five minutes at RT. To neutralize the reaction and protein precipitation 150 µl E3 were added. After centrifugation at 13,000 rpm for 5 minutes, the clear supernatant was transferred to a fresh tube and 320 µl of isopropanol were added. After centrifugation for 30 minutes at 13,000 rpm and 10°C the supernatant was removed. The pelleted plasmid DNA was then washed with 320 µl 70% ethanol (10 minutes, 13,000 rpm, 4°C), air-dried five minutes at room temperature and dissolved in 25 µl distilled water. The plasmid DNA was stored at 4 C. The solutions E1, E2 and E3 were prepared regarding the JETSTAR 2.0 Plasmid Kits manual (Genomed).

4.2.11 Plasmid preparation from *E.coli* in preparative scale (midi-prep) (JETSTAR 2.0 Plasmid Kit, Genomed)

E1	50 mM Tris, pH 8,0 10 mM EDTA 100 µg/ml RNase A	E4	600 mM NaCl 100 mM NaOAc, pH 5,0 (Acetic acid) 0,15% (v/v) Triton X-100
E2	200 mM NaOH 1% (w/v) SDS	E5	800 mM NaCl 100 mM NaOAc, pH 5,0 (Acetic acid)
E3	3,1 M KAc, pH 5,5 (Acetic acid)	E6	125 mM NaCl 100 mM Tris/HCl, pH 8,5

For the preparation of larger and cleaner amounts of plasmid DNA, Jetstar 2.0 Plasmid Kit (Genomed) anion exchange columns were used. First, 50 ml of LB medium with the appropriate antibiotic and 30 µl inoculated culture were incubated overnight at 37°C in a

shaker. The next day, the bacteria culture was dispensed into 50 ml Falcon and centrifuged for 10 minutes (4,000 rpm, RT). The supernatant was discarded and the pellet suspended in 4 ml of E1 buffer. The cells were lysed in 4 ml of E2 buffer, and after inverting several times the mixture was incubated for 5 min at RT. After adding 4 ml of E3 buffer, the mixture was again inverted several times and then centrifuged (6,000 rpm, 10 min, RT). The supernatant containing the plasmid DNA was then loaded onto a Genomed anion exchange column (previously equilibrated with 10 ml of E4 buffer). The plasmid DNA was bound to the matrix of the column and was washed twice with 10 ml of E5 buffer. The elution was then performed using 5 ml of E6 buffer in a 15 ml Falcon. After adding 3.5 ml of isopropanol, the mixture was distributed to four 2 ml reaction tubes. After centrifugation at 13,000 rpm at 4°C for 30 minutes, the plasmid DNA was precipitated and washed with 1 ml 70% ethanol (10 minutes, 13,000 rpm). The pellet was then air-dried for five minutes at room temperature, diluted in 30 µL distilled water and stored at 4°C

4.2.12 DNA restriction with endonucleases

Restriction endonucleases cut double-stranded DNA at specific sequences. The amount of the restriction enzyme needed to cleave the DNA with a particular concentration can be calculated as:

$$\text{Required Units/µg DNA} = \frac{48.5\ \text{kb (bp } \lambda) \times \text{Number of restriction sites in target DNA}}{\text{Size of DNA (bp)} \times \text{Number of restriction sites in } \lambda\text{-DNA}}$$

Restriction endonuclease digestion was performed according to the manual from Fermentas Heidelberg NEB using the enzymes and buffer provided. Reaction buffer was incubated in a final volume of 20 µl for one hour at 37°C. Subsequently, 10 µl of the digestions were applied to an agarose gel and analyzed.

4.2.13 Determination of plasmid DNA concentration

For quantification of DNA, RNA or protein samples the Thermo Scientific NanoDrop 2000 spectrophotometer was used. Nucleic acids can be quantified due to their maximum absorption at the wavelength of λ=260 nm and purified protein at λ=280 nm using the spectrophotometer.

4.3 Preparation and experiments with RNA

4.3.1 RNA isolation from *Drosophilae*, testes and larvae

The isolation of total RNA was carried out with TRIzol® (Invitrogen). For the isolation of RNA, the sample (30 *Drosophila* males, 30 virgin females, 30 larvae or 60 testes) was homogenized in 1 mL TRIzol® (1 ml/50-100 mg tissue) with a homogenizer stick and then incubated at RT for five minutes. This was followed by adding 0.2 ml of chloroform, and after 15 seconds of vigorous shaking, the mixture was again incubated for 3 minutes at RT. By centrifugation at 11,200 rpm, the mixture was separated into a lower red phenol-chloroform phase, an interphase, and a colorless upper aqueous phase. RNA remained exclusively in the aqueous phase. This was transferred to a new reaction tube. To precipitate the RNA 0.5 ml isopropanol was added. Then the mixture was incubated for 10 minutes at RT, centrifuged for 10 minutes (11,200 rpm, 4 °C) and the supernatant was discarded. The RNA pellet was then washed with 1 ml 75% ethanol (8,880 rpm, 5 minutes, 4°C) and air-dried for 10 minutes. The RNA was dissolved in 25 µl of RNase-free water for 10 minutes at 55°C, and stored at -20°C. As control, an aliquot was loaded to a 1.3% MOPS agarose gel or the concentration was measured using the spectrophotometer.

4.3.2 cDNA synthesis

The synthesis of first-strand cDNA was carried out using the Transcriptor First Strand cDNA Synthesis Kit; Roche, Mannheim.

The following conditions describe a first-strand cDNA synthesis preparation:

Transcriptor Reverse Transcriptase Reaction Buffer, 5x conc.	4 µl
Protector RNase Inhibitor, 40 U/l	0.5 µl
Deoxynucleotide Mix, 10 mM each	2 µl
Transcriptor Reverse Transcriptase, 20 U/l	0.5 µl
Random Hexamer Primer, 600 pmol/l	2 µl
DNA-free RNA	1 µg
RNase-free water	up to 20 µl

cDNA synthesis:

10 min	25 °C
30 min	55 °C
Inactivation for 5 min	85 °C

After the PCR the reaction tubes were stored on ice, filled with RNase-free water up to 50 µl of a total volume and stored at -20°C for further experiments.

4.3.3 Reverse Transcription Polymerase Chain Reaction (RT-PCR)

RT-PCRs were carried out with QIAGEN® OneStep RT-PCR Kit, Qiagen.

The reactions were prepared as following:

5x QIAGEN OneStep RT-PCR Buffer	4 µl
Q-Solution	4 µl
dNTP Mix (containing 10 mM of each dNTP)	2 µl
Forward primer	3 µl

Reverse primer	3 µl
QIAGEN OneStep RT-PCR Enzyme Mix	0.8 µl
RNase inhibitor (optional)	0.25 µl
Template RNA	1 pg-2 µg
RNase-free water	up to 20 µl

RT-PCR conditions:

Reverse transcription	30 min 50°C	
Initial PCR activation step	15 min 95°C	
Denaturation	0.5–1 min 94°C	25–40 cycles
Annealing	0.5–1 min 50–68°C	
Extension	1 min 72°C	
Final extension	10 min 72°C	

4.3.4 Quantitative PCR (qPCR)

Total RNA was extracted from 100 testes using TRIzol® (Invitrogen). Subsequently, the total RNA was treated with RQ1 RNase-free DNase (Promega). Thereafter, the RNA digested with 1 µg DNase was used for cDNA synthesis performed with the Transcriptor First Strand cDNA Synthesis Kit (Roche). qPCR was carried out with a Sybrgreen platform on a Bio-Rad CFX Cycler.

The reactions are prepared as follows:

iTaq™ Universal SYBR® Green Supermix (Bio-Rad),	7.5 µl
Diluted cDNA	2 µl
5µM Primer-Mix specific for the target gene	0.3 µl
ddH2O	5.2 µl

PCR conditions were: 95°C for 3 min; 55 cycles at 95°C for 10 s, 60°C for10 s, and 72°C for 30 s. A melting curve was generated to estimate the specificity of the reactions. Two biological replicates were used per sample. The values were normalized to the expression of *Rpl32*. A *t*-test was used to evaluate statistical significance.

4.4 Histological Methodologies

4.4.1 Determination of gene expression patterns using *in situ* hybridization in *Drosophila* testes

The whole-mount RNA *in situ* hybridizations (ISH) were carried out following the protocol (Morris et al., 2009). The protocol consisted on several steps as follow:

Probe Synthesis for *in situ* hybridization

Three µg of plasmid DNA were digested with the corresponding enzymes

Digestion Reaction

Plasmid DNA	3 µg
Enzymes	0.5 µl of each
NEB buffer	2 µl
ddH_2O	up to 20 µl

The mixture was incubated at 37°C for 30 min and then DNA was precipitated with ethanol with 1/10 Volume 3M Sodium acetate and 2.5 volume 96% Ethanol. After a 15 min incubation at -18°C and centrifugation (15 min, 13,000 rpm, 4°C), the pellet was washed with 70% Ethanol for 10 min at 4°C. After centrifugation (5 min, 13,000 rpm, 4°C), the pellet was air-dried for 5-10 min and suspended in 20 µl of sterile-nuclease free water. The probe was loaded in a 1.3% agarose gel for testing

RNA Probe generation for *in situ* hybridization

Linearized vector (DNA) ~100 ng	.... µl
RNA Labeling Mix	2 µl
10x Transcription Buffer	2 µl
Polymerase (T7 or SP6)	1 µl
ddH_2O	up to 20 µl

The reaction was incubated for two hours at 37°C and DNA was precipitated with ethanol with 1/10 Volume 3M Sodium acetate and 2.5 volume 96% Ethanol. After an incubation of 15 min at -18°C and centrifugation (15 min 13,000 rpm 4°C), the pellet is then washed with

70% Ethanol for 10 min at 4°C. After centrifugation (5 min 13,000 rpm 4°C), the pellet is air-dried for 5-10 min and is suspended in 50 µl of RNAse free water to be stored at -20°C. The probes are used in a dilution of 1:50.

Spot test for DIG labeled probes

For quality control of the DIG-labeled RNA probe, a spot test was performed. For this purpose, a dilution series of 1:10, 1:100, 1:1000 and 1:10,000 were prepared with RNase-free water. Then, one µl was spotted on a nylon membrane (Hybond N, Amersham) and covalently cross-linked by UV radiation from each dilution. Subsequently, the membrane was washed one minute in DIG buffer I and blocked for 30 minutes in PBT shaking gentle. Thereafter, the membrane was incubated for 30 minutes in α-DIG-AP-Fab antibody solution (1:5000 in PBT) at RT. This was followed by two washes for 5 minutes in DIG I and a further washing step for two minutes in DIG III. The subsequent staining reaction was performed by adding 2 ml of staining solution (9 µl NBT (100 mg/ml) + 7 µl X-phosphate in 2 ml of DIG III) in darkness. After 5 min, the membrane was removed from darkness and if the spot staining was reached up to 1:1000 dilution, the probes were of good quality of staining so they were stored until use at -20°C.

DIG I Buffer	0.1 M Tris/HCl, pH 7.5 0.15 M NaCl	DIG III	0.1 M Tris/HCl, pH 9.5 0,1 M NaCl 50 mM $MgCl_2$

ISH of RNA probe to *Drosophila* testes

in situ protocol was done in two or three days.

<u>DAY 1</u>

Drosophila testes were dissected in 1x PBS on ice.

<u>Fixation</u>

PBS was removed and 1 ml 3.7% F-PBS (Fresh) was added for fixation during 20 min. After three time washing in PBT (5 min each), digestion was done with Proteinase K up to 90 sec (10 µl Proteinase K (5 mg/ml) + 990 µl PBT). The digestion was stopped by adding 100 µl Glycine (20mg/ml) in 900 µl PBT and incubating for 5 min at RT. After washing twice with

PBT (5 min each), the tissue was fixed again in F-PBS (Fresh) for 20 min and washed twice in PBT afterwards.

Hybridization

Hybridization was started first by washing three times with PBT:HS, from the most concentrated to the more diluted one (3:1, 1:1, 1:3 PBT:HS, 10 min each). Subsequently, after washing three times with HS buffer (5 min each), the testes were transferred to a black block dish and separated equally into two clean reaction tubes. Thereafter, 100 µl of warm HS Buffer was added to each reaction tube and are incubated 1h at 55°C.

-Preparation of the probe-

The probe was diluted in 50 µl of HS buffer (1 µl probe: 50 µl HS), heated at 80°C for 3 min, and stored on ice. After 1h of incubation, the HS buffer was discarded from each reaction tube and 50 µl of probe were added correspondently for overnight (12-16h) incubation at 55°C

Hybridization Solution (HS)	50% Formamide
	5x SSC
	100 µg/ml Heparin
	100 µg/ml Salmon sperm DNA
	0.1% Tween-20

DAY 2

First the probe buffer was discarded from each reaction tube to make a quick wash with warm HS buffer, which was then followed by 15 min washing at 55°C with warm HS buffer. Subsequently, three washing steps were done at 55°C (15 min each) with HS:PBT from the most concentrated to the most diluted (3:1, 1:1, 1:3 HS:PBT). Finally, four washes with warm PBT (5 min each) were done. After the last wash, the reaction tubes were stored at RT and after removing the PBT, Anti-DIG-AP 1:2000 in PBT was added and the samples were incubated for 1 hour at RT or overnight at 4°C. In case of 1 hour incubation at RT, the protocol was followed in order to complete the experiment in 2 days.

DAY 3

Staining

After removing the antibody buffer, a quick wash with PBT was performed, followed by four washes in PBT (20 min each). Subsequently, the testes were washed three times in staining buffer (5 min each) and transferred with the pipette tip to a transparent block dish. Three and a half µl of NBT and 3.5 µl of X-Phosphate were added to 1 ml staining buffer and transferred to each transparent block dish and the reaction was developed in darkness. The incubation time was dependent on the probe. The staining was ended by washing with PBT (2-3 times 5 min each). After washing, the testes were either stored at 4°C for a couple of hours or overnight before mounting.

Staining Solution	0,1 M NaCl 0,1 M Tris, pH 9,5 1 mM Levamisole 0,1% Tween-20 0,05 M $MgCl_2$	EPON	51,5% (v/v) Epon 812 28% (v/v) Epon hardener DDSA 19% (v/v) Epon hardener MNA 1,5% (v/v) Epon accelerator DMP 30

Mounting

Mounting started first by dehydration steps through ethanol series 25% ► 50%► 75%► 100% (5min each). After the last step with 100% ethanol dehydration, the testes were collected by a gentle poke with a cut pipette tip. They were taken all inside of the 20 µl pipette tip and let to accumulate in the tip of the pipette by gravity flow. A little drop of EPON was applied to the microscope slide and the testes were let within a drop. Subsequently, the testes were distributed over the all EPON surface, covered with a coverslip. The slides were incubated at 60°C overnight. The results were analyzed once the slides were cooled.

4.4.2 Immunostaining protocol for testes squash preparations

This protocol is for immunostainings on testes squash preparations modified after (Hime et al., 1996). The protocol can be performed in two days.

DAY 1

Testes were dissected in PBS and transferred onto a small PBS drop on a polylysine coated slide. After covering with a coverslip (18x18 mm) and draining the PBS from the sides of the coverslip, the slide was immediately frozen in liquid nitrogen. Subsequently, the coverslip was flipped off using a razor blade and the slide was transferred in to a staining chamber containing pre cooled 95%ethanol and stored at -20°C until all slides were prepared and incubated for at least 15 minutes. For fixation, 3.7% F-PBS was deposited on each slide and incubated at RT for 7-10 minutes. Thereafter, the slides were washed twice in PBSTD for 15-30 min. later on in PBT for at least 10 min, and finally for 30 min in 3% BSA/PBT (Freshly prepared). After diluting the primary antibody in 3% BSA/PBT, 60 µl of AB dilution was added on each slide which were then covered with a coverslip (24x32 mm) and incubated overnight at 4°C in a humidified chamber.

DAY 2

After removing the coverslips, the slides were washed once for 15 min in PBT/3% BSA which is then followed by adding 60 µl of secondary AB dilution (Diluted in PBT/3% BSA) on each slide incubating for 1.5 hours at RT in humid chamber. Subsequently, the coverslips were removed and the slides were washed again once for 15 min in PBT/3% BSA. In the last step, 60 µl of DAPI (1:200) (Diluted in PBT/3 % BSA) were deposited on each slide, incubated for 20 min at RT in a humid chamber and followed by three washes with PBT/3% BSA. The slides were air-dried partially, embedded in Fluoromount and covered with a coverslip (24x32 mm). The slides were stored at 4°C until analysis at the microscope.

4.4.3 Blocking with immunizing peptide

The necessary amount of antibody was diluted in blocking buffer to the final volume needed for the two experiments. Subsequently, this was equally divided into two tubes. In the first tube (named blocked), the blocking peptide was added to a final concentration of 1 µg/ml. In the second tube (named control), an equivalent amount of buffer was added. Both tubes were incubated with agitation, at RT for 30 minutes, or at 4°C overnight.

The staining protocol was performed on the two identical samples, using the blocked antibody for one and the control for the other. The staining that disappears when using the blocked antibody was specific to the antibody.

4.4.4 Decondensation of *Drosophila* spermatids

Prior to fixation, squashed seminal vesicles were treated with 10 mmol/L DTT, 0.2% Triton X-100 and 400 U of heparin in ddH_2O, for 20-30 min (modified after Li et al., 2008, personal communication Dr. David Miller, Leeds, Hundertmark and Theofel, submitted manuscript). The slides were then washed quickly in PBS and fixated with 3.7% F-PBS at RT for 7 minutes. The immunofluorescence staining was carried out essentially as described in the chapter 4.4.2.

4.5 Preparation and experiments with proteins

4.5.1 Protein extraction from *Drosophila* testes and seminal vesicles

20 testes or 80 seminal vesicles were dissected in 1x PBS on ice. Dissected testes or seminal vesicles were homogenized in 20 µl 2×SDS sample buffer by pipetting a few times up and down, followed by sonication for 30 min in an ultrasonic bath at 4°C room. After this step samples can be stores at 4°C until loading or until needed. Before loading incubate the sample tubes for 10 min at 37°C. Load the whole sample into an SDS-Gel.

4.5.2 Western blot Analysis **(Bio-Rad)**

10x Tank blot buffer	25 mM Tris/HCl, pH 8.3 129 mM glycine

20% (v/v) Methanol (in addition 1x buffer)

10x TBS	20 mM Tris/HCl, pH 7.7 140 mM NaCl	TBSTT	1x TBS 0.05% Tween-20 0.2% Triton X-100

Staining Solution	Methanol 40% (v/v) Acetic acid 10% (v/v) Coomassie Brillant Blue 0.05% (w/v)	Destaining solution	Methanol 40% (v/v) Acetic acid 10% (v/v)

Western blots were performed using standard methods. The protocol was completed in two or three days. Gel percentage selection was dependent on the size of the protein of interest. A 4-20% gradient gel separates proteins of all sizes very well.

DAY 1

Proteins separation by gel electrophoresis

Load equal amounts of protein (20 µl) into the wells of a mini (8.6x6.7 cm) or midi (13.3x8.7 cm) format SDS-PAGE gel, along with molecular weight markers. Run the gel at first at 100 volts. Increase the voltage to 130-150 volts to finish to run the gel in about 1-2 hours. After using the SDS gel electrophoresis, the proteins were separated, the gel apparatus was opened, and the gel was washed for 10 minutes in 1x tank blot buffer on a swivel.

Transferring the proteins from the gel to the membrane

Subsequently, the blot can be assembled. For this, first 6 Whatman papers and nitrocellulose membrane were cut to the size of the gel. The 6 Whatman papers as well as two sponges were immersed in tank blot buffer and the membrane was moistened with ddH_2O. The blotting apparatus was assembled according to the following scheme, and run overnight at 30 volts or at 100 volts for about 2 hours at 4°C.

- Pol
Sponge
3 Whatman papers
Gel
Nitrocellulose membrane

3 Whatman papers
Sponge
+ Pole

DAY 2

Antibody incubation

The next day, the apparatus was dismantled and the membrane was washed for 10 minutes in 1x TBS. To check the efficiency of the transfer, the separation gel can be stained with Coomassie and then pivoted to destaining, which can be recognized by distinct protein bands. In order to saturate unspecific binding sites on the membrane, the membrane was blocked for about one hour in 5% milk powder/TBS. Subsequently, the nitrocellulose membrane was incubated with the primary antibody (diluted in 5% milk powder/TBS) overnight at 4°C.

DAY 3

The next day, the membrane was washed twice with TBSTT and once with TBS (each 10 min), followed by one hour incubation at RT with the peroxidase-coupled secondary antibody (diluted in 5% milk powder/TBS). After incubation, four washes with TBSTT (each 10 min) were necessary.

Imaging and data analysis

For the subsequent reaction, the chemiluminescent substrate was applied to the blot according to the manufacturer's recommendation (ECL-ECL Novex® Chemiluminescent Reagent Kit, Invitrogen). Novex® ECL Chemiluminescent Substrate Reagent Kit is a two-part reagent consisting of a luminol and an enhancer for the detection of horse radish peroxidase. Reagent A and Reagent B were mixed in equal volumes before application to the blot. The peroxidase coupled to the secondary antibody catalyzes a chemiluminescent reaction of the reagent mixture, which was visualized with a chemiluminescence Sensitive film.

4.6 Experimental approaches to separate head and tail from *Drosophila* sperm

For methods described in this section double transgenic flies *dj-eGFP,Prot-B-DsRed* with dual sperm color were used (Köttgen et al., 2011). Dj-eGFP was expressed in sperm tail in green and Prot-B-DsRed was expressed in sperm head in red, allowing to differentiate head and tail under the microscope.

4.6.1 Sonication of *Drosophila* sperm

Two to three hundred seminal vesicles were dissected in 1x PBS, sperms were taken out of the seminal vesicles and stored in 1x PBS on ice. After dissection, in order to get rid of contaminants, the reaction tube was shortly centrifuged and the sperm pellet was then resolved with fresh PBS. To prevent heating of the biological material, the sample was sonicated in the corresponding conditions always on ice (different power outputs (10-70%) using the same length of sonication with a series of short pulses (2x15s, 15s intervals)). To see the efficiency of sonication, a small amount of the sample was analyzed under the microscope. After this step the samples were stored at 4°C until next experiment.

4.6.2 Percoll and sucrose gradient ultracentrifugation

Sperm cells were dissected from 200-300 seminal vesicles in ice-cold PBS and sonicated as explained in section 4.6.1. After confirming the separation of tail and head under the microscope, the sample was centrifuged (10 minutes, 5,000 rpm, 4°C). While centrifugation the gradients were prepared in 2 ml reaction tubes. The supernatant was discarded and the pellet dissolved in 550 µl or 350 µl PBS (correspondingly for Percoll and sucrose gradient).

Percoll Gradient

Different Percoll gradients concentration were prepared using DMEM (mammalian cell culture medium), therefore the gradient was easily visible due to the presence of phenol red. The gradient was prepared as shown below adding 500 µl of each to the reaction tube, bottom: 90%, middle: 70%, top: 40% (500 µl each).

Preparation of different Percoll gradients concentrations:

Bottom 90% > 150 µl DMEM+ 1350 µl Percoll
Middle 70% > 450 µl DMEM+ 1050 µl Percoll
Top 40% > 900 µl DMEM+ 600 µl Percoll

Sucrose Gradient

Different sucrose gradients concentration were prepared using sterile water. The step gradient was prepared as shown below adding 500 µl of each to the reaction tube:

300 µl 60% sucrose
300 µl 70% sucrose
300 µl 75% sucrose

The sample was applied on the top of the gradient (500 µl to Percoll gradient and 300 µl to sucrose gradient), and ultracentrifuged (30 minutes, 6,000g, 4°C).

4.6.3 Chemical treatment of *Drosophila* sperm

Treatment of *Drosophila* sperm with Dibucaine-HCl

Dissected sperms from 10 seminal vesicles in 500 µl freshly prepared 25 mM Dibucaine-HCl were pipetted up and down for 2 min. A small amount from the sample was then analyzed under the microscope.

Treatment of *Drosophila* sperm with Nocodazole

Dissected sperms from 150-200 seminal vesicles was sonicated as described in Section 4.6.1. The sample was then incubated for 24 hours at 24°C with 10 μM Nocodazole – a microtubule destabilize microtubules - in a rocker. After incubation and in order to remove nocodazole sample was washed twice with Schneider's *Drosophila* medium. Finally, the sample was centrifuged (2 minutes, 13,000 rpm, 7 °C), dissolved in 500 μl Schneider's *Drosophila* medium.

5 Results

5.1 Functional analysis of Prtl99C during spermiogenesis

Drosophila protamines (ProtA and ProtB) are not essential for male fertility (Rathke et al., 2010). However, it is very likely that sperm of protamine-deficient flies still contain proteins that perform functions similar to that of protamines. Therefore, our lab used transcriptome data (Flybase) to identify and study further sperm chromatin relevant genes. In the search for transition proteins, the expression pattern of CG15510-eGFP revealed that the protein was present in the mature sperm (Rathke PhD Thesis, 2007; Rathke et al., 2007). This expression pattern was verified and correlated to the stages of spermatogenesis, Histone and Tpl94D expression (Figure 4). The fusion gene is expressed after histone removal and overlaps with Tpl94D expression in agreement with Rathke PhD Thesis, 2007. Thus CG15510 is as a new promising candidate gene for encoding for a protein of sperm chromatin. Due to its male specific transcript and its chromosomal localization, we named this gene *Protamine like 99C (Prtl99C)*.

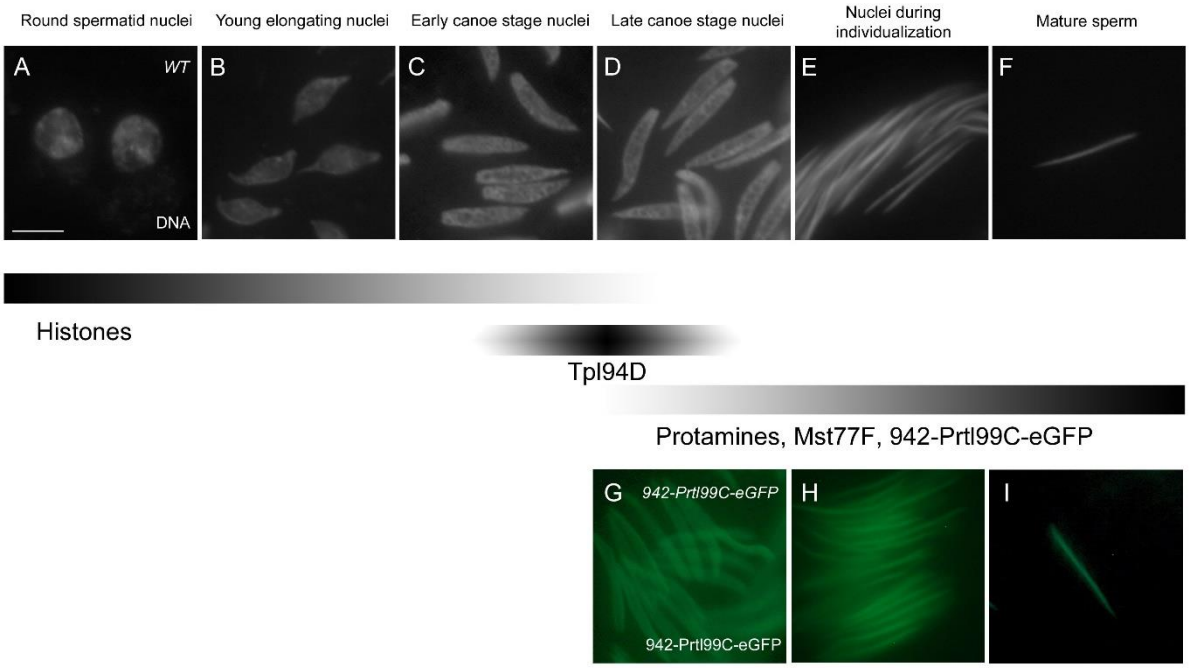

Figure 4 Overview of *Drosophila* spermiogenesis and expression pattern of 942-Prtl99C-eGFP. (A-F) Different stages of post-meiotic spermatid nuclei stained with Hoechst to visualize DNA. The scheme below displays some of the identified chromatin components which are expressed during spermiogenesis. (G-I) 942-Prtl99C-eGFP (CG15510-eGFP) expression in nuclei of late canoe stage spermatids, spermatid nuclei during individualization and nuclei of mature sperm. In agreement with Christina Rathke, PhD Thesis 2007.

CG15510-eGFP fusion gene with the presumptive promoter and 5' UTR of 942 bp upstream of the start codon, was named afterwards *942-Prtl99C-eGFP*. During this work, I concentrated on the function of Prtl99C and the importance of more potential protamine-like proteins in *Drosophila*.

5.1.1 Prtl99C as a candidate for sperm protein of *Drosophila*

Prtl99C, which codes for an HMG-box protein, is specifically transcribed in the testes (Chintapalli et al., 2007). Apart from the HMG-box domain, the predicted gene contains a nuclear localization signal (NLS) in the N-terminal and a central low complexity region (c-LCR) (Figure 5A-B).

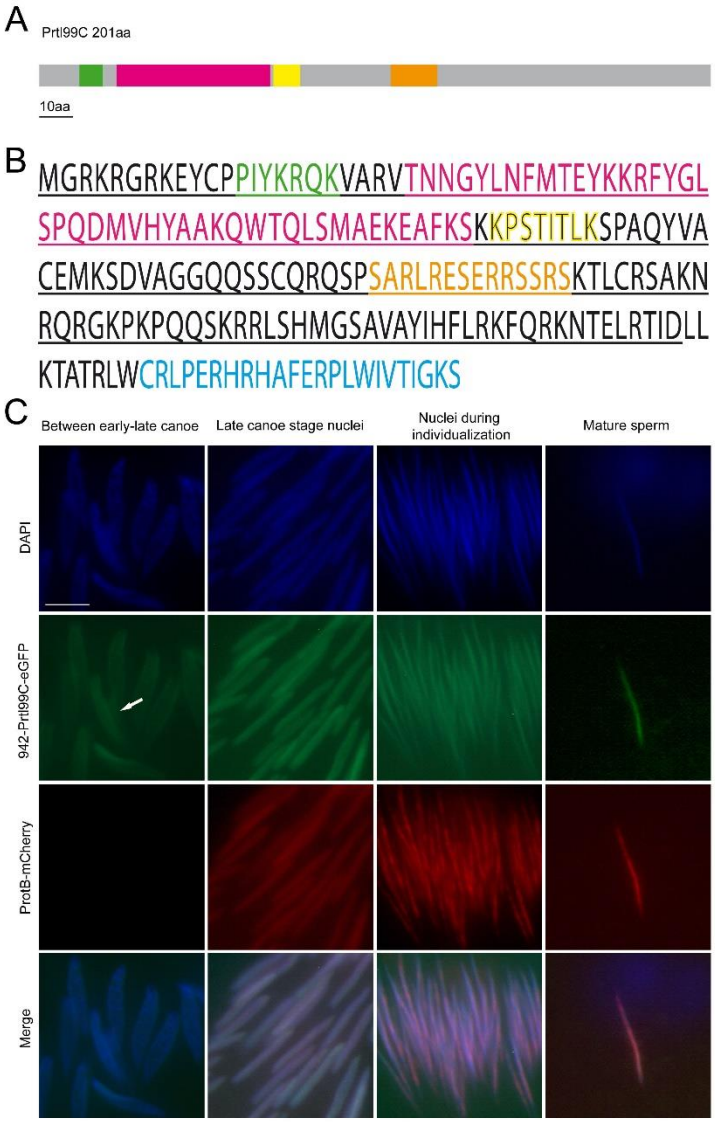

Figure 5 Prtl99C encodes a highly basic protein (A) Schematic overview of the full-length Prtl99C protein. NLS, green (aa 12–19); HMG-box, pink (aa 23–69); eight internal amino acids, yellow found in isoform Prtl99C-PD that are lacking in isoform Prtl99C-PC (aa 69–77). c-LCR, orange (aa 105–119) (B) Primary structure of protein Prtl99C with nuclear localization signal (NLS; green letters), high mobility group (HMG-box; pink letters), eight amino acids (yellow letters) which differs between isoforms PD and PC, and central low complexity region (c-LCR; orange letters). Prtl99C antibody was raised against a peptide derived from the C-terminus (blue letters). The maintained sequence of the protein Prtl99C (aa 1–150) in Prtl99C-ΔC mutant is underlined. (C) First row: Dapi staining to visualize DNA in double transgenic flies expressing 942-Prtl99C-eGFP and ProtB-mCherry to compare their expression patterns. Second row: Expression of 942-Prtl99C-eGFP starts between the early and late canoe stages before protamines are expressed (arrow) and remains in mature sperm. Third row: ProtB-mCherry expression starts at the late canoe stage and remains in mature sperm. Fourth row: Merged photo of fluorescence images. Bar, 5 μm.

The biochemical properties of Prtl99C are similar to many other known chromatin components of *Drosophila* sperm. However, sequence similarities to mammalian proteins were not found. Due to the abundance of arginine (12.4%) and lysine (11.0%) residues, the Prtl99C protein is basic (predicted pI of 11.48). Prtl99C also contains five cysteines (2.5%) (Figure 5B) and has a predicted molecular mass of 23.6 kDa (Flybase).

Prtl99C is present at cytological position 99C2-3, on chromosome arm 3R and is predicted to encode three transcripts (St Pierre et al., 2014) (http://flybase.org/) which one of them -*Prtl99C-RC*- is predicted to differ by eight internal amino acids (Figure 5A-B, yellow letters).

The fusion protein 942-Prtl99C-eGFP showed a post-meiotic expression pattern similar to protamines (Figure 4, 5C). The 942-Prtl99C-eGFP expression started first at the late canoe stage, shortly before protamines appeared (Figure 5C, arrow) and remained in mature sperm (Figure 5C). Prtl99C is therefore likely a component of sperm chromatin.

5.1.2 *Prtl99C* encodes a protein of the sperm chromatin

5.1.2.1 *Prtl99C* is transcribed in the male germ line from the primary spermatocyte stage onward

To determine if Prtl99C is indeed testis specifically expressed, I conducted reverse transcription polymerase chain reactions (RT-PCR) with primers detecting all transcripts using RNA from larvae (mixture of males and females), adult females, carcass (males without reproductive tract) and adult testes. *β3-tubulin* was used as a positive control. *Prtl99C* mRNA was expressed in larvae and adult testes, but not in females or carcass (Figure 6A). These results showed that *Prtl99C* is testis-specifically transcribed.

Furthermore, *in situ* hybridizations were performed using a *Prtl99C*-specific antisense probe to detect the cellular and subcellular distribution of *Prtl99C* mRNA within *Drosophila* testes. Rich distribution of *Prtl99C* transcripts was observed from early spermatocytes until late spermatids. However, the hub region and seminal vesicles were free of staining (Figure 6B). The 5’ UTR, coding region and the 3’ UTR of all predicted transcripts are highly

identical with the exception that an additional 5' exon is predicted for *Prtl99C-RB*, which would lead to a longer 5' UTR (Figure 6C). Therefore, in order to clarify if all the predicted transcripts were transcribed in testes several RT-PCRs with specific primers to each isoform were performed.

Firstly, RT-PCR using primers within the exons of predicted 5' UTR region of the RB transcript (St Pierre et al., 2014) showed that the predicted transcript *Prtl99C-RB* does not exist. Secondly, sequencing results of the RT-PCRs products gave evidence for the existence of *Prtl99C-RD* that differs in length by eight internal amino acids (predicted protein difference depicted in Figure 5B, yellow letters). However, we do not know if *Prtl99C-RC* is transcribed at low levels and was underrepresented in sequencing.

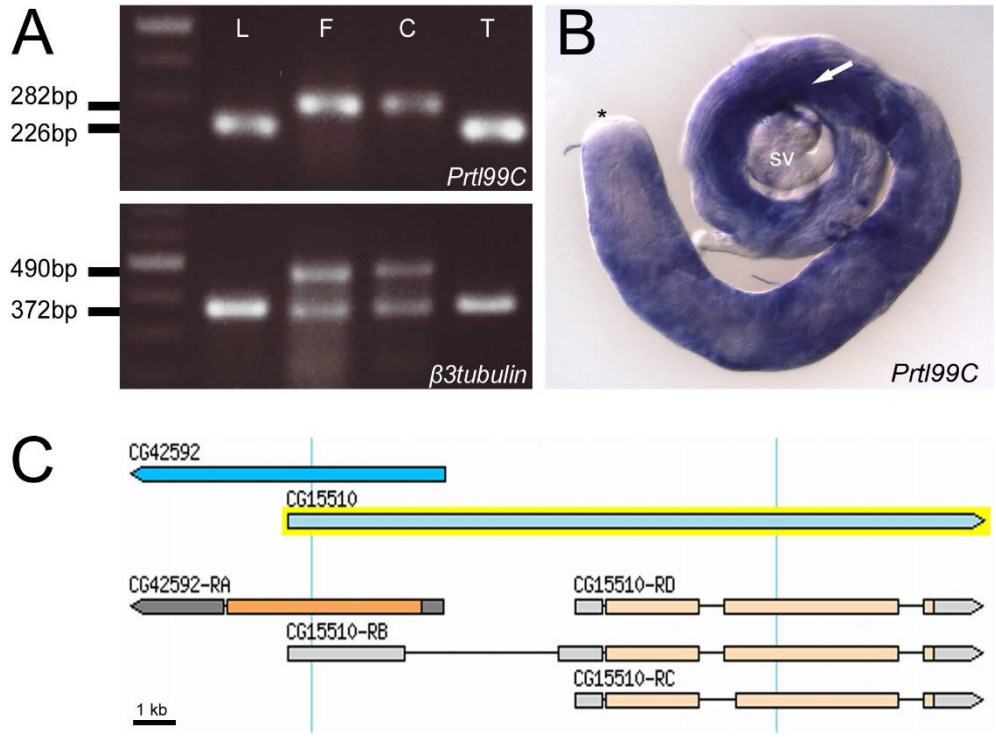

Figure 6 Male specific *Prtl99C* is transcribed during spermatogenesis and encodes for isoform *Prtl99C-RD* (*CG15510-RD*) (A) RT-PCR of *Prtl99C* from wild-type larvae (L), adult virgin females (F), carcass males (C) and adult testes (T). Upper photo, *Prtl99C*-specific primers; lower photo, *β3-tubulin*-specific primers as control. The *Prtl99C*-specific primers amplified a 226-bp cDNA fragment from the open reading frame of *Prtl99C* in adult testes and in larvae but not in carcass males or in adult females. In carcass males and in adult females a 282-bp DNA fragment was amplified from genomic DNA contamination of the RNA, as primers flank a small intron of 56-bp. Lower photo, Aa 372-bp cDNA fragment of the *β3-tubulin* gene was amplified as control. The cDNA *β3-tubulin* fragment was visible in all samples, whereas DNA contamination shown by a 490-bp fragment was visible only in carcass males and adult females. Marker: 2-Log DNA Ladder (NEB). (B) *in situ* hybridization of testis with an RNA probe specific for *Prtl99C* transcripts (dark staining). Arrow, post-meiotic stage in spermatids; *, hub region; and sv, seminal vesicles. (C) Schematic representation of the genomic region of *Prtl99C* (*CG15510*) and the predicted isoforms: *Prtl99C-RB*, *Prtl99C-RC*, *Prtl99C-RD*. Photo captured from http://flybase.org/.

5.1.2.2 Prtl99C is expressed during spermiogenesis

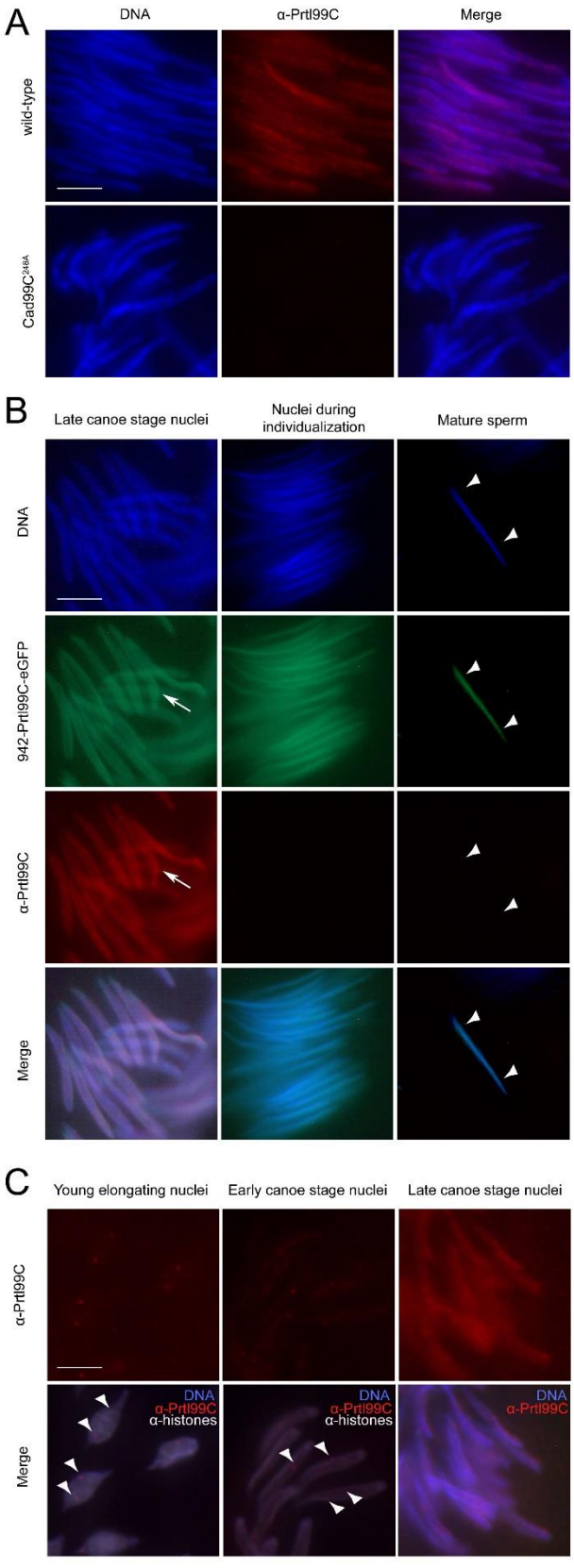

To analyze the expression pattern of the endogenous Prtl99C protein we decided to raise a suitable antibody. Anti-Prtl99C was raised in rabbit against a C terminal peptide (aa 179 to aa 201) and the affinity-purified antibody was applied in a dilution of 1:500 (Pineda Antibody-Service; http://www.pineda-abservice.de) (Fig. 5B, blue letters).

To check the specificity of anti-Prtl99C antibody in immunofluorescence, I first performed immunostainings using anti-Prtl99C antibody on wild-type testes and on a Prtl99C deficiency (homozygous mutant *Cad99C*^{248A}, see Figure 9 for chromosomal situation).

Figure 7 Anti-Prtl99C detects Prtl99C at late canoe stage. (A) Anti-Prtl99C is specific for Prtl99C. First column: Hoechst staining to visualize chromatin of squashed spermatid nuclei from testes of wild-type flies and the Prtl99C deficiency mutant homozygous *Cad99C*^{248A}. Second column: Anti-Prtl99C staining. Prtl99C was detected in late canoe stage of wild-type testes but not in homozygous *Cad99C*^{248A} testes. Third column: Merged photo of fluorescence images. (B) Anti-Prtl99C antibody staining of testes from transgenic flies expressing 942-Prtl99C-eGFP. First row: Visualization of DNA via Hoechst staining. Second row: 942-Prtl99C-eGFP expression. Third row: Endogenous Prtl99C detected with anti-Prtl99C antibody. Fourth row: Merged photo of fluorescence images. All rows: arrows, expression at late canoe stage; arrowheads, expression in mature sperm. (C) Anti-Prtl99C (First row) and anti-histones antibody staining of testes from wild-type flies. Second row: Merged photo of fluorescence images (anti-Prtl99C+anti-histones and Hoechst (DNA)), arrowheads, and expression of Prtl99C in small dots in histone positive spermatids. Red: Prtl99C, white: histones, blue: DNA. Bar, 5 µm.

Anti-Prtl99C detected nothing at late canoe stage of homozygous *Cad99C*^{248A} mutant testes, demonstrating its specificity in immunofluorescence (Figure 7A). By immunostaining testes from flies expressing 942-Prtl99C-eGFP, the localization of the endogenous Prtl99C and the transgenic protein, 942-Prtl99C-eGFP could be compared.

Surprisingly anti-Prtl99C showed the appearance of Prtl99C, specifically at the late canoe stage (Figure 7B, arrow), and moreover, Prtl99C was not detectable in the nuclei of spermatids during individualization nor in nuclei of mature sperm like 942-Prtl99C-eGFP (Figure 7B, arrowheads). These observations indicated that Prtl99C might not be accessible to the antibody when the chromatin is more compacted.

Furthermore, double immunostaining of anti-Prtl99C together with anti-histones revealed that endogenous Prtl99C started to be expressed in small dots already from the young elongation stage (Figure 7C, arrowheads). These histone positive spermatids showed a very faint anti-Prtl99C staining. The expression of Prtl99C was increasing while the majority of the histones were being removed and showed the intense expression at late canoe stage (Figure 7C).

5.1.2.3 Prtl99C is expressed in mature sperm nuclei

In consideration of the different results obtained by 942-Prtl99C-eGFP fusion protein and the anti-Prtl99C antibody, we checked the specificity of the antibody biochemically. Western blotting (WB) demonstrated that a Prtl99C protein of 25 kDa (predicted approx. 23kDa, Flybase) is detectable in protein extracts from both, testes and seminal vesicles of wild-type flies. This proved that the protein persists in mature sperm (Figure 8A, arrow). In addition, the Prtl99C protein was not detectable in protein extracts from homozygous *Cad99C*^{248A} mutants (Figure 8A). An anti-Actin antibody, which bound to the 45-kDa β-Actin protein, was used as a positive control in all samples. The protein extracts were prepared at the same time under the same conditions. However, occasionally a non-specific band appeared in WB of testes or seminal vesicles as a protein source at about 28 kDa (Figure 8A, asterisks).

Moreover, to determine if the WB band was specific, an immunizing peptide blocking experiment was performed. The anti-Prtl99C antibody was neutralized by incubating with Prtl99C peptide that corresponds to the epitope recognized by the antibody. As a result, no band was seen with the blocked antibody in WB (Figure 8B).

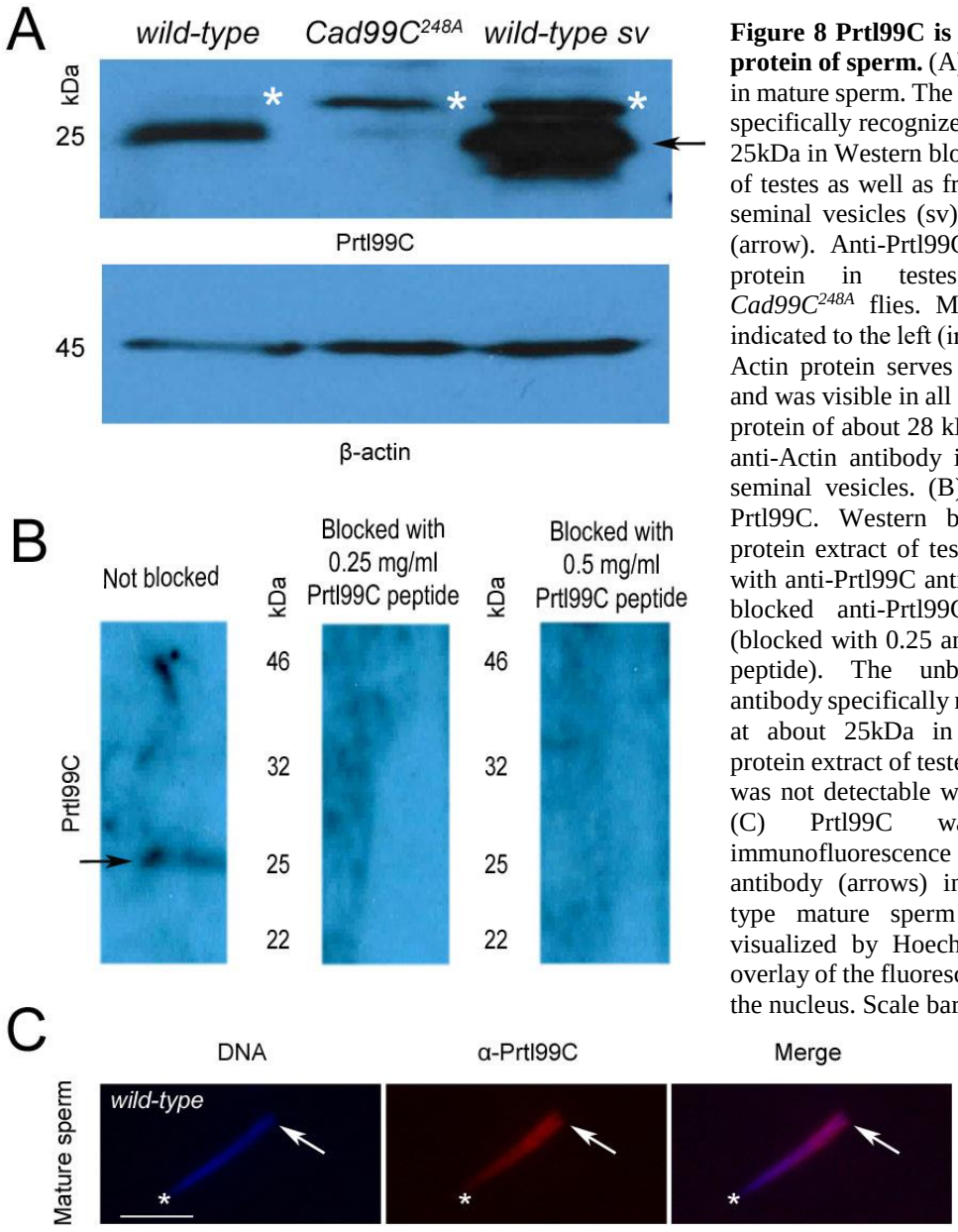

Figure 8 Prtl99C is a new chromosomal protein of sperm. (A) Prtl99C is expressed in mature sperm. The anti-Prtl99C antibody specifically recognized the protein at about 25kDa in Western blot from protein extract of testes as well as from protein extract of seminal vesicles (sv) from wild-type flies (arrow). Anti-Prtl99C did not detect the protein in testes of homozygous *Cad99C*^{248A} flies. Molecular weights are indicated to the left (in kDa). The 45 kDa β-Actin protein serves as a loading control and was visible in all extracts. *, unspecific protein of about 28 kDa. Lower row panel: anti-Actin antibody in Western blots. sv, seminal vesicles. (B) Specificity of anti-Prtl99C. Western blot performed from protein extract of testes of wild-type flies with anti-Prtl99C antibody in parallel with blocked anti-Prtl99C with its peptide (blocked with 0.25 and 0.5 mg/ml Prtl99C peptide). The unblocked anti-Prtl99C antibody specifically recognized the protein at about 25kDa in Western blot from protein extract of testes whereas the protein was not detectable with blocked-antibody. (C) Prtl99C was detected via immunofluorescence with anti-Prtl99C antibody (arrows) in decondensed wild-type mature sperm nuclei. DNA was visualized by Hoechst staining. Merged: overlay of the fluorescence images. *, tip of the nucleus. Scale bar: 5 µm.

Sometimes, due to high compaction of the chromatin at the late spermiogenesis the antibodies cannot gain access in cytological preparations (Tirmarche et al., 2014). In order to visualize the localization of Prtl99C in mature sperm, I used decondensation protocol (Hundertmark and Theofel, submitted manuscript) to decondense sperm from wild-type seminal vesicles and stain them with anti-Prtl99C antibody. Indeed, the expression of Prtl99C was seen in a

large region of the nucleus (Figure 8C). The protein seemed to accumulate towards the flagella, nevertheless as the chromatin is artificially opened, it is not correct to correlate this cellular localization with its endogenous pattern. (Figure 8C, arrow). Encouraged by these results, we conclude that Prtl99C is a chromatin component of the mature sperm.

5.1.3 Prtl99C is essential for male fertility

5.1.3.1 Deletion of Prtl99C and three neighboring genes leads to male sterility

In order to investigate whether Prtl99C is essential for male fertility in *Drosophila,* further genetic analyses were performed. To elucidate the function of Prtl99C, we first analyzed an existing mutant, $Cad99C^{248A}$ (Schlichting et al., 2006). The allele $Cad99C^{248A}$ is a deletion mutant which removes besides *Prtl99C*, *Cad99C*, *Atg16* and the predicted gene *CG42592* (Figure 9A). Male and female flies carrying this deletion in a homozygous situation are viable (Schlichting et al., 2006) but males are infertile (Table S1). Indeed, we observed rarely motile sperm in the seminal vesicles of homozygous $Cad99C^{248A}$ males (Figure 9B, f).

Whole mount testis squash preparations of homozygous $Cad99C^{248A}$ males demonstrated normal germ cell development until late stages of spermiogenesis (Figure 9B, a-d). Starting from the individualization stage, wild type appearing cysts (not shown) and cysts containing disorganized spermatid bundles with abnormal nuclei were observed indicating a distortion in late post-meiotic stages (Figure 9B, e). In these disorganized spermatid cysts, long coiled spermatid nuclei were observed (Figure 9B, e; arrow and arrowhead). Despite this, the few mature sperm which got into the seminal vesicles also displayed abnormal nuclear morphology (Figure 9B, f). A part of this, the sperm nuclei had a coiled looking structure (Figure 16, column 5 arrow) or appeared too long (Figure 16, column 6) and even hooked like (Figure 9B, f).

Following elongation and nuclear shaping, spermatids become individualized by a process called individualization. Individualization complex composed of 64 aligned actin cones are formed during this process and can be visualized by phalloidin staining (Fabrizio et al., 1998). As the phenotype started to appear during individualization, we checked whether

the individualization cones are formed properly. In homozygous *Cad99C*^{248A} mutants, investment cones were formed and individualization complexes were observed (Figure 9C). These results suggested that the sterility was not caused by a defect in the initiation of spermatid individualization.

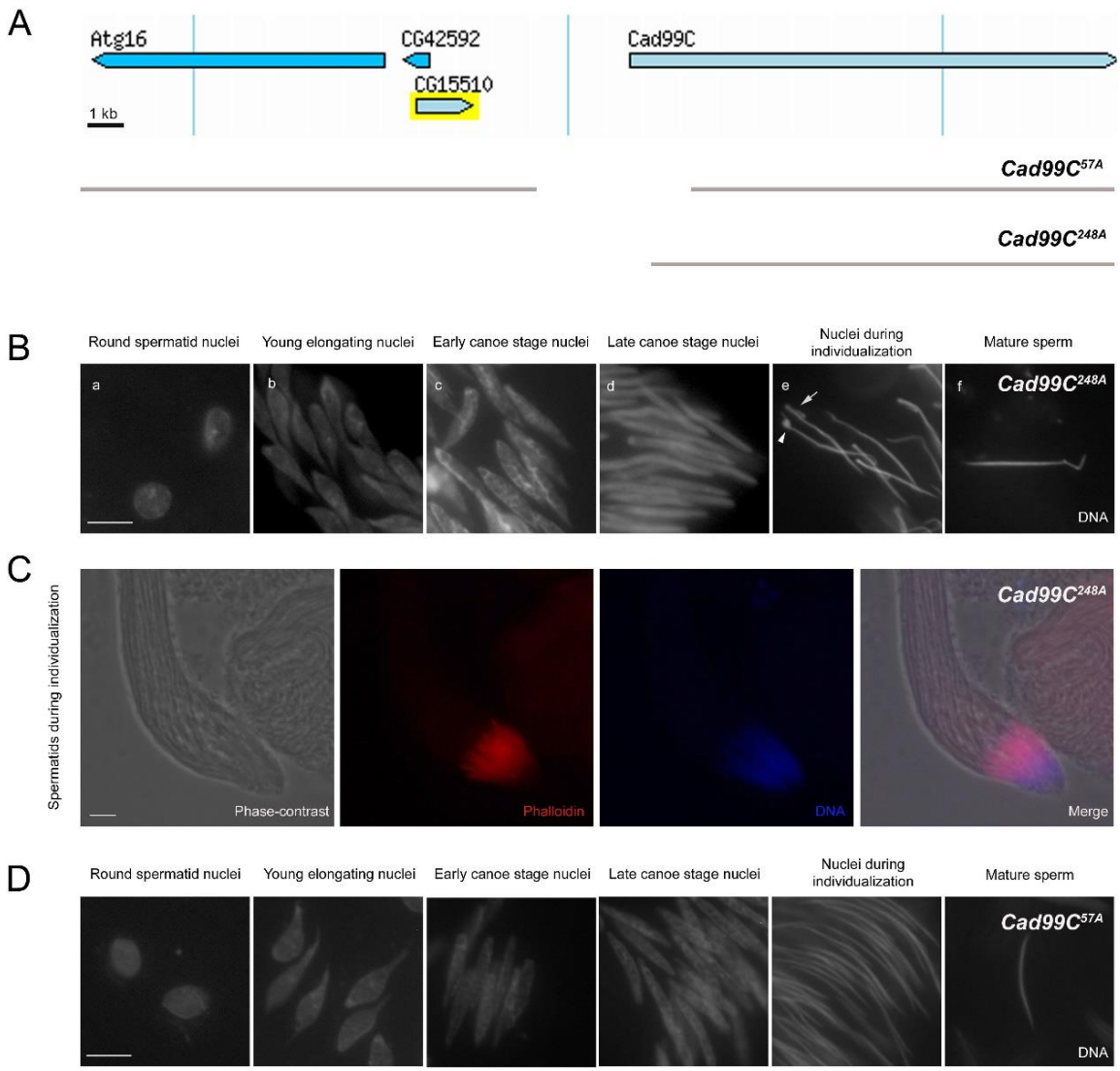

Figure 9 Spermiogenesis of *Cad99C*^{248A} and *Cad99C*^{57A} mutants (A) Schematic representation of the genomic region of *Prtl99C* (CG15510) and three neighboring genes: *Atg16*, *CG42592* and *Cad99C*. Photo captured from http://flybase.org/. The extent of the *Cad99C*^{248A} and *Cad99C*^{57A} deletions in *Cad99C* mutant alleles are presented below (grey lines) as described in Schlichting et al., 2006. (B) Spermiogenesis was normal up to individualization stage in homozygous *Cad99C*^{248A} mutants. (a–f) Hoechst staining of squashed spermatid nuclei from testes of homozygous *Cad99C*^{248A}. (e) Disorganized cysts during individualization stage (arrow) with abnormal nuclei showing a knob-like structure (arrowhead). (f) Rarely found mature sperm in seminal vesicles were longer than wild type nuclei and displayed abnormal hooked like morphology. (C) Individualization cones were formed properly in homozygous *Cad99C*^{248A} flies. Squash preparations of *Cad99C*^{248A} mutant testes stained with Hoechst and Phalloidin to visualize DNA or F-actin. Actin cones were formed and individualization complexes were observed in *Cad99C*^{248A} mutant flies. (D) Hoechst staining of squashed spermatid nuclei from testes of homozygous *Cad99C*^{57A}. Spermiogenesis was normal *Cad99C*^{57A} mutants. Scale bars: 5 µm.

To evaluate if the deletion of *Cad99C* is responsible for spermatogenesis defects, we analyzed homozygous $Cad99C^{57A}$ (Schlichting et al., 2005) mutant flies which are solely null for Cad99C protein (Figure 9A). Whole mount testis squash preparations of $Cad99C^{57A}$ males demonstrated normal spermiogenesis (Figure 9D). Moreover, analysis of $Cad99C^{57A/248A}$ showed normal spermiogenesis and their seminal vesicles were full of motile sperm (data not shown). All these results indicated that Cad99C apparently is not required for male fertility.

5.1.3.2 Transcription of the three neighboring genes and their potential contribution to sterility

5.1.3.2.1 In contrast to *Cad99C*; *Atg16*, *CG42592* and *Mst99C* are transcribed in testes

To determine if the neighboring genes of *Prtl99C* are transcribed in testes and clarify the genes that may contribute to $Cad99C^{248A}$ phenotype, RT-PCRs using mRNA from adult testes were performed. Specific primers for each gene were designed to amplify a cDNA fragment from the open reading frame of *Atg16*, *CG42592*, *Prtl99C* and *Cad99C*. In FlyAtlas: the *Drosophila* gene expression atlas, genes *Atg16* and *CG42592*, but not *Cad99C* are transcribed in adult testis at low levels (Chintapalli et al., 2007).

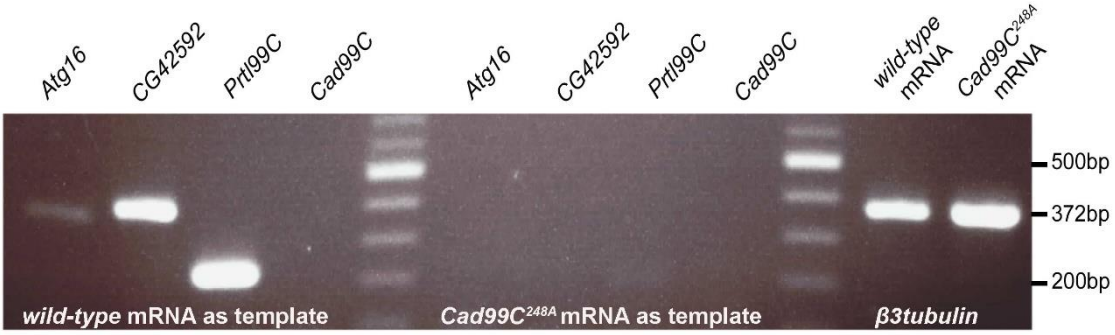

Figure 10 Neighboring genes of *Prtl99C: CG42592* and *Atg16* but not *Cad99C* are transcribed in testes. RT-PCR was performed to detect transcripts. *Prtl99C*'s neighboring genes *CG42592* and *Atg16* but not *Cad99C* were transcribed in wild-type testes. Whereas in homozygous $Cad99C^{248A}$, *Prtl99C* and its three neighboring genes were not transcribed showing the specificity of the RT-PCR. Amplification of *β3-tubulin* mRNA as control.

The RT-PCR results showed that except *Cad99C* all the other neighboring genes have transcripts in adult testis, which make them all potential candidates to cause or contribute to sterility (Figure 10). Thus, in agreement with the previous chapter and with the microarray

expression data from different dissected tissues of adult flies (FlyBase), we stated that genes others than *Cad99C* are likely responsible for male sterility in the *Cad99C*^{248A} deletion.

5.1.3.2.2 P-element insertions to *Atg16* do not affect spermiogenesis

One of the other neighboring genes, *Autophagy-specific gene 16 (Atg16)* encodes a protein required for Atg8a lipidation (Pircs et al., 2012), therefore, we did not expect *Atg16* to play a role in spermiogenesis. Nevertheless, we performed further investigation to clarify if *Atg16* affects fertility. The minos insertion, *Mi{MIC}Atg16*^{MI00187}, is located in the open reading frame (ORF) 6750 bps after the translation start site and leads to an stop codon in the C-terminal region (Figure 11A). According to RT-PCRs, a stable *Atg16-ΔC* transcript was transcribed (data not shown). Homozygous males showed normal spermiogenesis and motile sperm in their seminal vesicles (Figure 11B). Nevertheless, we cannot exclude that a partially functional protein was synthesized and stable. Moreover the P-element insertion, *P{EP}Atg16*^{G5082}, in the 5' untranslated region of *Atg16* (Figure 11A) led to the same result (data not shown), making it very likely that *Atg16* does not have an essential role in spermatogenesis.

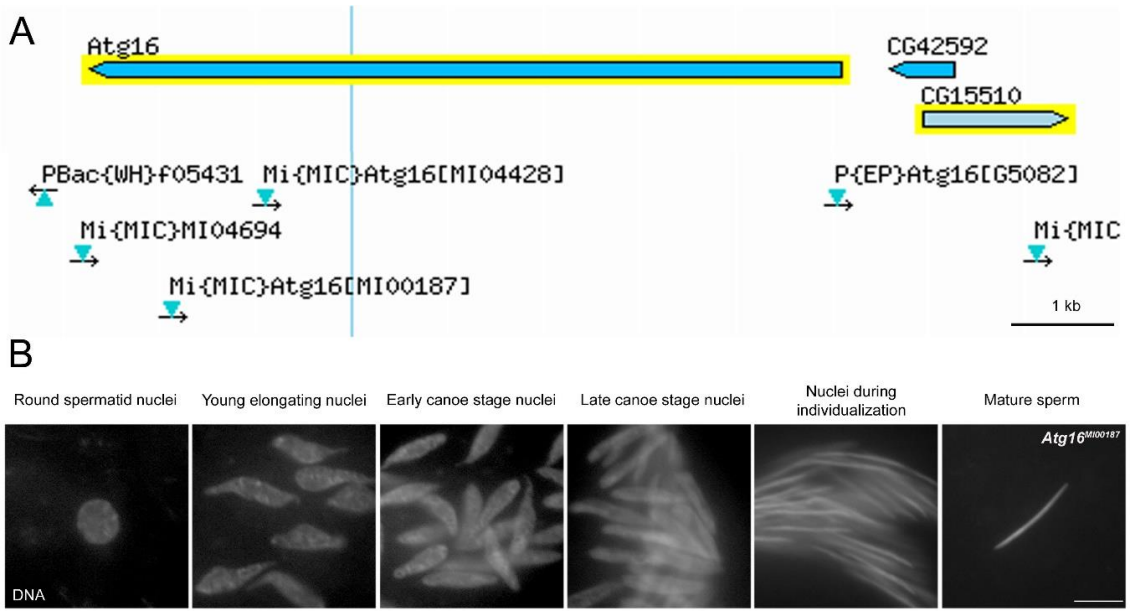

Figure 11 Atg16 does not play a role during spermiogenesis (A) Schematic representation of the genomic region of *Atg16* and its neighboring genes: *Prtl99C (CG15510)* and *CG42592*. Triangles indicates available P-element and Mi-element insertion fly lines. Photo captured from http://flybase.org/. (B) Hoechst staining of squashed spermatid nuclei from testes of homozygous *Atg16*^{MI00187} revealed that spermiogenesis is as in wild type. Scale bar: 5 µm.

5.1.3.2.3 CG42592 is expressed in cytoplasm of spermatocytes and during meiotic divisions

CG42592 is a newly annotated gene in FlyBase and no information is available in the literature. *CG42592* gene locus is mapped to 99C2-2 in the 3R chromosome. With the predicted molecular mass of 15.7 kDa and a pI of 6.75 (Chintapalli et al., 2007), CG42592 is predicted to have 4 transmembrane domains (Figure 12A) (http://smart.embl-heidelberg.de/).

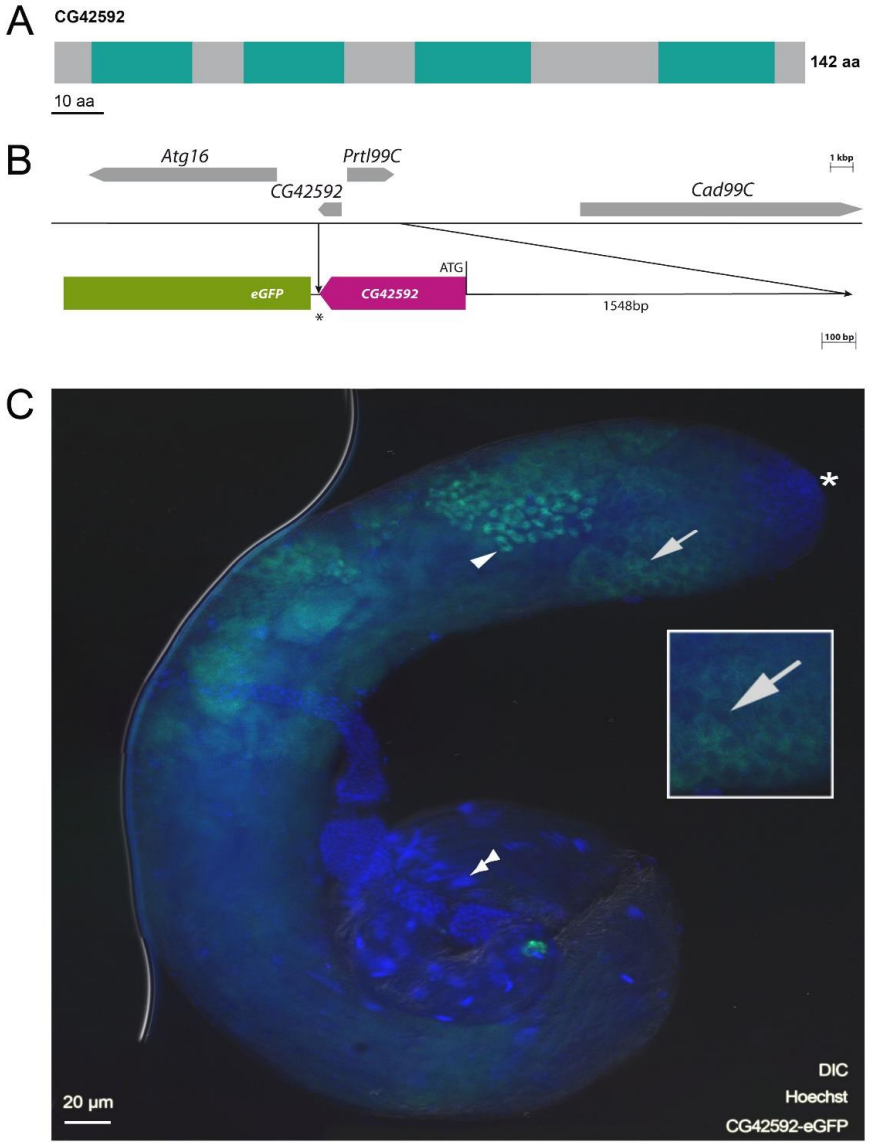

Figure 12 CG42592 is only expressed in the cytoplasm of spermatocytes. (A) Schematic overview of the full-length CG42592 protein. The four transmembrane domains are indicated with green color (aa 7–26, 36–55, 68–90, 114–136). (B) Schematic drawing of the *eGFP* fusion gene constructs used for analysis of expression pattern of CG42592. (C) Whole mount of *CG42592-eGFP* testis stained with Hoechst, showing CG42592-eGFP expression. The insert shows the high magnification to visualize the cytoplasmic expression of CG42592-eGFP. Arrow, cytoplasm of spermatocytes; arrowhead, meiotic division; double arrowhead, elongating spermatid; and *, tip of the testis.

CG42592 was transcribed in testes as shown in Section 5.1.3.2.1. In accordance to these data, this gene likely encodes an integral membrane protein in testis. Nevertheless, to observe the cellular localization of the protein, we generated a transgenic fly line expressing CG42592-eGFP fusion protein under control of its own gene regulatory region (Figure 12B).

CG42592-eGFP was expressed only in the cytoplasm of the spermatocytes and during meiotic division (Figure 12C, arrow and arrowhead). There was neither signal in the nuclei before meiosis nor at the late stages of development (Figure 12C, double arrowhead). Therefore, CG42592 unlikely has a function related to the chromatin.

5.1.3.3 Prtl99C rescues the sterility of *Cad99C^{248A}* mutants

5.1.3.3.1 *942-Prtl99C-eGFP* in *Cad99C^{248A}* mutant background

In order to clarify if Prtl99C could rescue the sterility and the phenotype of *Cad99C^{248A}*, transgenic flies carrying *942-Prtl99C-eGFP* on the second chromosome were used for rescue crossings. The introduction of only one copy of *942-Prtl99C-eGFP* in *Cad99^{C248A}* mutant background was able to rescue spermiogenesis defects and male sterility (Figure 13A).

We rarely observed motile sperm in the seminal vesicles of homozygous *Cad99C^{248A}* (Figure 13C compare to wild type 13B). In contrast, the seminal vesicles of rescued flies were filled with motile sperms (Figure 13D).

These data confirmed that *Atg16* and *Cad99C* are not essential for male fertility. Therefore, we concluded that the *Prtl99C* genomic region is required for male fertility. Besides *Prtl99C,* this region contains *CG42592*, which is predicted to be transcribed from the opposite strand of *Prtl99C* (Chintapalli et al., 2007), thus *CG42592* was included in our rescue construct and might contribute to the rescue capability of *942-Prtl99C-eGFP*.

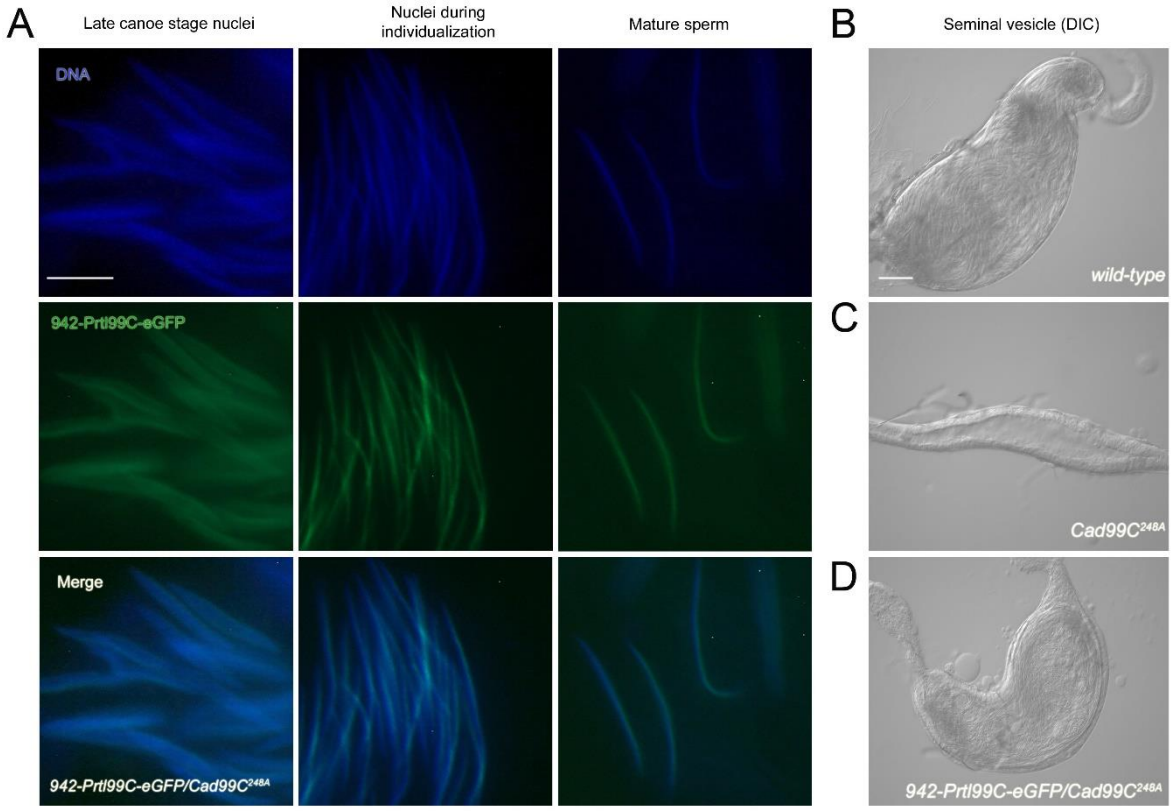

Figure 13 942-Prtl99C-eGFP rescues sterility of *Cad99C^{248A}* males. (A) Squash preparation of *Cad99C^{248A}* testis expressing 942-Prtl99C-eGFP. First row: stained with Hoechst to visualize DNA. Second row: 942-Prtl99C-eGFP expression. Third row: Merged photo of fluorescence images. Spermatid nuclei as well as mature sperm nuclei appeared wild type. (B–D) DIC images of seminal vesicles of three-day-old males. (B) Wild type, (C) *Cad99C^{248A}* and (D) *Cad99C^{248A}* males expressing 942-Prtl99C-eGFP.

5.1.3.3.2 *386-Prtl99C-eGFP* in *Cad99C^{248A}* mutant background

As *CG42592* was still not annotated while generating *942-Prtl99C-eGFP* (Rathke, 2007), the presumptive promoter region of *Prtl99C* was taken and *CG42592* was also present in that construct (see PhD thesis Rathke, 2007 for the generation of *942-Prtl99C-eGFP*). In order to clarify that the capability of the rescue with *942-Prtl99C-eGFP* was due to *Prtl99C* and not to *CG42592*, I generated a corresponding *eGFP* fusion gene for *Prtl99C* excluding completely the sequence of *CG42592* from the 5'upstream sequence of *Prtl99C* by taking only 386 bp in front of ATG, therefore, we named it *386-Protamine like 99C-eGFP (386-Prtl99C-eGFP)* (Figure 14A and see Supplemental Information for generation of the transgenic construct).

I introduced *386-Prtl99C-eGFP* in the homozygous *Cad99C*^{248A} mutant background. The expression of one or two copies of *386-Prtl99C-eGFP* in the homozygous *Cad99C*^{248A} mutant background was able to rescue male sterility (Table S1). In contrast to Cad99C^{248A} (Figure 14C), the seminal vesicles of rescued flies were filled with motile sperms (Figure 14D) like in wild type (Figure 14B). Spermatid nuclei as well as the shape of mature sperm nuclei appeared wild type (Figure 14E).

This rescue experiment showed clearly that CG42592 is not required for male fertility. Accordingly, we conclude that Prtl99C is essential for male fertility.

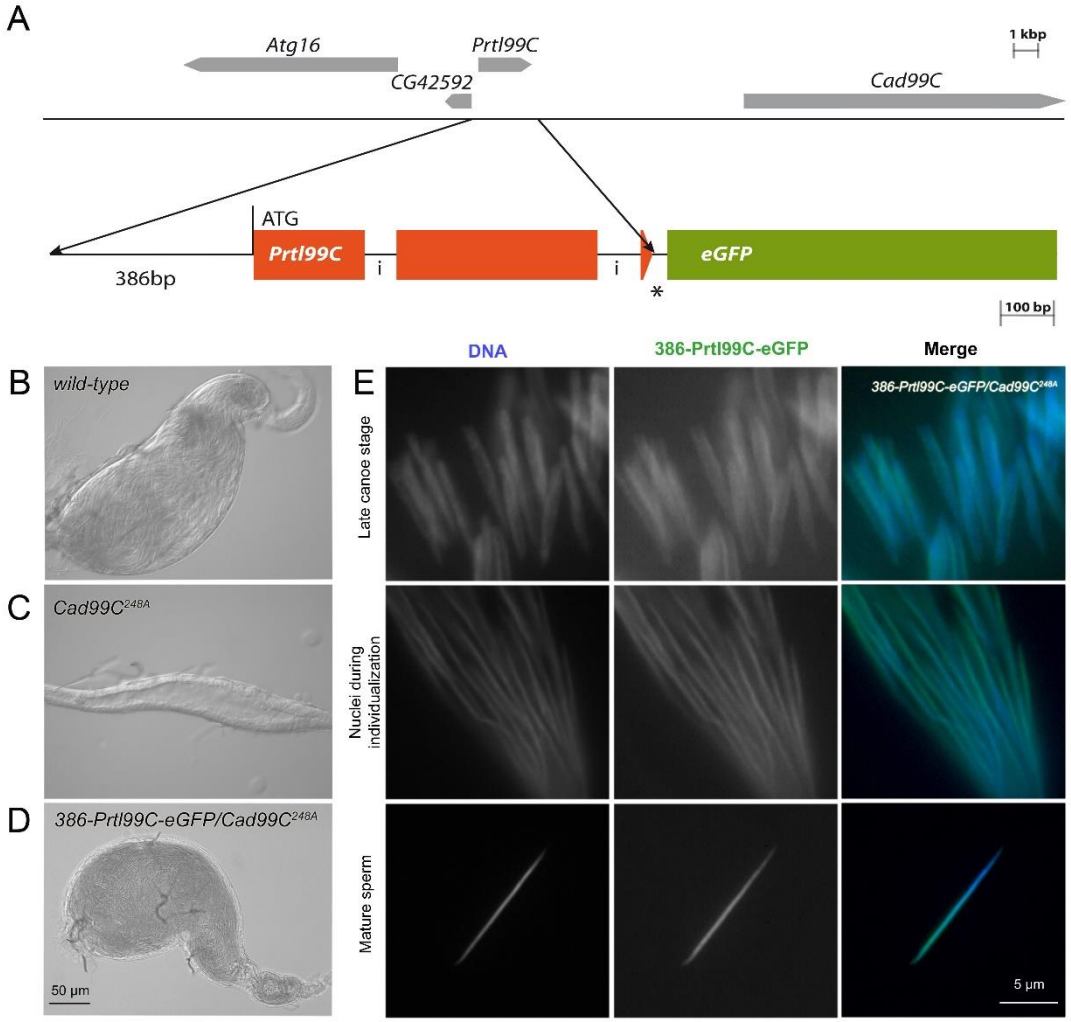

Figure 14 386-Prtl99C-eGFP rescues sterility of *Cad99C*^{248A} males. (A) Schematic drawing of *Cad99C*^{248A} region and the *386-Prtl99C-eGFP* fusion gene used for rescue experiments. i: intron, * : multiple cloning site in frame with *Prtl99C* and *eGFP*. (B–D) DIC images of seminal vesicles of three-day-old males. (B) Wild type, (C) *Cad99C*^{248A} and (D) *Cad99C*^{248A} males expressing 386-Prtl99C-eGFP. (E) Squash preparation of homozygous *Cad99C*^{248A} testis expressing 386-Prtl99C-eGFP. Hoechst staining to visualize nuclei. Spermatid nuclei as well as mature sperm nuclei appeared wild type.

5.1.4 Different *Prtl99C* mutants cause elongation of the chromatin region in sperm

5.1.4.1 Knockdown of *Prtl99C* by RNA interference (RNAi)

Silencing gene expression by RNA interference (RNAi) is a dynamic tool to complement classical mutagenesis and to evaluate single gene mutants in *Drosophila melanogaster* (Jonchere and Bennett, 2013). To approach the solely function of *Prtl99C* with another method, we analyzed RNAi-mediated knockdown of *Prtl99C* with binary UAS/GAL4 system to target dsRNA expression in different cell types or stages of development (for a review, see Southall and Brand, 2008).

For RNAi against *Prtl99C*, KK line (v106856) from the Vienna *Drosophila* Resource Centre was used (Dietzl et al., 2007). The expression was driven from spermatogonia to early spermatocyte stage using *bam-Gal4* driver line. *bam-Gal4* (Bam-Gal4/Bam-Gal4, Sp/CyO, Bam-Gal4/MKRS) female virgins were crossed with homozygous RNAi transgenic males at 30°C (Caporilli et al., 2013; Chen and McKearin, 2003). Both, undriven *Prtl99C*^{RNAi} (*v106856*) and *bam-Gal4* fly stocks were viable at 30°C and showed no defect in spermatogenesis (data not shown). For that reason, we considered them as controls for our RNAi experiments. The RNAi hairpin construct used to generate v106856 had no off-targets and *Prtl99C* was described as the only on-target (see Supplemental Information for the target sequence Dietzl et al., 2007).

5.1.4.1.1 The level of *Prtl99C* transcripts was strongly diminished in *Prtl99C* knockdown testes

We first checked the efficiency of the knockdown by performing *in situ* hybridizations on *wild type* and *bam-Gal4>Prtl99C*^{RNAi} testes using specific *Prtl99C* antisense probe to check the transcript level (Figure 15A). In contrast to *wild type* testes (Figure 15A, arrow), *Prtl99C* transcripts were not detectable from early spermatocytes onward in *bam-Gal4>Prtl99C*^{RNAi} testes (Figure 15A).

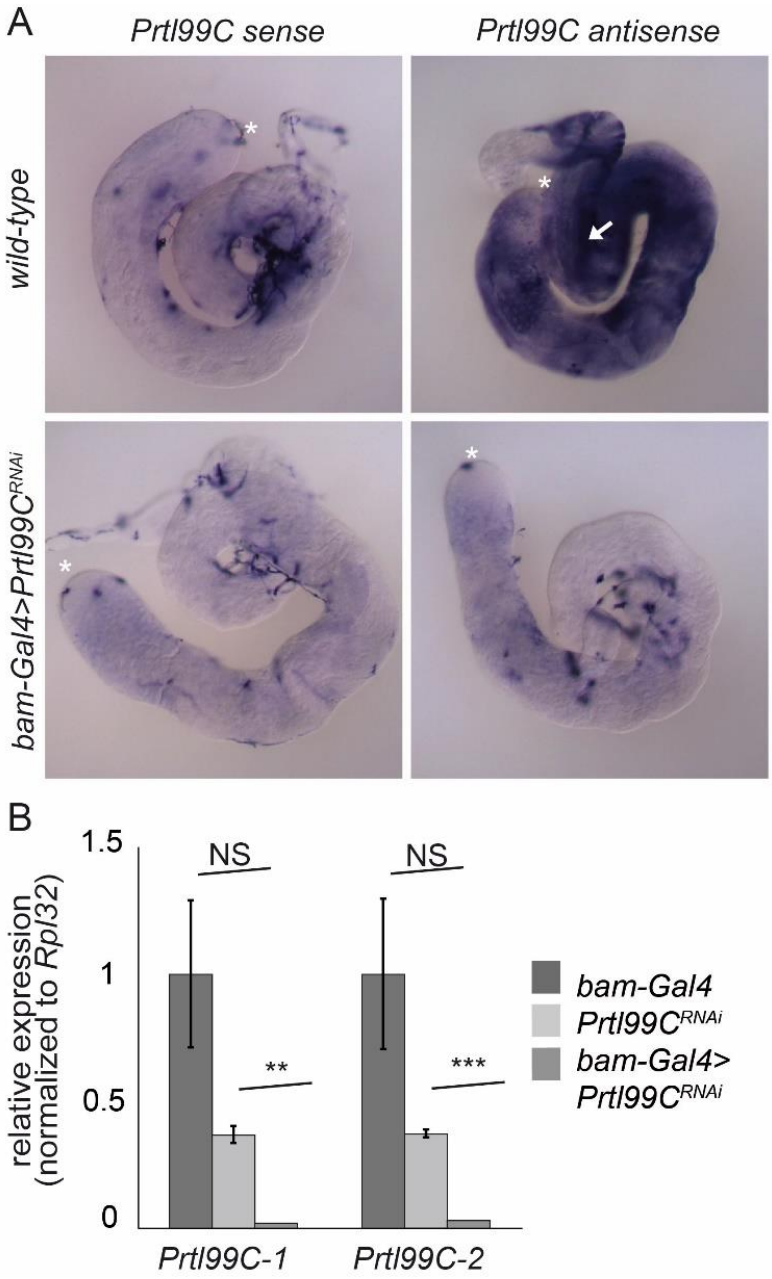

Figure 15 Prtl99C transcripts were strongly diminished in *bam-Gal4>Prtl99C*^{RNAi} testes compared to controls.

(A) *In situ* hybridization of wild type and *bam-Gal4>Prtl99C*^{RNAi} testes with an RNA probe specific for *Prtl99C* transcripts (dark staining). Arrow, post-meiotic stage ; *, hub region. (B) Quantitative PCR (qPCR) using cDNA of *bam-Gal4*, *Prtl99C*^{RNAi}, and *bam-Gal4>Prtl99C*^{RNAi} testes with two different *Prtl99C* specific primer pairs: Prtl99C-1 (RTpcrMst99C-Fw and Mst99C-qRv) and Prtl99C-2 (Mst99C-qFw and CG15510-ISH-Rv). Transcript level of Prtl99C was significantly reduced in *Prtl99C* knockdown situation in comparison to both controls. P-values for significance: ** $p \leq 0.01$ and *** $p \leq 0.001$; NS, not significant.

Furthermore, to see the reduction quantitatively, we checked the level of *Prtl99C* transcripts by quantitative PCR (qPCR). cDNAs from *bam-Gal4*, *Prtl99C*^{RNAi}, and *bam-Gal4>Prtl99C*^{RNAi} were used as template with two different primer pairs specific for *Prtl99C*. We normalized the values to the expression of the housekeeping gene *Rpl32* as an internal control. Indeed, *Prtl99C* transcripts were strongly decreased in *bam-Gal4>Prtl99C*^{RNAi} testes compared to controls of the individual strains (Figure 15B, in collaboration with MSc Ina Theofel). Together, these results showed a high efficiency of the knockdown on *Prtl99C* transcript level.

5.1.4.1.2 The Prtl99C protein was not detectable in *Prtl99C* RNAi mediated knockdown

In order to check if down-regulation of *Prtl99C* via RNAi altered the levels of Prtl99C protein, protein extracts from *bam-Gal4*, *Prtl99C*^{RNAi} and *bam-Gal4>Prtl99C*^{RNAi} testes were analyzed by Western blotting with anti-Prtl99C antibody. An anti-Actin antibody, which recognizes the 45 kDa β-Actin protein, was used as a loading control in all samples.

In conclusion, in contrast to controls (*bam-Gal4* and *Prtl99C*^{RNAi}), the Prtl99C protein of about 25 kDa was not detectable in *bam-Gal4>Prtl99C*^{RNAi} protein extract indicating a very efficient *Prtl99C* knockdown by RNAi (Figure 16).

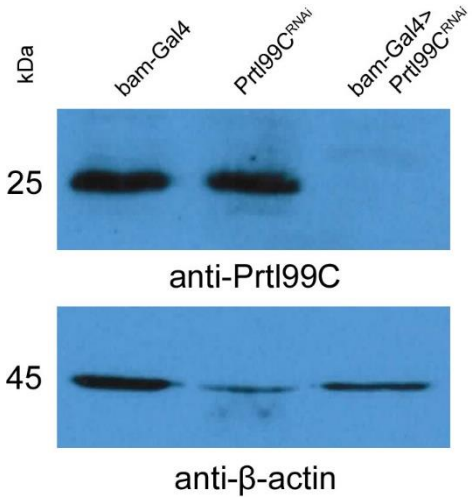

Figure 16 Prtl99C protein was not detectable in *bam-Gal4>Prtl99C*^{RNAi} testes. Western blots using protein extracts from *bam-Gal4*, *Prtl99C*^{RNAi}, and *bam-Gal4>Prtl99C*^{RNAi} testes. Upper row: anti-Prtl99C antibody; lower row: control anti-Actin antibody.

5.1.4.1.3 *bam-Gal4>Prtl99C*^{RNAi} sperm nuclei have a longer chromatin region compared to wild type

After confirming the knockdown efficiency, we analyzed the *bam-Gal4>Prtl99C*^{RNAi} flies in detail. First, we checked the fertility of these males. Interestingly, *bam-Gal4>Prtl99C*^{RNAi} males were nearly sterile (Table S1), however, while looking under the phase-contrast microscope I could see few motile sperm coming out of the seminal vesicles (data not shown). Furthermore, histological examination of *bam-Gal4>Prtl99C*^{RNAi} flies revealed that spermiogenesis was relatively normal (data not shown), nevertheless, the length

of mature sperm nuclei was affected. In order to look at more *bam-Gal4>Prtl99C*^{RNAi} sperm and compare with controls, I stained squashed seminal vesicles of *wild type*, *Prtl99C*^{RNAi} (from 30°C) and *bam-Gal4>Prtl99C*^{RNAi} (from 30°C) with Hoechst and anti-Mst77F antibody.

The protein Mst77F expression is restricted to post-meiotic male germ cells. Anti-Mst77F marks distinct chromatin regions within mature sperm nuclei (Rathke et al., 2010). As Anti-Mst77F works better than anti-protamines antibody in immunofluoresence, I chose anti-Mst77F in combination with Hoechst to visualize the mature sperm nuclei.

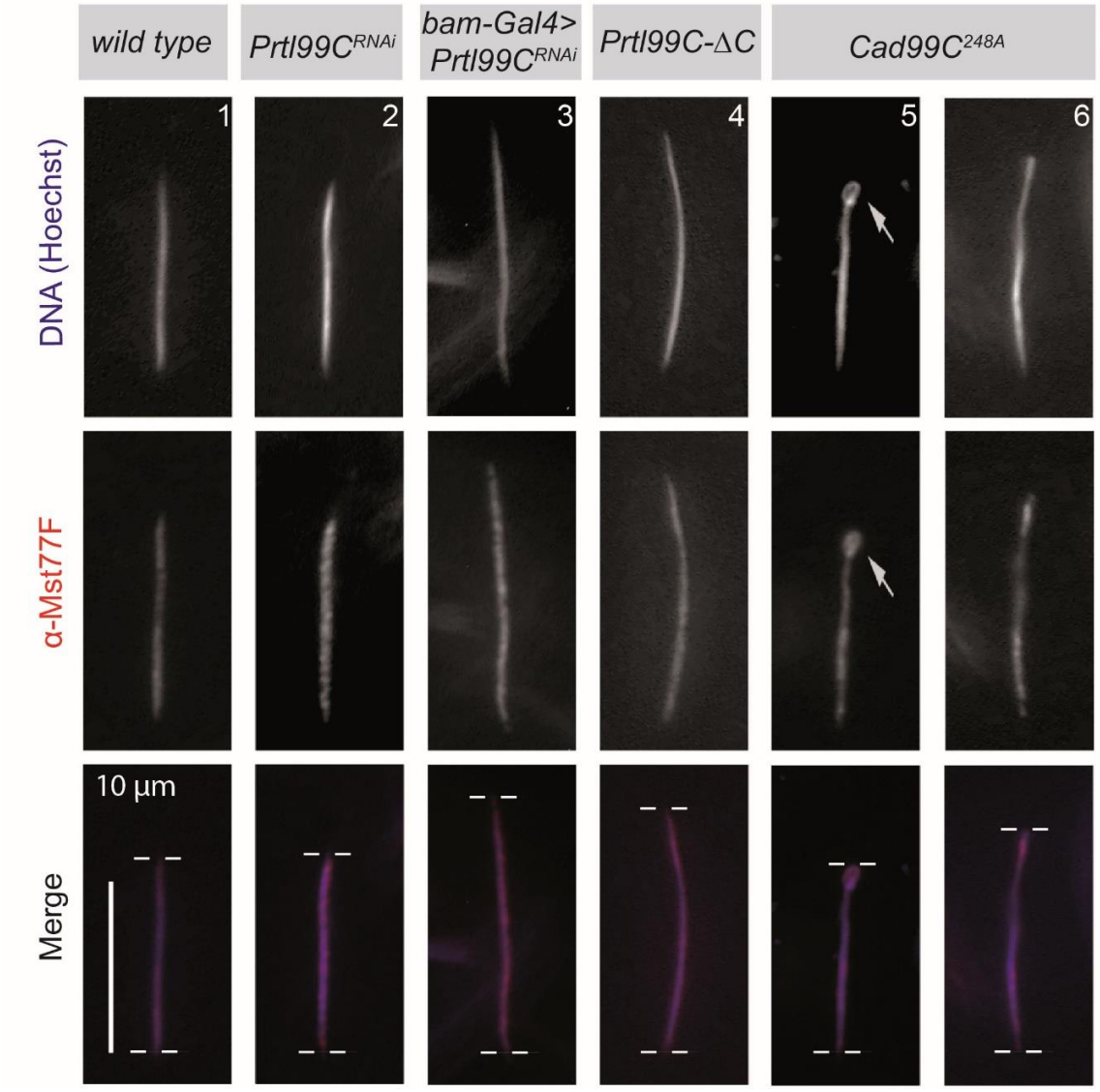

Figure 17 Defects in *Prtl99C* result in extended length of the chromatin area of sperm heads. Individual sperm heads from squashed preparations of *Drosophila* seminal vesicles from *wild type* (column 1), *Prtl99C*^{RNAi} control at 30 °C (column 2), *bam-Gal4>Prtl99C*^{RNAi} (column 3), *Prtl99C-ΔC* mutant (column 4), and *Cad99C*^{248A} mutant flies (columns 5, 6). Row 1: DNA stained with Hoechst dye labeling DNA. Row 2: Detection of Mst77F using anti-Mst77F antibody. Row 3: Merge: overlay of the fluorescence images; dashes indicate the ends of the DNA region in the nuclei. Arrows, coiled or hooked nuclei.

Intriguingly, *bam-Gal4>Prtl99C*^{RNAi} flies had extended chromatin region (Figure 17A, column 3) compared to non-driven *Prtl99C*^{RNAi} at 30°C (Figure 17A, column 2) and to wild type (Figure 17A, column 1). Nevertheless, the nuclei showed the typical needle-like morphology despite the longer length, suggesting that Prtl99C might play a role in chromatin compaction, but not in nuclear shaping.

5.1.4.2 *Prtl99C-ΔC* mutants cause elongation of the chromatin region in sperm nuclei and show reduced fertility

A further opportunity to approach the particular function of a gene is the analysis of P-element induced mutations. For this reason, the minos insertion, *Mi{MIC}CG15510*^{MI10224}, located in the open reading frame of *Prtl99C* was analyzed (St Pierre et al., 2014) (Figure 18A).

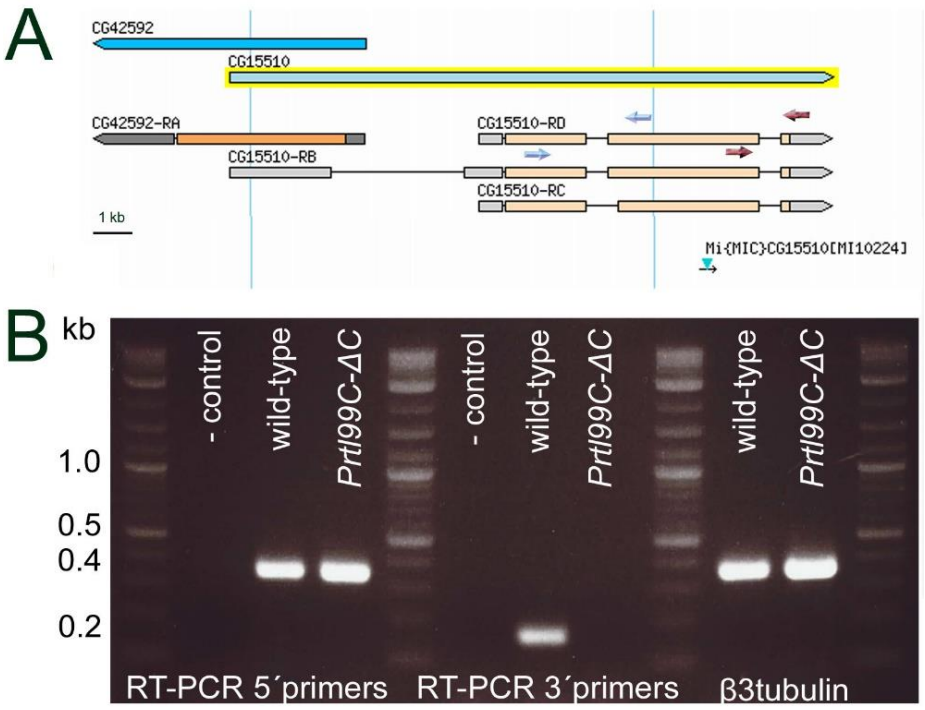

Figure 18 Minus-element insertion leads to a *Prtl99C-ΔC* stable transcript (A) Schematic representation of the genomic region of *Prtl99C* (*CG15510*) with the minos insertion *Mi{MIC}CG15510*^{MI10224}. Primer pairs used for RT-PCR are also indicated: *Prtl99C* 5'-specific primers (blue arrows), *Prtl99C* 3'-specific primers (red arrows). Photo captured from http://flybase.org/. (B) *Prtl99C-ΔC* encodes a stable transcript. RT-PCR of *Prtl99C* using RNA from wild type and *Prtl99C-ΔC* adult testes. The *Prtl99C* 5'-specific primers amplified a 365-bp cDNA fragment from the ORF of *Prtl99C* in wild type and *Prtl99C-ΔC* testes. The *Prtl99C* 3'-specific primers amplified a 167-bp cDNA fragment from the ORF of *Prtl99C* in wild type but not *Prtl99C-ΔC* testes. Amplification of *β3-tubulin* cDNA as control.

Before the flies could be examined more closely, the Minus-insertion strain had to be verified initially for the insertion site. I performed single-fly PCRs with genomic DNA of *Mi{MIC}CG15510*^{MI10224} flies using the 5′ and 3′ specific primers from the Minus-element vector in combination with *Prtl99C* genomic region primers (PCR1 primers: RTpcrMst99C-Fw and MIMIC5-1, PCR2 primers: MIMIC5-1 and MI10224-3Rv). Both primer pairs gave the expected products (666 bp and 507 bp respectively) that the insertion site of the P-element could be therefore verified by sequencing (data not shown). After proving the insertion site, we determined that this minos insertion leads to an early stop codon 100 aa after the HMG-box motif, most likely resulting in a truncated *Prtl99C-ΔC* protein at a size of 169 aa. This protein contains all the major domains of the protein but has lost the very C-terminal 32 aa (Figure. 4A, underlined letters).

In order to see if a shorter transcript exists, I performed RT-PCR with RNA from adult testes using two specific primer pairs, one pair located 5' to the transposon insertion site (Figure 18A, blue arrows) and the other located 3' to the site (Figure 18A, red arrows). The 5' corresponding primers amplified a cDNA fragment from the ORF, in contrast to the 3' primers. Therefore, we confirmed that a stable *Prtl99C-ΔC* transcript was transcribed (Figure 18A-B).

5.1.4.2.1 Prtl99C-ΔC-eGFP shows the same expression pattern as 942- or 386-Prtl99C-eGFP

As a consequence that anti-Prtl99C was raised against a C-terminal peptide (aa 179 to aa 201), we could not use anti-Prtl99C in order to confirm if the stable *Prtl99C-ΔC* transcripts were translated at all (Figure 19A). As an alternative to strengthen our hypothesis that a truncated protein may exist, we generated an e-GFP fusion protein, with the presumptive promoter and 5' UTR of 386 bp upstream of the start codon. Prtl99C-ΔC-eGFP included all the major domains of the protein but missed the C-terminal 32 aa expressing a shortened ORF similar to the *Prtl99C-ΔC* mutant (Figure 19B, see Supplemental Information for generation of the transgenic construct).

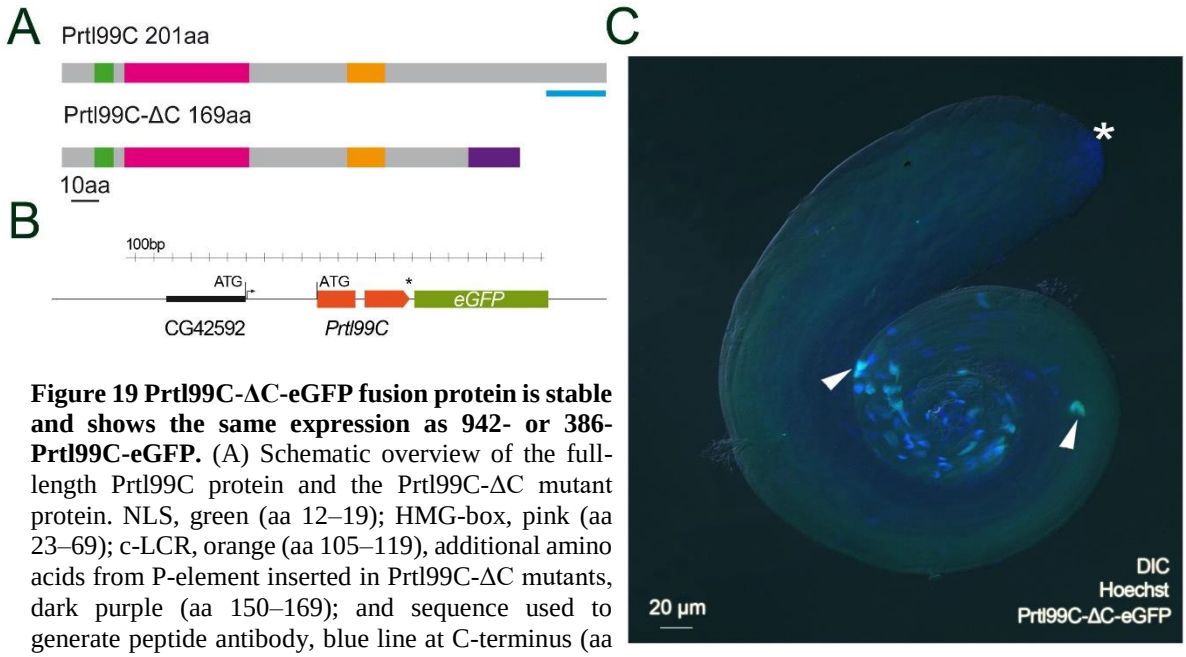

Figure 19 Prtl99C-ΔC-eGFP fusion protein is stable and shows the same expression as 942- or 386-Prtl99C-eGFP. (A) Schematic overview of the full-length Prtl99C protein and the Prtl99C-ΔC mutant protein. NLS, green (aa 12–19); HMG-box, pink (aa 23–69); c-LCR, orange (aa 105–119), additional amino acids from P-element inserted in Prtl99C-ΔC mutants, dark purple (aa 150–169); and sequence used to generate peptide antibody, blue line at C-terminus (aa 179–201).
(B) Schematic drawing of the *Prtl99C-ΔC-eGFP* construct. *: multiple cloning site in frame with *Prtl99C* and *eGFP*. (C) Whole-mount of *Prtl99C-ΔC-eGFP* expressing testis stained with Hoechst. Prtl99C-ΔC-eGFP is expressed in the nucleus of spermatids from late canoe stage onwards (arrowheads). *, tip of the testis.

Certainly, Prtl99C-ΔC-eGFP expression pattern was exactly the same as full ORF *eGFP* fusion genes, *942-Prtl99C-eGFP* or *386-Prtl99C-eGFP* (Figure 19C). This helped us to see that the 32 C-terminal amino acids were not essential for the correct expression pattern of Prtl99C.

5.1.4.2.2 The nucleus length of *Prtl99C-ΔC* mature sperm is longer

Clearly, *bam-Gal4>Prtl99C*^{RNAi} flies showed a failure in chromatin compaction and fertility. Moreover, to check if Prtl99C-ΔC protein is still functional, we analyzed *Prtl99C-ΔC* line in detail. Interestingly, homozygous *Prtl99C-ΔC* males showed severely reduced fertility similar to *bam-Gal4>Prtl99C*^{RNAi} males (Table S1). Furthermore, histological examination of *Prtl99C-ΔC* flies revealed that spermiogenesis was relatively normal (Figure 24A-B), nevertheless, the length of sperm nuclei was also affected (Figure 17). Hoechst and anti-Mst77F immunostainings of squashed seminal vesicles from homozygous *Prtl99C-ΔC* males also showed extended chromatin region (Figure 17, column 4) compared to wild type

sperm nuclei (Figure 17, column 1). Surprisingly, also these mature sperm nuclei were needle-like despite the longer length (Figure 17, column 4). From these results, we concluded that the C-terminal is responsible for correct chromatin compaction and affects male fertility.

5.1.4.2.3 *Prtl99C-ΔC-eGFP* in *Cad99C^{248A}* mutant background

In order to clarify if the N-terminal part of Prtl99C could rescue the sterility and the phenotype caused by *Cad99C^{248A}*, transgenic flies carrying *Prtl99C-ΔC-eGFP* on the second chromosome were used. The introduction of only one copy of *Prtl99C-ΔC-eGFP* was able to rescue male sterility partially (Table S1).

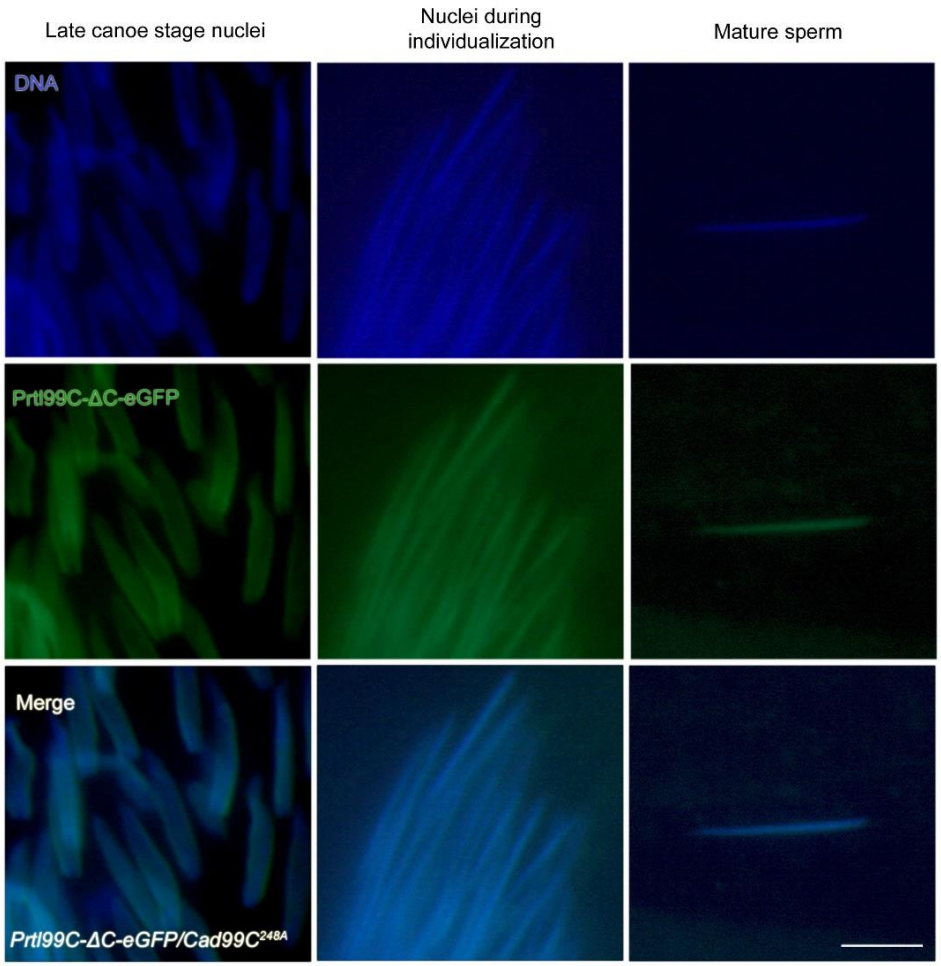

Figure 20 Prtl99C-ΔC-eGFP rescues substantially the phenotype caused by *Cad99C^{248A}* deletion. Squash preparation of *Cad99C^{248A}* testis expressing Prtl99C-ΔC-eGFP. First row: stained with Hoechst to visualize DNA. Second row: Prtl99C-ΔC-eGFP expression. Third row: Merged photo of fluorescence images. Spermatid nuclei as well as mature sperm nuclei appeared wild type. Scale bar: 5 µm.

Prtl99C-ΔC-eGFP;Cad99C^{248A} males showed reduced fertility where only few bottles were observed with very few offspring (Table S1). Nevertheless, spermiogenesis was substantially rescued (Figure 20). Squashed testes stained with Hoechst revealed normal spermatid development (Figure 20). The seminal vesicles of rescued flies were mostly filled with motile sperm however the sperm nuclear lengths were longer compared to wild type (data not shown). In conclusion, the N-terminal of Prtl99C was able to do a partial rescue which pointed out that for a fully function of the protein also the C-terminal is required.

5.1.4.3 Nuclear elongation of Prtl99C mutants is manifested already at the individualization stage

Based on the similar results obtained from the analysis of RNAi-mediated knockdown (*bam-Gal4>Prtl99C*^{RNAi}) and *Prtl99C-ΔC* mutant, we decided to measure more sperm nuclei of different genotypes in order to look for the average length compared to wild type. For this end, I stained squashed testes and seminal vesicles of each fly strain and measured the Hoechst-dye-positive area of 20 spermatid nuclei during individualization (from testes squashes) and 20 mature sperm nuclei (from seminal vesicles squashes), which I referred as "length of the nuclei" for simplicity (Figure 21). From the measurements, I saw that during individualization wild-type nuclei were slightly longer than wild-type mature sperm nuclei, indicating that the chromatin compaction still goes on until the sperm completes its maturation (Figure 21).

There was also a variation in the length of wild-type nuclei, in agreement with electron microscopy data (Tokuyasu, 1974), which may be a reflection of whether the genome contains an X or Y chromosome. Thus, the volumes of sperm nuclei are proportional to their DNA content (Hardy, 1975).

The measurement of homozygous *Prtl99C-ΔC* and *bam-Gal4>Prtl99C*^{RNAi} nuclei displayed different results than wild type. Both, *Prtl99C-ΔC* and *bam-Gal4>Prtl99C*^{RNAi}, spermatid nuclei during individualization and mature sperm showed longer nuclei compared to wild type, which indicated that the extension of the nucleus was manifested already at the stage before becoming a mature sperm (Figure 21 and Table S2).

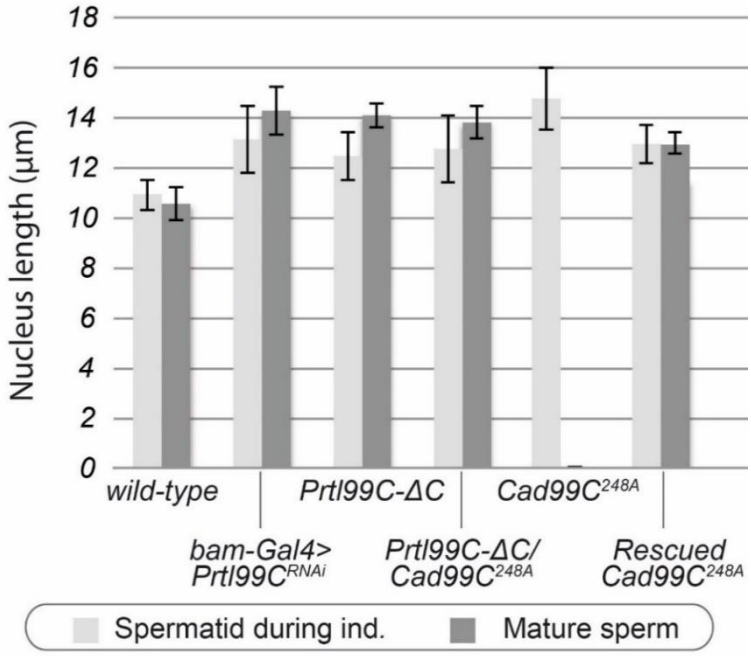

Figure 21 Nuclear elongation of Prtl99C mutants is manifested already at the individualization stage. Average length of nuclei during individualization and of mature sperm from wild type and various fly strains in which Prtl99C is affected (n = 20). Only morphologically linear nuclei were measured.

In the heterozygous *Prtl99C-ΔC* (one wild-type, one *Prtl99C-ΔC* copy) there was a slight elongation (11.3 µm) of nuclear length compared to wild type (10.5 µm) which might indicate a slight dominant negative effect, nevertheless, these males were fertile. Moreover, the trans crossing of Prtl99C-ΔC in *Cad99C*^{248A} background was also an important check point for these measurements. In these flies, only the C-terminal of Prtl99C was missing. On the other hand, the other genes (*Atg16*, *CG42592*, and *Cad99C*) of the *Cad99C*^{248A} region were present in one wild-type copy. These flies were semi-fertile, furthermore, exhibited also longer nuclei length starting from the stage during individualization (Figure 21 and Table S2).

So far as the extension of the nuclei was manifested already at the stage during individualization, we wanted to check whether this happens also in *Cad99C*^{248A} mutant. These males were sterile and their seminal vesicles were poor in mature sperm, however, I could measure linearly displayed spermatids from cysts during individualization. Compared to wild type, also homozygous *Cad99C*^{248A} males had longer nuclei length during individualization (Figure 21 and Table S2). Taken together, within the measured different genotypes, the mature sperm nuclear length was about 1/3 longer in all strains compared to wild type and the extension clearly started during individualization.

To examine whether the rescue of Prtl99C has a reducing effect on the length of the nuclei, I analyzed the homozygous rescue males *386-Prtl99C-eGFP;Cad99C^{248A}*. The rescued *Cad99C^{248A}* males exhibited shorter nuclei length (12.99 µm) compared to *Cad99C^{248A}* (14.72 µm) (Figure 21). As the rescue capability of transgenic Prtl99C could not reach to the endogenous expression of the protein, this decrease in nuclei length is likely significant. Thus, we conclude that Prtl99C has a crucial role for proper chromatin compaction in spermiogenesis.

5.1.5 Sperm nuclei of homozygous protΔ and Prtl99C mutants are longer than sperm nuclei of Prtl99C mutants

Deletion of both *Drosophila* protamines leads to 20% abnormally shaped nuclei, however, these flies are still fertile (Rathke et al., 2010). As Prtl99C and protamines expression patterns are very similar, we asked whether the deletion of protamines has an additive effect on the length of the nuclei. For this purpose, we established a double mutant line *protΔ; Cad99C^{248A}*. *protΔ2* mutant line was used from the deletion mutant collection (Rathke et al., 2010). For simplicity, we named it *protΔ*.

Not surprisingly, homozygous *protΔ; Cad99C^{248A}* double mutants were male sterile, like *Cad99C^{248A}* single mutants (Table S1). Squashed testes preparations immunostained with Hoechst revealed that late spermiogenesis of these mutants was strongly disarranged (Figure 22A). During individualization the majority of the cysts showed a stronger phenotype than those of single mutants. While some cysts looked exclusively like those of the wild type (Figure 22A-b), the spermatid nuclei in most cysts were abnormal. Often the arrangement of sperm heads within a cyst was disturbed (Figure 22A-d), a part of the nucleus was coiled around itself (Figure 22Aa, e, and f), and the nuclei were longer (Figure 22Aa-f).

After those observations, to see if the nuclear length was also affected in the single *protΔ* mutation, I first measured the nuclear length of *protΔ* mutant nuclei from squashed testes and seminal vesicles immunostained with Hoechst. Very interestingly *protΔ* nuclei during individualization were slightly longer than *protΔ* mature sperm nuclei, similar to my observation in wild type. However, the nuclear length was also increased in *protΔ* mutants

(11.49 µm) compared to wild type (10.55 µm) but not as much as in *Prtl99C* knockdown (14.26 µm) (Figure 22B and Table S2).

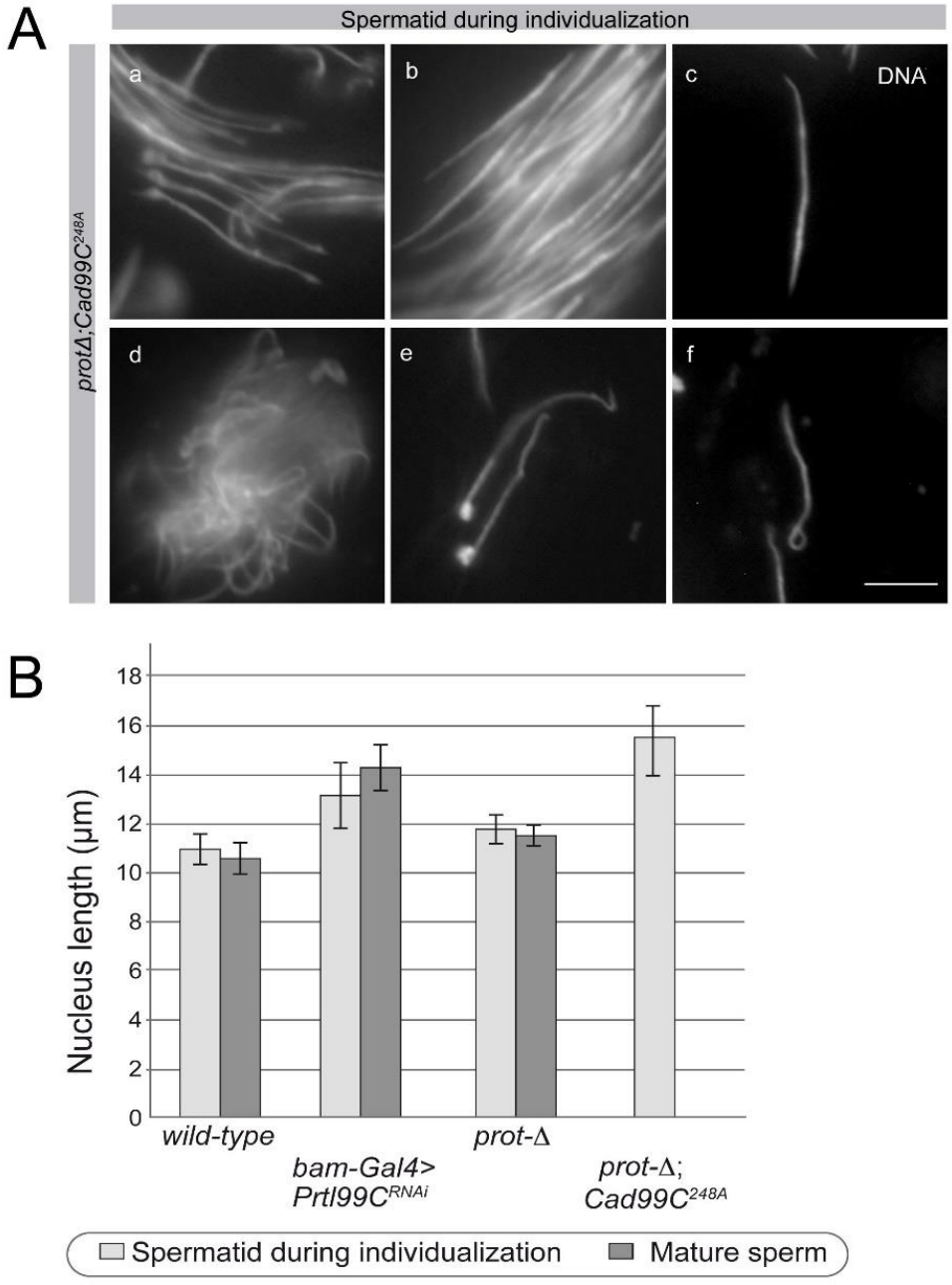

Figure 22 Deletion of both protamines and Prtl99C enhance the nucleus length. (A) Homozygous *protΔ*;*Cad99C*^{248A} double mutants showed a strong nuclear phenotype than *protΔ* or *Cad99C*^{248A} at the stage during individualization. (a–f) Hoechst staining of squashed spermatid nuclei from testes of *protΔ*;*Cad99C*^{248A} mutants. Chromatin of *protΔ*;*Cad99C*^{248A} spermatids during individualization were longer, and the sperm phenotype was stronger than that of the *Cad99C*^{248A} mutant. Scale bar: 5 µm. (B) Average length of nuclei during individualization and of mature sperm from wild type and various fly strains in which *Prtl99C* or/and *ProtA* and *ProtB* are affected (n = 20). Only morphologically linear nuclei were measured.

Furthermore, the measurement of nuclear length of homozygous *protΔ; Cad99C*^{248A} spermatid nuclei during individualization showed that loss of protamines enhances the *Prtl99C* mutant phenotype. The length of nuclei of *protΔ; Cad99C*^{248A} mutant (15.45 µm) was longer than those of *Prtl99C* mutants (Table S2). The spermatid nuclei during individualization were still needle-like shaped, but their length increased from 14.3 µm to 15.5 µm (Figures 22B and Table S2). Thus, the reason of this nuclear elongation was due to the additive effect of the loss of protamines. In conclusion, these data imply that the chromatin is compacted by several proteins like ProtA, ProtB and Prtl99C.

5.1.6 The removal of histones and loading of Mst77F and Protamines are independent of Prtl99C

The previous experiments clearly demonstrated the additive compaction of chromatin by protamines and Prtl99C. In *Drosophila*, ProtA, ProtB, and Mst77F are major components of the mature sperm chromatin (Jayaramaiah Raja and Renkawitz-Pohl, 2005; Rathke et al., 2010). Functional differences or similarities between these proteins could be taken in consideration. For this purpose, we asked whether each protein is expressed properly in the absence of the other. In other words, we wanted to check if the loading of Prtl99C was dependent on protamines. To address this question, I performed anti-Prtl99C staining on squashed homozygous *protΔ* testes. Anti-Prtl99C staining was restricted at the late canoe stage in *protΔ* mutants as observed in wild type (Figure 23).

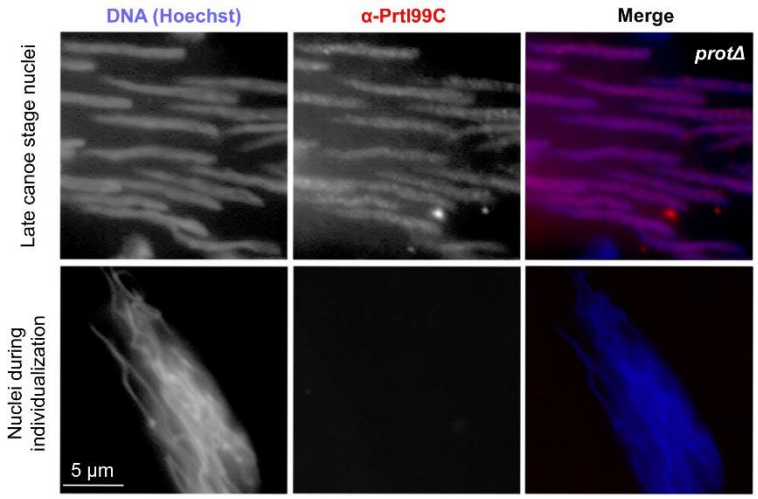

Figure 23 Prt99C is expressed normally in *protΔ* mutants. Anti-Prtl99C antibody staining of homozygous *protΔ* testes. Visualization of DNA via Hoechst staining. Endogenous Prtl99C detected with anti-Prtl99C antibody. Merged photo of fluorescence images. DNA (blue), Prtl99C (Red).

To see if Prtl99C is dispensable for histone-to-protamine or to Mst77F transition, we further investigated histone-to-protamine dynamics immunofluorescently using anti-histones, anti-ProtA, and anti-Mst77F antibodies in homozygous *Prtl99C-ΔC* mutants and *bam-Gal4>Prtl99C*^{RNAi} flies. In fact, disappearance of histones as well as loading of Mst77F and protamines was not altered in these mutants (Figure 24A, B, and C). We also observed the same results by staining the homozygous *Cad99C*^{248A} mutant males (Figure 24C). In summary, these results showed that loading of protamines and Mst77F does not depend on Prtl99C, and Prtl99C loading is independent of protamines.

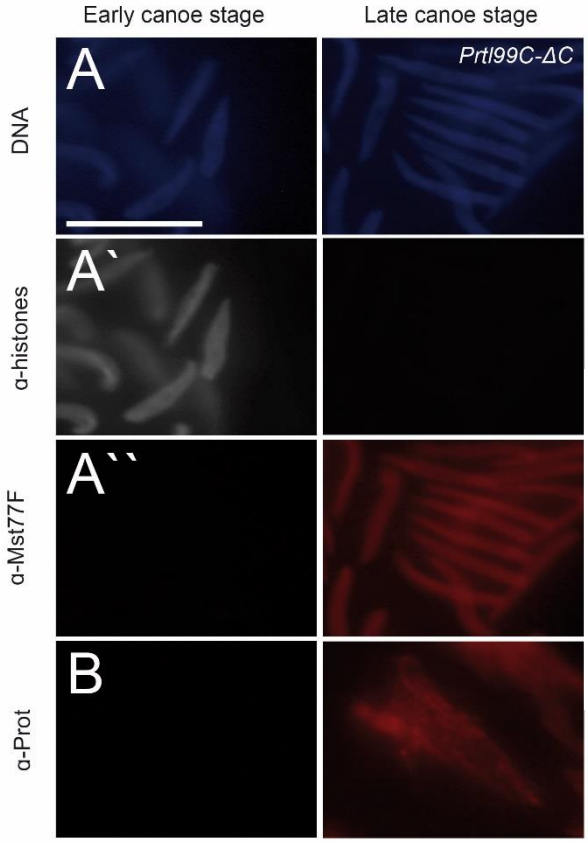

C

Strain	Transition from Histones to Mst77F and Protamines
Cad99C^{248A}	normal
bam-Gal4>Prtl99C^{RNAi}	normal
Prtl99C-ΔC	normal

Figure 24 Histone degradation and expression of Mst77F and protamines are independent of Prtl99C. (A-B) Transition from histones (A`) to Mst77F (A``) and to protamines (B) in spermatid nuclei of mutant *Prtl99C-ΔC* was not affected. DNA stained with Hoechst dye (blue), histones (white), Mst77F (red) and protamines (red). Scale bar: 10 μm. (C) Summary of the transition from histones to Mst77F and to protamines in various fly strains in which Prtl99C is affected.

5.1.7 Majority of the sperm chromatin relevant proteins seem to localize in different chromatin regions

To elucidate the chromatin status of *Drosophila* male genome, we checked the distribution of Prtl99C, Mst77F, protamines and CID in mature sperm. The histone H3 variant CENP-A (CID in *Drosophila*) is a highly conserved epigenetic mark which

determines centromere localization and is associated with the inner kinetochore (Blower and Karpen, 2001; Panchenko et al., 2011). In order to see the structural relationships between centromeric chromatin and chromosomal proteins, and to investigate further if different proteins occupy distinct subdomains, I decondensed sperm from wild-type seminal vesicles and immunostained with anti-Prtl99C, anti-Mst77F, anti-ProtA, and anti-CID antibodies (Figure 25). The expression of Prtl99C, Mst77F and protamines was seen in a large region of the nucleus (Figure 25A). In contrast to conventional IF, we rarely observed distinct regions of sperm chromatin where a specific protein was localized; however, the centromers were free of Prtl99C, Mst77F and protamines (Figure 25Ba-b, arrows). In summary, as far as the immunofluoresence imaging on decondensed nuclei allowed us, we saw the centromeric chromatin free of basic chromosomal proteins. Unfortunately, it was not possible to distinguish the occupancy of each basic protein by fluorescence microscope.

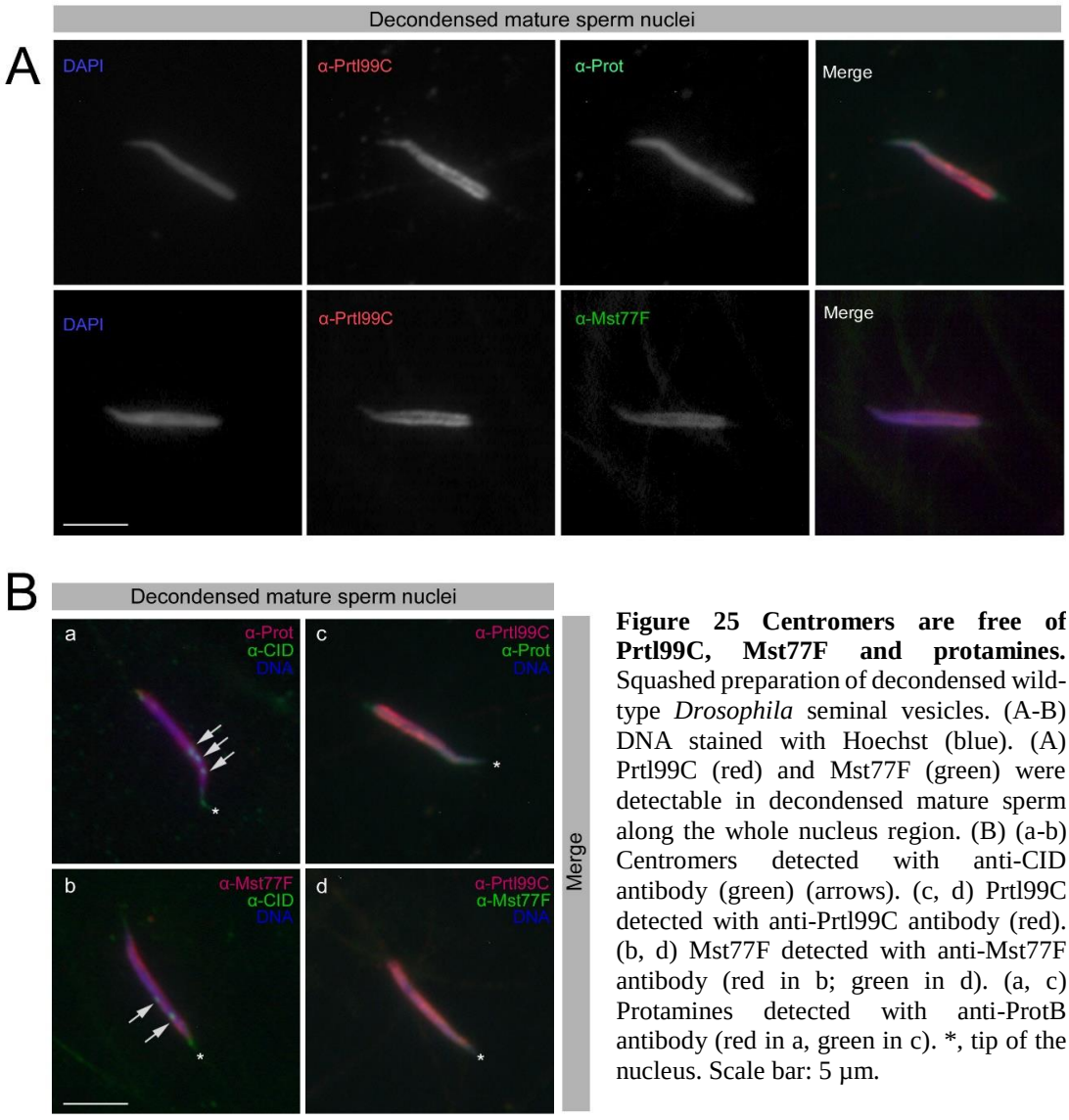

Figure 25 Centromers are free of Prtl99C, Mst77F and protamines. Squashed preparation of decondensed wild-type *Drosophila* seminal vesicles. (A-B) DNA stained with Hoechst (blue). (A) Prtl99C (red) and Mst77F (green) were detectable in decondensed mature sperm along the whole nucleus region. (B) (a-b) Centromers detected with anti-CID antibody (green) (arrows). (c, d) Prtl99C detected with anti-Prtl99C antibody (red). (b, d) Mst77F detected with anti-Mst77F antibody (red in b; green in d). (a, c) Protamines detected with anti-ProtB antibody (red in a, green in c). *, tip of the nucleus. Scale bar: 5 µm.

5.1.8 Prtl99C cannot rescue *protΔ* phenotype

Previous experiments showed that Mst77F-eGFP does not rescue the crumpled phenotype of the *protΔ* mutants (Rathke et al., 2010). To complement our immunofluorescence stainings data and to study whether Prtl99C can partially replace protamines, we further performed a rescue experiment similar to Rathke C. et al, 2010. Therefore, it was important to know whether Prtl99C might be functionally redundant to protamines or behaves like Mst77F in the context of rescue capability. *386-Prtl99C-eGFP* transgene was brought into homozygous *protΔ* background and spermiogenesis was analyzed. Squashed testes immunostained with Hoechst revealed the similarity of the rescue performed with Mst77F-eGFP. Indeed, 386-Prtl99C-eGFP could not rescue the malformed sperm heads phenotype (Figure 26). In agreement with Section 5.1.6 from this chapter, we conclude that protamines cannot be replaced by Prtl99C. Evidently, protamine A and B, as well as Mst77F are likely loaded independently of Prtl99C during post-meiotic chromatin reorganization.

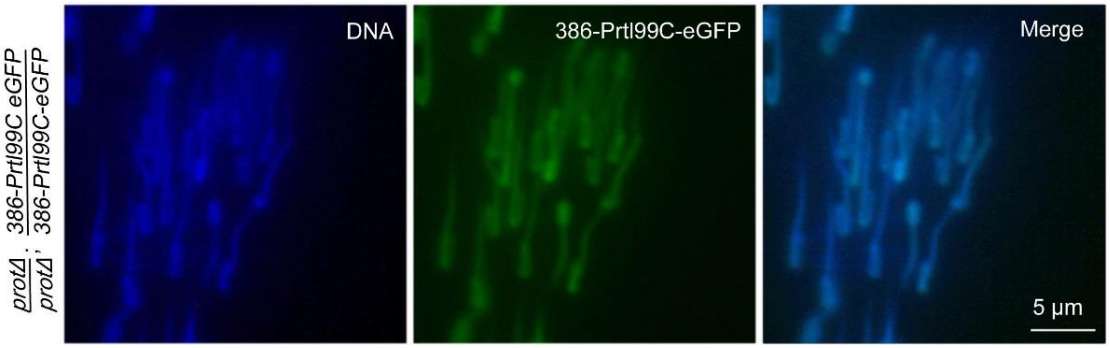

Figure 26 386-Prtl99C-eGFP is not able to rescue the sperm head phenotype of *protΔ* mutants. Squashed preparation of homozygous *protΔ* testis rescued with 386-Prtl99C-eGFP was stained with Hoechst to visualize DNA. No reduction of the crumpled phenotype of the *protΔ* mutants was seen.

5.2 *Drosophila* sperm head enrichment assays

As mentioned earlier, our data point out the presence of more protamine-like proteins in chromatin remodeling during *Drosophila* spermatogenesis. In order to find out more protamine-like proteins, two different strategies were chosen. The first strategy was to isolate

Drosophila sperm heads in order to enrich for a potential "*Drosophila* sperm nuclei proteome". Herewith, subcellular proteomics (using only sperm heads) would allow the identification of less concentrated proteins. The second strategy was pursued by the evaluation of the existing whole testis and sperm proteome data.

For sperm head enrichment assays we used double transgenic flies *dj-GFP,Prot-B-DsRed* with dual sperm color. dj-GFP was expressed in sperm tail in green and Prot-B-DsRed was expressed in sperm head in red (Figure 27) (Köttgen et al., 2011). This combination of tags allowed us to distinguish tail and head as an easy control assay for fractionation.

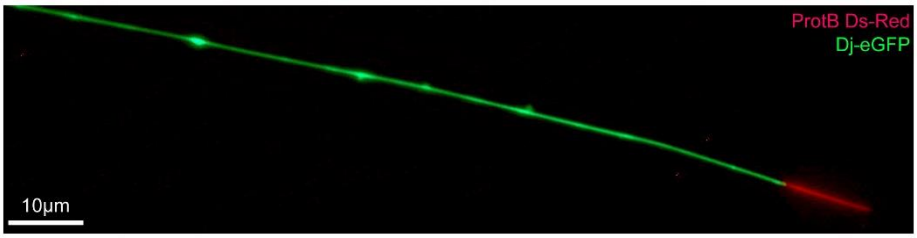

Figure 27 A part of a *Drosophila* mature sperm. Double transgenic flies expressing Dj-eGFP in sperm tail (green) and Prot-B-DsRed in sperm head (red).

5.2.1 Sonication power effect on *Drosophila* sperm

1.8 mm in length, *Drosophila melanogaster*'s sperm is 50 time longer than human sperm (Brill and Wolfner, 2012). In the last published *Drosophila* sperm proteome, DmSP-II, protein extract of whole sperm was used, and surprisingly, even known sperm proteins, like Snky (sperm membrane protein) or Mst77F (sperm chromatin component), were not found (Wasbrough et al., 2010). *Drosophila* sperm tail is approximately 200 time longer than the head, which is approximately 9µm in length (Tokuyasu, 1974), therefore no wonder that a protein extract from whole sperm would be enriched mainly for tail proteins.

In order to get a clear subcellular fractionate (only sperm heads) before proteomic analysis, we first tried to separate the head from the tail. Sonication was described as the most efficient technique for human sperm tail isolation (Amaral et al., 2013), accordingly I also sonicated sperm from *dj-GFP,Prot-B-DsRed* flies. Indeed, by sonication the tail was chopped into small pieces and the head was separated from the tail (Figure 28).

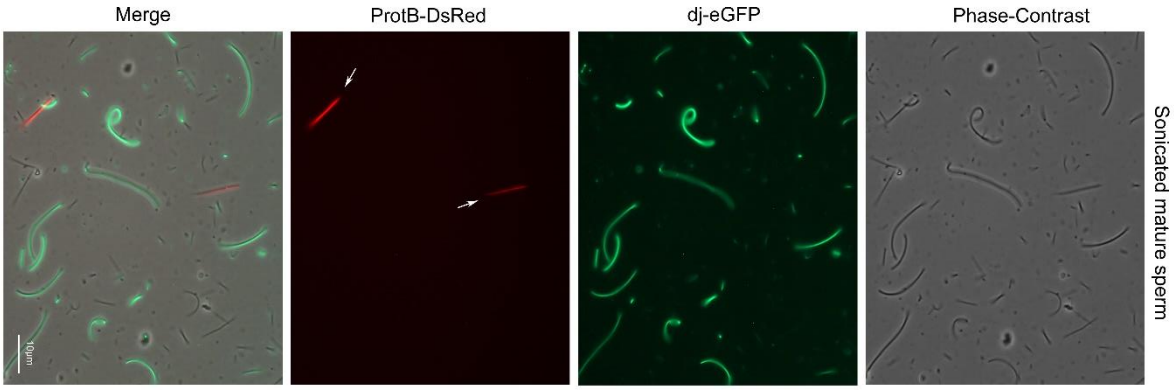

Figure 28 Effect of sonication on *Drosophila* sperm of males expressing dj-GFP in sperm tail (green) and Prot-B-DsRed in sperm head (red). Sperm heads separated from the tail are marked with arrows.

To determine the optimum sonication conditions, I applied different power outputs (10-70%) using the same length of sonication time with a series of short pulses (2x15s, 15s intervals) (Table 1 and Figure 29).

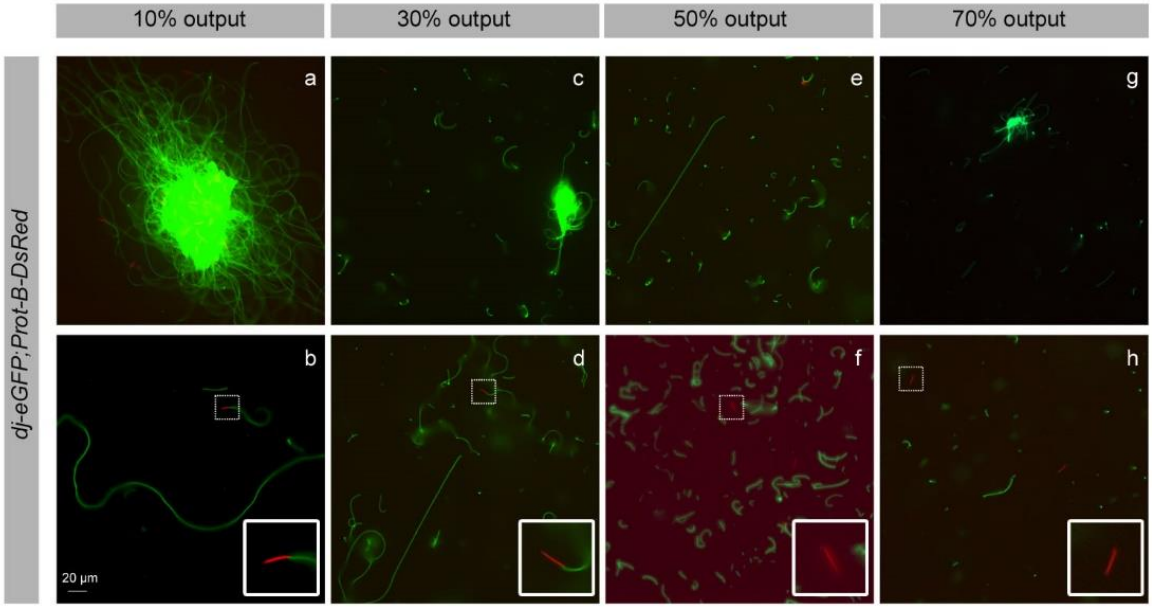

Figure 29 Different sonication power on *Drosophila* sperm expressing dj-GFP in sperm tail (green) and Prot-B-DsRed in sperm head (red). (a-b) 10% output (a) sperm tails were intertwined to each other (b) the sperm head was still intact with the tail. (c-d) 30% output (c) small intertwined sperm clouds were still present whereas (d) the sperm head was still intact with the tail. (e-f) 50% output (e) sperm tails were chopped in diverse length and (f) the head was separated from the tail. (g-h) 70% output (g) small intertwined sperm clouds were also present, with 70% output (h) the length of the tail residues were smaller, the head was separated from the tail and still looking needle-like shaped. The inserts show the high magnification to visualize the sperm heads.

10% output	Not homogenous sample. Nuclei still attached to the tail piece (Figure 29b). Large sperm tail clouds bearing intact sperm (Figure 29a). Diverse length of tail pieces.
30% output	Not homogenous sample (Figure 29c). Some nuclei were separated from the tail; however, large sperm aggregates bearing intact sperm were present (Figure 29d). Diverse length of tail pieces.
50% output	Nuclei were separated from the tail (Figure 29f). Diverse length of tail pieces (Figure 29e), nevertheless, much smaller compared to 30% output. Sperm tail clouds were still present.
70% output	Nuclei were separated from the tail and its shape was still needle-like shaped (Figure 29h). Diverse length of tail pieces with small tail clouds were present (Figure 29g).

Table 1 Summary of the observation for each sonication conditions which were applied (power outputs from 10 to 70%). (See Figure 29).

In summary, 70% output with 2x15s, 15s intervals was the optimum condition in order to get sperm heads separated from the tails. Nevertheless, even with this power, small intertwined sperm clouds were still present (Figure 29g).

5.2.2 Tests for *Drosophila* sperm head fractionation using gradient centrifugations

For the physical separation of head and tail pieces we tried several experiments using gradient ultracentrifugation. The sperm nucleus contains highly condensed and packed chromatin, therefore is quite dense. In order to separate sperm heads and tail pieces, we used sucrose and Percoll gradients which are based on separation via density difference between sperm head and tail.

- **Ultracentrifugation using Percoll and sucrose gradients**

Percoll is a classic medium for density gradient centrifugation and is commonly used to fractionate human or mouse sperm cells. In order to fractionate *Drosophila* sperm heads

and tail pieces, I applied sonicated *Drosophila* sperm sample to a Percoll gradient and analyzed each fraction. After ultracentrifugation, I observed one upper and one lower opaque band, took samples of each fraction and looked under the fluorescence microscope. In both fractions sperm heads and tail pieces were present (data not shown). Therefore, in contrast to mammalian samples, Percoll gradient did not work with *Drosophila* sperm to separate nuclei from tail residues.

As an alternative to Percoll gradient, I also applied sonicated *Drosophila* sperm sample to a sucrose gradient (60%, 70%, and 75%) and analyzed each fraction. After centrifugation, only one layer appeared in the upper region of the tube due to the phase difference. I first analyzed the tube under the UV without aspirating any material to see any possible layer from the transgenes; however, I did not see a specific band. Then, I started to take small fractions and looked under the fluorescence microscope. Starting from the upper phase, I could see tail residues together with nuclei. In the intermediary and lower phase I observed the same results (data not shown). In conclusion, these conditions were not sufficient to fractionate sperm heads or tail pieces in different phases.

- **Treatment of *Drosophila* sperm with Nocodazole**

Nocodazole, a microtubule-destabilizing drug, blocks axoneme assembly or maintenance (Riparbelli et al., 2013). Here, we checked whether we could resolve the intertwined tail pieces by affecting the microtubule stability and dynamics. For this end, sonicated sperm were incubated with Nocodazole. After overnight incubation sperm heads and tail were still in shape together with degraded tail residues. Nevertheless, there were still uncoiled intertwined sperm bundles (data not shown). In summary, Nocodazole was not efficient to dissolve/dissociate the intertwined sperm bundles.

- **Treatment of *Drosophila* sperm with Dibucaine-HCl**

Dibucaine is a local anesthetic used to induce flagellar removal in *Chlamydomonas reinhardtii* (Nishikawa, 2010) and is generally used to deflagellate cells. In our experiments, we used dibucaine before sonication in order to dissolve the intertwined sperm bundles formed by the junction of several sperm. Freshly dissected *Drosophila* sperm were pipetted up and down several time with Dibucaine-HCl and then analyzed under the fluorescent microscope. After examination under the microscope, I didn't see any deflagellation effect

on sperm clouds. Unfortunately, Dibucaine-HCl was not sufficient to dissolve the intertwined sperm cells (data not shown)

In conclusion after sonication, the centrifugation techniques and the chemical treatments that I applied were not successful to obtain large quantities of sperm heads free of tail fragments.

5.3 Conclusions

On the basis of my data so far, I consider that the identification of Prtl99C may significantly advance the knowledge of male fertility. The fact that the *Drosophila* genome condenses approximately 10 fold stronger than its mammalian counterpart raises the possibility that more chromatin components exist in *Drosophila*. Therefore, further experiments addressing the identification of novel nuclear sperm proteins have to be carried out to understand the exact mechanism of *Drosophila* spermatogenesis and to give insight to researchers working on mammalian spermatogenesis. Eventually a subcellular *Drosophila* sperm proteomics and chromatin immuno-precipitation (ChIP) followed by sequencing (ChIP-Seq) - with antibodies against the newly identified and the so far known chromatin components- will elucidate the region specific composition of the sperm chromatin more extensively.

5.4 Outlook

My data so far indicated an additive effect of protamines and Prtl99C on chromatin condensation but nevertheless the sperm chromatin appears compact in double mutants of Prtl99C and protamines (*protΔ; Cad99C*^{248A}).

We hypothesize that there are other sperm chromatin proteins. In order to identify such proteins I first approached to enrich *Drosophila* sperm heads for a potential "*Drosophila* sperm nuclei proteome", which was unsuccessful due to contamination of mainly tail residues. The second approach pursued the analysis of whole testis and sperm proteome data. Dorus and colleagues published the first "*Drosophila melanogaster* sperm proteome" (DmSP) in 2006, where they identified 381 proteins from the whole sperm (Dorus et al., 2006). This work was followed by the "*Drosophila melanogaster* sperm proteome II" (DmSP-II), where they identified 766 new proteins and updated the sperm proteome data containing a total of 1108 proteins (Wasbrough et al., 2010). Very recently, our lab performed a developmental proteomics using larval, pupal and adult testes named "The *Drosophila melanogaster* stage-specific testis proteome" (DmTP) and identified a total of 6641 proteins. Among the obtained data, 355 proteins were specific for adult testes (Gärtner et al., in preparation, Gärtner PhD Thesis, 2014). This subgroup of proteins was very interesting for the identification of new protamine-like proteins.

Therefore, I first looked for very basic proteins which were also identified in DmSP-II. From the outcome, I checked for mutant availability and analyzed in total five candidates (CG12860, CG4691, CG17377, CG31542 and CG6332) (Table 2). To unravel if those five candidates are sperm chromatin components acting in chromatin compaction, I analyzed P-element insertions for each candidate (see material section for fly strains and site of insertion of the P-element). Squashed testes preparations immunostained with Hoechst revealed that spermiogenesis of these mutants and the length of nuclei was normal (data not shown). Nevertheless, we cannot exclude that any partially functioning protein was synthesized and stable, in particular as often the P-element is inserted in the 5'UTR or upstream region. Thus, we aimed to search insertions in the open reading frame for genes of particular interest.

Among these candidates, CG6332 caught our attention as it is predicted to contain a "Testicular haploid expressed repeat (THEG)" and has 29% homology with the human testicular haploid expressed gene protein isoform 1 (http://blast.ncbi.nlm.nih.gov/; see Figure S1 for alignment). The minos insertion, *Mi{ET1}CG6332*^{MB01798}, in the open reading frame of *CG6332* was controlled for the insertion site of the minos element. Therefore, we performed single-fly PCRs with genomic DNA of *Mi{ET1}CG6332*^{MB01798} flies using the 5′ and 3′ specific primers from the minos element vector in combination with *CG6332* genomic region primers (PCR1 primers: 6332-5Fw and MIMIC5-1, PCR2 primers: MIMIC5-1 and 6332-3Rv). By sequencing the PCRs, we could confirm the insertion site of the minos-element which leads likely to a truncated shorter protein of 236 aa in comparison to the wild-type protein of 353 aa. Surprisingly the minos insertion led to complete male sterility (n=20), and this might be due to the loss of the C-terminal part of the protein which is most conserved to the mammalian homolog. Furthermore, in phase contrast microscopy late spermatid cysts displayed very tight organization, raising us the question whether a defect during individualization might occur as any individualized spermatids were observed (data not shown). Due to time limit, I could not continue further on the examination of this protein, however, it will be necessary to generate transgenic lines or/and to raise an antibody to see the subcellular localization and to gain further insight into the functional role of CG6332 in *Drosophila* spermatogenesis.

Name	IP	MW (kDa)	Protein Domains/Motifs prediction	FlyAtlas Anatomical Expression Data
CG12860	9.76	36.6	Protein of unknown function DUF1431, cysteine-rich, *Drosophila*	Very high expression
CG4691	10.38	30.8	Protein of unknown function DUF1431, cysteine-rich, *Drosophila*	Very high expression
CG17377	8.45	18.6	-	Very high expression
CG31542	8.63	21.2	-	Very high expression
CG6332	10.6	40.5	Testicular haploid expressed repeat	Very high expression

Table 2 Details of five candidate genes analyzed for chromatin compaction.

5.4.1 Potential loading factors for Prtl99C

In higher eukaryotes, dramatic structural changes in chromatin occur during sperm development. In somatic cells these alterations are proposed to be moderated by several mechanisms such as ATP-dependent chromatin remodelers and histone chaperons (Becker and Workman, 2013). One of those ATP-dependent chromatin remodeling complexes, ISWI, plays a role in DNA replication, DNA repair, transcriptional regulation and chromosome structure maintenance. Interestingly, it has been reported that HMG-box containing proteins increase their binding capacity to DNA by cooperating with ISWI (Toto et al., 2014). In *Drosophila* spermatogenesis, ISWI is expressed specifically at the late canoe stage and is shown to play an essential role in the loading of Mst77F and Protamines into the sperm chromatin (Doyen et al., 2015). Besides this, chromatin assembly factor 1 (CAF1) subunits act in sperm chromatin organization. During histone-to-protamine switch, CAF1-p180 disassembles from the chromatin and CAF1-p75 associates and acts as a protamine loading factor (Doyen et al., 2013). Moreover, during *Drosophila* spermatogenesis, the nuclear protein CCCTC-binding factor (CTCF) is present during pre-meiotic stages and remains until the late canoe stage as monitored in conventional immunofluorescence. CTCF is predicted to insulate active genes to keep chromatin accessible for RNA polymerase II as discussed in Rathke et al., 2007. Unfortunately, up to date any CTCF mutagenesis studies in flies were published. Very recently, *ISWI* mutants (Deuring et al., 2000) and *ISWI* knockdown (*C135 > ISWI*^{RNAi}) males were investigated in the context of chromatin dynamics during spermiogenesis. Doyen and colleagues reported ISWI being essential for spermatogenesis together with its role in promoting rapid repackaging of paternal genome after fertilization. *ISWI* knockdown males are male sterile. While *ISWI* hypomorphic males show significantly reduced fertility, their sperm are not properly compacted, giving rise to elongated nuclei as we observed in Prtl99C mutants (Doyen et al., 2015).

Here, we investigated the relationship of Prtl99C with loading factors, chromatin remodelers and insulators during *Drosophila* spermatogenesis. For this purpose, I analyzed RNAi-mediated knockdown of *CAF1-p180, CAF1-p75, ISWI,* and *CTCF* with the UAS/GAL4 binary system to target dsRNA expression in different cell types or stages of development in order to see the expression pattern of Prtl99C.

For RNAi experiments, KK and GD fly lines from the Vienna *Drosophila* Resource Centre and from Bloomington Drosophila Stock Center were used (for details see materials section) (Dietzl et al., 2007). Among all the lines, only *CTCF* RNAi sequence had been reported to have two off targets, *CG11352* and *CG42230*; however, according to *Drosophila* gene expression atlas, they are transcribed in adult testis at low levels (Chintapalli et al., 2007) so they unlikely may contribute to a phenotype during spermatogenesis (see supplemental information for the target sequence (Dietzl et al., 2007). The expression was driven from spermatogonia until early spermatocyte stage using *bam-Gal4* driver line (Caporilli et al., 2013; Chen and McKearin, 2003) or in spermatocytes using *C135-Gal4* driver line (Doyen et al., 2013). The *bam-Gal4* (Bam-Gal4/Bam-Gal4; Sp/CyO; Bam-Gal4/MKRS) or *C135-Gal4* (Sp/CyO; C135-Gal4/C135-Gal4) female virgins were crossed with homozygous RNAi transgenic males at 30°C. All RNAi lines and driver fly stocks were viable at 30°C and showed no defects in spermatogenesis (data not shown), for that reason we considered them as negative controls for our RNAi experiments.

Histological examination of all RNAi experiments revealed that the expression pattern of Prtl99C was not altered (Table 3) and spermiogenesis was normal except in *bam-Gal4>CTCF*^{RNAi} flies (Table 3, asterisk). Surprisingly, *bam-Gal4>CTCF*^{RNAi} flies showed abnormal canoe stage nuclei positive for Prtl99C. These late spermatid nuclei were looking apparently fat and the organization within cysts were disorganized indicating a distortion in late post-meiotic stages (Figure 30, arrow). In contrast, in control flies spermiogenesis was normal (Figure 30, arrows). Fertility test of *bam-Gal4>CTCF*^{RNAi} males revealed full male sterility correlating to a reduced CTCF levels during spermatogenesis (Rathke C. personal communication, BSc Christina Müller-Weisbrod). In summary, neither knockdown of ISWI nor CTCF did affect the expression pattern of Prtl99C. Moreover, loss of CAF1 had no influence on the expression pattern of Prtl99C. Caf-p75 is a known protamine chaperone and accordingly anti-protamine staining was performed as positive controls of these experiments. Unfortunately, I did not observe a knockdown of protamines in contrast to Doyen et al., 2013. Future experiments should clarify if the copy number of RNAi construct needs to be increased to achieve an efficient knockdown. In accordance with the previous chapter, we conclude that the loading of Prtl99C is independent of protamines or of Mst77F incorporation.

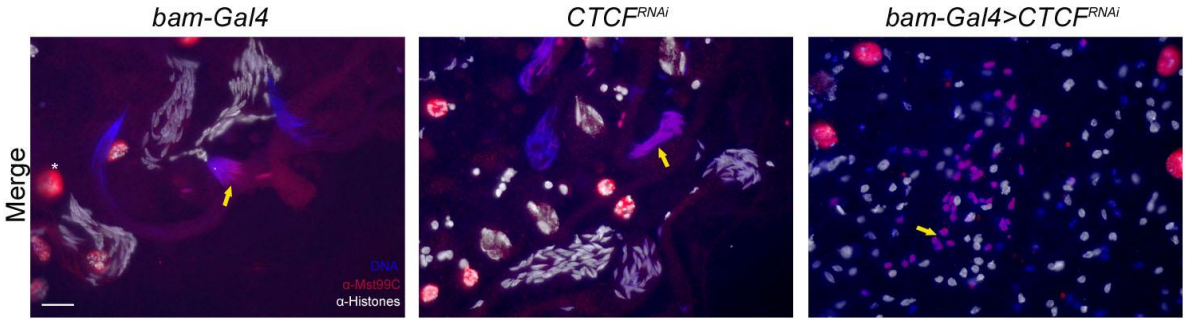

Figure 30 Spermiogenesis is disturbed in *bam-Gal4>CTCF^{RNAi}* flies however Prtl99C expression is not affected. Overview to *bam-Gal4*, *CTCF^{RNAi}* and *bamGal4>CTCF^{RNAi}* testes. Merge: overlay of the fluorescence images in which DNA was stained with Hoechst dye (blue), Prtl99C using anti-Prtl99C antibody (red) and histones (white) using anti-histones antibody. Yellow arrows indicate Prtl99C positive late canoe cysts. *bam-Gal4>CTCF^{RNAi}* flies showed apparently misshaped canoe stage nuclei which were still Prtl99C positive. Red strong signal in somatic cells is background caused by anti-Prtl99C antibody. Scale bar: 20 µm.

Name of the target gene	Driven with *bam-Gal4*	Driven with *c135 -Gal4*
	Prtl99C expression pattern	
ISWI	normal	normal
CAF1-p75	normal	normal
CAF1-p180	normal	normal
CTCF	normal*	normal

Table 3 Summary of RNAi experiments performed against *ISWI, CAF1-p75, CAF1-p180* and *CTCF*. Prtl99C expression was normal in all RNAi-mediated knock-down experiments driven with bam-Gal4 or c135-Gal4. (*) *bam-Gal4>CTCF^{RNAi}* flies showed a phenotype during spermiogenesis (see Figure 30).

The identification of different molecular chaperons for each individual chromatin associated sperm protein would argue for independent loading of these proteins. Therefore, this should be clarified in particular with respect to additive effect for chromatin compaction.

6 Discussion

Understanding the sperm epigenetics is pivotal to figure out the causes of male infertility. Major characteristics during spermatogenesis are condensation and proper packaging of the sperm chromatin. Both in mammals and flies, this is achieved by the incorporation of male specific proteins known mainly as protamines preceded by several players such as histone modifications, transition proteins, etc. (reviewed by Minocherhomji et al., 2010; Rathke et al., 2014). Currently, our knowledge regarding this large-scale genome compaction is still limited. Until a decade ago, there was only evidence for sperm specific transcripts (Mst) with the potential to encode small basic proteins in *Drosophila* (Andrews et al., 2000; Ashburner et al., 1999; Russell and Kaiser, 1993). First; expression pattern of *Drosophila* protamines and Mst77F were characterized but deleting them caused only minor phenotype thus evidence was gained that more proteins are involved in the packaging of mature sperm genome (Rathke et al., 2010; Jayaramaiah Raja and Renkawitz-Pohl, 2005). Indeed, a few years after, relevant studies showed that in contrast to mice (Cho et al., 2001), *Drosophila* protamines are not essential for male fertility (Rathke et al., 2010; Tirmarche et al., 2014). *Drosophila* sperm lacking protamines are more sensitive to X-rays. Haplo-insufficient protamine mutants of mice carry more DNA breaks. Nevertheless, the *protamine* mutant phenotypes of mice and *Drosophila* were not disruptive as expected. Loss of one copy of mice protamine 1 or protamine 2 resulted in haploinsufficiency and disturbed the processing of protamine 2 (Cho et al., 2003). With the identification of more male specific proteins expressed during spermiogenesis, now, we do see that *Drosophila* chromatin compaction is a dynamic process with the involvement of several players.

In this thesis, I aimed to identify further *Drosophila* sperm specific proteins acting especially in chromatin condensation and male fertility. Prtl99C is identified as a novel sperm chromatin binding protein displaying an expression pattern similar to that of protamines. Prtl99C is essential for male fertility, in addition, similar to protamines, it contains an HMG-box domain. Prtl99C compacts paternal genome, therefore, its absence leads to extended chromatin region. Significantly, our results suggest a function of Prtl99C as a structural protein involved in the condensation of the *Drosophila* sperm genome during post meiotic spermatid maturation (Chapter 5.1). The fact that male specific proteins – protamine A, B

and Prtl99C - compact the DNA in an additive manner raises the possibility that more male specific chromatin components exist. For that purpose, I intended to develop a protocol to extract proteins from enriched sperm nucleus for proteomics use (Chapter 5.2). Since the experimental studies for sub fractionation of sperm cell were unsuccessful, my major research focused on to the characterization of Prtl99C and other male specific candidates (Chapter 5.3).

6.1 Protamine-like proteins in sperm

The size and amino acid sequence of proteins used to package sperm DNA vary significantly from invertebrates to vertebrates. The protamine family is thought to be evolved from specialized histones through protamine-like proteins (Balhorn, 2007). Moreover, it has been postulated that the dynamic condensation of sperm is facilitated by the appearance of intermediate proteins between histones and protamines. This allows consecutively nuclear shaping (Chiva et al., 2011). In frogs, the genus *Rana* sperm DNA is packed with histones while *Xenopus* sperm is packed both with histones and protamine-like intermediate proteins, furthermore, the *Bufo* sperm DNA is packed with histones and protamines (Zini and Agarwal, 2011). As we can see, a lot of variations may be well possible even between similar species. Importantly, the major difference between sperm-specific nuclear basic proteins and somatically expressed proteins is the high content of arginine and lysine on sperm proteins. These amino acids are known to be present in all somatically expressed proteins at low level (~5%) (Reviewed by Balhorn and Balhorn, 2011). Even in a lower level than in protamines (70% arginine), protamine-like proteins at a size of 100 to 200 amino acids are rich in lysine and arginine content (35-50%) in vertebrates (Balhorn, 2007, Table 4).

Drosophila protamines (Mst35Ba and Mst35Bb) are considered as homologs of mammalian protamines due to their significant similarities in cysteine, lysine and arginine content. Likewise, *Drosophila* Mst77F shows 39% similarity to mouse HILS1 (Jayaramaiah Raja and Renkawitz-Pohl, 2005), however recent data indicate, that protein domains are rather different between HILS1 and linker histones (Doyen et al., 2015; Kost et al., 2015). Prtl99C is a small basic protein richer in arginine rather than cysteine content (Table 4).

Tpl94D, Prtl99C and protamines are predicted to be part of the unknown function 1074 (DUF1074) family (UniProt, 2015). A very recent work summarized and revealed additional candidates for the presence of male specific transcript (MST)-HMG-box domain in *Drosophila* sperm chromatin proteins (Doyen et al., 2015). MST-HMG-box domain in Mst77F and in uncharacterized proteins such as MST33A, CG30356, and CG42355 resembles a truncated form of the canonical HMG-box and DUF1074. While a full length HMG-box is present in several known male specific proteins of *Drosophila* such as Protamines (Gärtner et al., 2015), Tpl94D (Rathke et al., 2007), Prtl99C (this thesis). However, there is no evidence of sequence homology of these proteins with their mammalian homologs. Not surprisingly, MST-HMG-box proteins are not found in mammals (Doyen et al., 2015). Mst77F contains in addition a coiled-coil domain, proven to allow homo-dimerization and an intrinsically unstructured C-terminal domain (CTD) which allows DNA binding at least in vitro (Kost et al., 2015). Prtl99C does not reveal significant sequence homology neither with histones nor with *Drosophila* protamines. The identification of the uncharacterized MST-HMG-box proteins will help to understand the diversity and the precise function of intermediate basic proteins in *Drosophila* spermiogenesis.

Name	Total #aa	% Cysteine	%Lysine	% Arginine
hProt1	51	11.8	0	47.1
hProt2	102	4.9	2.0	32.4
dProtA	146	6.8	14.4	12.3
dProtB	144	6.9	15.3	10.4
Mst77F	215	4.7	13.5	9.8
Prtl99C	201	2.5	11.0	12.4

Table 4 Summary of the basic amino acid (lysine and arginine) and cysteine percentages in several chromatin condensing proteins from human and *Drosophila*.

6.2 Chromatin condensation during *Drosophila* spermiogenesis

Both mammalian and fly sperm consist of proteins acting in chromatin organization, DNA packaging and chromatin modification (Castillo et al., 2014; Rathke et al., 2014). The

overall aim of all these processes are to guarantee a compact chromatin structure in order to minimize DNA damage and protect the paternal genome.

Spermatogenesis in *Drosophila* is defined by continuous expression of HMG-box and MST-HMG-box proteins which are thought to organize DNA condensation (Doyen et al., 2015; Gärtner et al., 2015; Rathke et al., 2007). These male specific proteins are structurally different from somatically expressed chromosomal proteins. Both in mammals and flies this is likely achieved by the presence of arginine and lysine residues to neutralize DNA. Arginine residues are rich in protamines and they bind to the chromatin within the major groove of DNA (Kanippayoor et al., 2013). It has been shown that lysine is less successful in densely packing DNA than arginine, therefore, DNA packed by only lysine rich peptides would permit more DNA damage (DeRouchey et al., 2013). Human protamines almost do not contain lysine residues, whereas, in *Drosophila,* among protamines and Prtl99C the ratio between arginine and lysine is almost the same (Table 4). It remains unclear how DNA condensation occurs with proteins of different amino acid compositions and why *Drosophila* protamines and Prtl99C have a higher lysine percentage than mammalian protamines.

Apart of the positively charged amino acids, male specific nuclear proteins contain also cysteines which form disulfide bonds (Table 4). For instance, by inducing the coiling and condensation of DNA into much larger toroidal chromatin subunits, it is proposed that highly positively charged protamines are able to coil DNA in a different manner than histones (Balhorn, 2007).

The formation of zinc bridges with thiols of cysteines and disulfide bonds between the protamines intercalated into different DNA strands bring further condensation and stability to the sperm chromatin (Wouters-Tyrou et al., 1998; Rousseaux and Khochbin, 2011). Furthermore, protamines have also several phosphorylation sites which are thought to prevent specific sites from DNA interaction (Balhorn, 2007). These properties are giving male specific proteins a unique function in order to compact the chromatin and stabilize the paternal genome before fertilization.

Besides their high isoelectric points, male specific nuclear proteins contain several domains which give them distinct properties. For example, Mst77F contains a coiled-coil domain as a homodimerization domain and a region of low complexity at the C-terminal which mediates DNA binding. LCR-containing proteins have likely more binding partners

than proteins that have no LCRs (Coletta et al., 2010). Recent in vitro studies demonstrated DNA and chromatin aggregation by multimerization caused by Mst77F alone. These properties contribute to condense DNA and in chromatin organization during spermiogenesis (Kost et al., 2015). Prtl99C, different to Mst77F, contains a central low complexity region (Chapter 5.1.1).

6.3 Role of Prtl99C

To get insight into the biological function of Prtl99C, we analyzed several fly lines in which Prtl99C was affected. Mutant *Drosophila* male lacking *Prtl99C* are sterile (*Cad99C*^{248A}). The rescue of the *Cad99C*^{248A} mutation by 386-Prtl99C-eGFP proved that the sterility of *Cad99C*^{248A} mutant was due to the lack of *Prtl99C*. Furthermore, depletion of *Prtl99C* or a truncated version of Prtl99C (Prtl99C-ΔC) led to reduced male fertility. Withal, the introduction of Prtl99C-ΔC-eGFP to the Cad99C^{248A} mutation rescued the sterility partially. In other words, Prtl99C-ΔC, which still contains the N-terminal HMG-box domain and central low complexity region, is not fully functional. Taken together, our results proved that Prtl99C is required for male fertility and its C-terminal contributes significantly to fertility (Chapter 5.1.3).

6.3.1 Role of Prtl99C in male fertility

Although we know that Prtl99C is essential for male fertility, we do not know precisely the reason behind. It is proposed that the major function of protamines is for fertilization, and not for embryogenesis. Round spermatid injection (ROSI) with protamine deficient sperm leads to normal development in mouse suggesting that protamines are not essential for the development of the embryo (Ward, 2010). As Prtl99C has characteristics similar to protamines we do expect a role of Prtl99C for fertilization and not in embryogenesis. Alternatively, sterility can be due to swimming defect as sperm swimming is crucial in male fertility determination (Luke et al., 2015). Surprisingly, very few but motile sperm were

observed in *Cad99C*^{248A} mutant seminal vesicles (Chapter 5.1.3.1). Therefore, Prtl99C likely is not causing a motility defect but rather affecting fertility in other aspects.

6.3.2 Role of Prtl99C in chromatin compaction

Importantly, any alteration in head size and shape can influence sperm competition (Luke et al., 2015). Lack of Prtl99C in *Cad99C*^{248A} mutant leads to nuclear defects in late spermiogenesis starting from the stage of individualization. Nuclear elongation is the common phenotype observed in all analyzed lines in which *Prtl99C* is affected (Chapter 5.1.4). Sperm nuclei of *Prtl99C* mutants were up to 40% longer than wild type ones. Those of *protΔ* mutants were moderately elongated, at 9% longer of the size of that of wild type (Figure 31A). This small elongation in *protΔ* mutants was significant as these sperm were more sensitive to DNA damage, reflected in an increase in induced mutations (Rathke et al., 2010). Sperm nuclei of *protΔ; Cad99C*^{248A} were up to 47% longer than the wild type length, i.e., the effect was additive (Figure 31B); as these mutants are infertile, the sensitivity to mutagens cannot be tested genetically. Potentially also Mst77F mutants would lead to an extension of the chromatin areas. Unfortunately, because of its dual function in chromatin organization and nuclear shaping these flies do not have individualized sperm. The nuclei are tid shaped when a deletion is placed in trans to a point mutation (Jayaramaiah Raja and Renkawitz-Pohl, 2005). Therefore no further mutants - for example caused by transposon insertion in the open reading frame - could be analyzed for this possibility.

In mammals, even though sperm condensation is not directly linked with sperm head shaping, the incorporation of protamines obliquely gives rise to a vigorous sperm head, in turn, poorly packed chromatin is associated with enlarged or abnormal head shapes (Balhorn, 2007). It is bizarre that very few sperm can individualize and reach the seminal vesicles in Prtl99C deficiencies, however, a defect like elongation of sperm chromatin region might be sufficient to lead to infertility

Murex brandaris, a mollusk, has a complex nuclear protein transition as histones are replaced by protamine precursors and condensing chromatin is continually associated with the inner and outer nuclear envelope. It has been demonstrated that the form and the volume

of the nucleus simultaneously influences the organization and arrangement of the chromatin condensation pattern (Chiva et al., 2011). However, our observations with Prtl99C revealed that chromatin condensation influences the volume of the nucleus but not the shape as we did not observe alterations in wild type needle-like shape. The different observations between our group and Chiva et al., is likely due to the morphological differences between *Drosophila* and *Murex brandaris* sperm nucleus.

A

Strain	Mean length of nuclei (µm) ± SD	% from wild type
wild type	10.55 ± 0.33	100.0
bam-Gal4>Prtl99C^{RNAi}	14.26 ± 0.47	135.1
Prtl99C-ΔC	14.09 ± 0.26	133.6
Prtl99C-ΔC/Cad99C^{248A}	13.80 ± 0.32	130.9
*Cad99C^{248A}**	14.72 ± 0.61	139.6
protΔ	11.48 ± 0.21	108.8
protΔ;Cad99C^{248A*}	15.49 ± 0.71	146.8
Rescued Cad99C^{248A}	12.99 ± 0.22	123.1

B

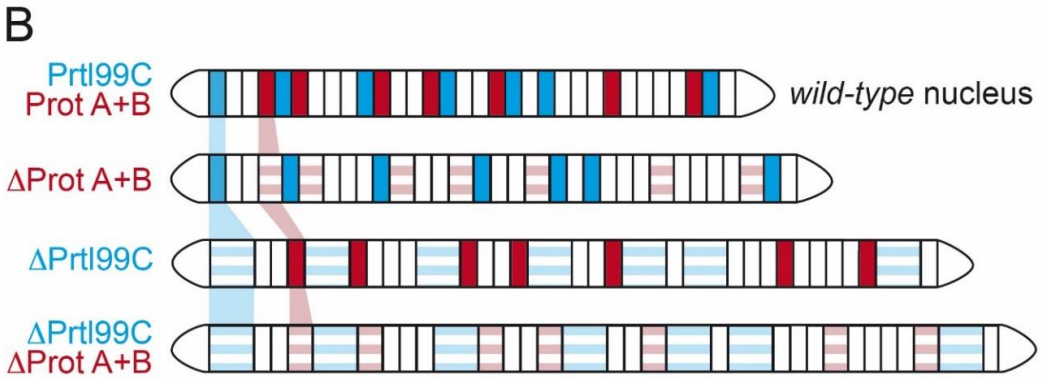

Figure 31 Lack of sperm nuclear basic proteins leads to less compacted chromatin thus enhances the nucleus length. (A) Mean length and standard deviation (SD) of nuclei of mature sperm in wild type and six mutants (n = 20). The percentage of the deviation from the wild-type sperm (100%) is given. *, mean length during individualization, as these strains are sterile. (B) Simple model showing the additive effect of loss of Prtl99C and protamines. Representation of colors: Protamines (red), Prtl99C (blue), and other proposed unidentified putative proteins (white areas). Histones are not shown. The model shows how the length of a nucleus locally increases upon loss of protamines (light red horizontal stripes) or upon loss of Prtl99C (light blue horizontal stripes), and the additive effect of the loss of both protamines and Prtl99C

On the other hand, it is still obscure how human sperm morphology is associated with its function. To understand how protamine deficiency is associated with sperm head morphology, Utsuno and colleagues, compared patient's protamine-deficient and non-

deficient spermatozoa using elliptic Fourier analysis. They observed considerable alterations in sperm head shape and size in protamine-deficient spermatozoa and indicated that sperm head morphology may slightly be a reflection of protamine levels in human (Utsuno et al., 2014). Accordingly, these findings help to understand why loss of Prtl99C leads to longer sperm nucleus length.

Propitious fertilization is possible with properly compacted sperm of good quality (Oliva, 2006). Very recently Ausio et al. examined structural organization of sperm chromatin from three vertebrates (bony fish, birds and mammals) (Ausio et al., 2014). Calculating DNA packing densities in sperm nuclei of each species they showed that mouse has the highest compaction compared to the rooster and zebrafish. The differences in DNA compaction are interesting to better understand the structural organization of the sperm chromatin. Up to date no structural examination of *Drosophila* sperm has been performed besides ultrastructural analysis (For review see Fuller, 1993; Yasuno and Yamamoto, 2014). These authors observed an uneven distribution of chromatin in the nucleus in transgenic flies carrying ProtamineB-eGFP in addition to the internal protamine genes.

It would be very intriguing to see how protamine-containing chromatin structure is and how Prtl99C packs DNA to complement the role of other sperm-specific basic proteins. In cooperation with Dr. Wolfgang Fischle Lab (Göttingen), we aimed to analyze structural effects of Prtl99C *in vitro* and *in vivo* on chromatin and its interaction with DNA. Unfortunately, we were not able to express Prtl99C protein in *Escherichia coli* (data not published). Accordingly, and with the results of this work showing Prtl99C compacting paternal genome, we can only assume that Prtl99C likely interacts with DNA. Thus, biochemical and biophysical experiments are essential to prove if Prtl99C is indeed a DNA/chromatin architectural protein.

Based on our data so far, we concluded that Prtl99C is responsible for chromatin organization and essential for male fertility. As the sperm nuclear morphology is altered, we assume that the fertility is indirectly affected. Further examinations are required in order to elucidate the main reason of infertility in Prtl99C deficiencies.

6.4 Mst77F and Protamines are deposited to the sperm chromatin independent of Prtl99C

We checked the distribution of Mst77F and protamines in homozygous *Prtl99C* mutants as well as the distribution of Prtl99C in homozygous *protΔ* males. In both cases, histone removal and loading of Mst77F, protamines or Prtl99C proceeded as in wild type situation, indicating that they were independently localized to the chromatin (Chapter 5.1.6). Moreover, additional expression of 942- or 386- Prtl99C-eGFP did not rescue the morphologic sperm head defect of *protΔ* males as is known from Mst77F-eGFP (Rathke et al., 2010) (Chapter 5.1.8). The independent loading of different chromosomal proteins to sperm suggests a spatial difference. Moreover, the loading of protamines requires CAF1-p75, while CAF1 is not required for Mst77F loading (Doyen et al., 2013). These results let us to suggest that Prtl99C, protamines and Mst77F are loaded independently into DNA and likely have individual distinct functions during chromatin reorganization.

A recent work described Mst77F as a critical element in the hierarchical assembly of sperm chromatin (Doyen et al., 2015). Depletion of *Mst77F* via RNAi showed the essentiality of Mst77F for the loading of protamines. Since the diminished level of *Mst77F* transcripts were not checked quantitatively, the 18 *Mst77F* pseudogenes (*Mst77Y-1 to Mst77Y-18*) found on the Y chromosome in *Drosophila melanogaster* were not taken into consideration while interpreting the knockdown experiments. The *Mst77F* pseudogenes contribute about 25% of the MST transcripts (Krsticevic et al., 2010; Russell and Kaiser, 1993). For instance, *in-situ* probe for *Mst77F* and microarray assay likely detected signal from transcripts of several of the 18 *Mst77F* pseudogenes in male germ cells (Barckmann et al., 2013), therefore, it is well possible that the RNAi target sequence knockdown also some of the pseudogenes. If so, the effect might be due to knocking down both the transcripts from MST copy at 77F on the third chromosome and/or the MST copies on the Y chromosome. When in fact, ProtB-eGFP was deposited properly on the sperm chromatin of male flies carrying an Mst77F point mutation in trans to a deficiency. Moreover, the introduction of ProtB-eGFP was not able to rescue the scattered tid nuclear phenotype of late spermatids of this genetic situation (Jayaramaiah Raja and Renkawitz-Pohl, 2005). Therefore, Doyen et al. 2015, should clarify how trustable was the knockdown phenotype of *C135>MST77F*^{RNAi} regarding chromatin compaction defects

and consider to revise the role of Mst77F which they proposed. Apart from that, they should also consider that Mst77F starts to appear already at early spermatids related to its additional function with microtubules, with which Mst77F seems to co-localize under the light microscope. The Mst77F point mutation seems to only have an effect on nuclear shaping function of Mst77F (Jayaramaiah Raja and Renkawitz-Pohl, 2005). Thus, this mutant cannot be used to address any role concerning chromatin compaction. The knockdown experiment of Doyen and colleagues, could have also affected the nuclear shaping function of Mst77F as the malformed nuclei and absence of mature sperm were reported (Doyen et al., 2015).

6.5 Model for additive chromatin compaction by independent loading of different proteins to condense the sperm chromatin

Our previous and current data shows distinct accumulation and/or punctuated pattern along the chromatin among the independent attitude of male specific proteins (This work, Rathke et al., 2010). Therefore, on the strength of our results, we speculate that *Drosophila* sperm chromatin is condensed by several proteins that act in an additive manner to the compaction of sperm chromatin. For instance, lack or dysfunction of one protein induces extension of sperm nuclei, and further lack or dysfunction of another protein induces an additive elongation of sperm nuclei (Figure 32). Even if the potential additive elongation due to the lack of Mst77F has still not been proven, we know that Mst77F is associated with both DNA and chromatin condensation (Kost et al., 2015). Accordingly, we suggest that the lack of Mst77F would induce an additional elongation of the nuclei length in sperm (Figure 32).

Importantly, our model does not intend to reflect any temporal segregation but we hypothesize that DNA sequences bound with different proteins (Mst77F, Prtl99C, protamine A and B, and perhaps other unidentified proteins) may package different regions of the paternal genome (Figure 32, Chapter 5.1.5). Clearly, we cannot exclude that some areas are compacted by an interaction of these proteins. Moreover, proteomics data showed the presence of histones in *Drosophila* sperm (Dorus et al., 2006; Miller et al., 2010). Here, in

our model, we do not concentrate neither on the presence nor on the role of histones in sperm. However, recent findings in mammals can help to dissect the packaging strategy of the paternal genome. It seems that specific sequences are bound specifically to sperm basic proteins whereas others are associated with histones. In humans about 8% of the sperm DNA is arranged by histones (Castillo et al., 2014). Relevant data obtained from human spermatozoa showed the non-random distribution of histones and their association with specific genes (Ward, 2010). In a former study, the presence of sperm histones was linked to weak protamination, but later the presence of these histones let to the hypothesis that sperm chromatin might be able to transfer epigenetic information that influence post-fertilization events (Carrell, 2012). At the moment, many researchers are interested in sperm histone dynamics as they are considered to transfer the paternal genetic information to the next generation (Castillo et al., 2014).

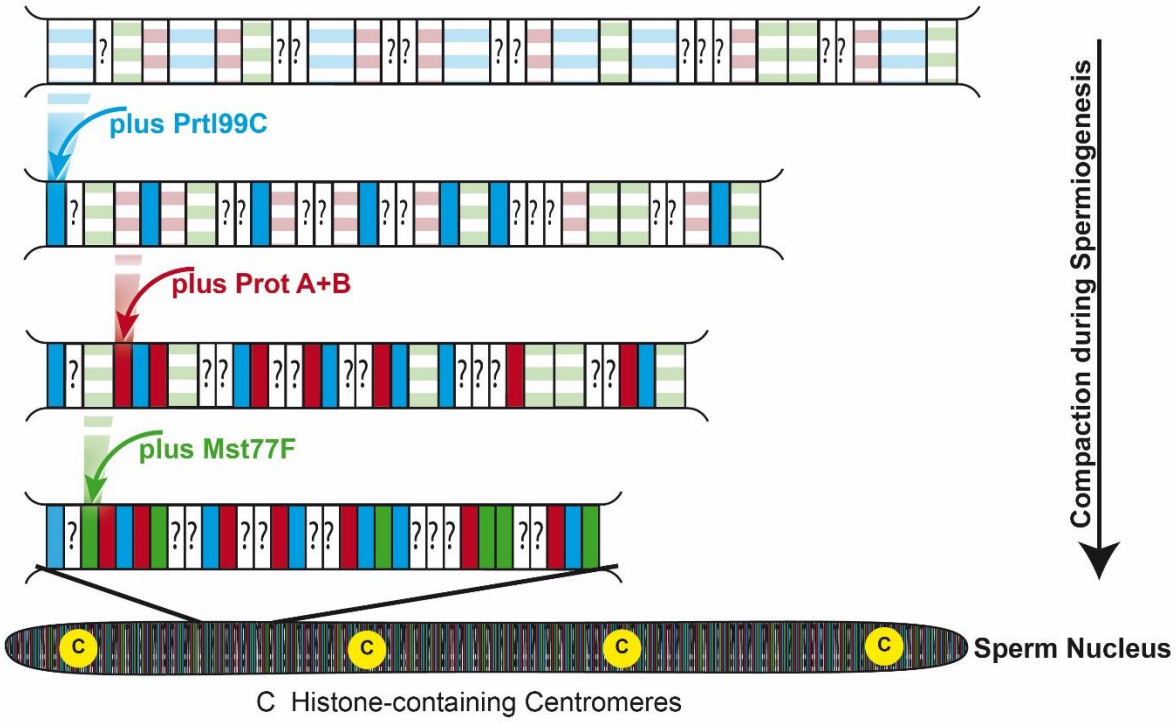

Figure 32 Model of chromatin compaction achieved by additive effects of several proteins in *Drosophila* sperm. The spermatid chromatin contains areas for binding of Prtl99C (light blue horizontal stripes), protamines (light red horizontal stripes), Mst77F (light green horizontal stripes), and other proposed unidentified putative proteins (?). Histones are not shown. We proposed that these areas are independently compacted by deposition of Prtl99C (blue), Protamines (red), and Mst77F (green). Other unidentified putative proteins (?) may contribute to the compaction. This leads to a fully compacted chromatin of the sperm nucleus.

Our lab also aimed to address the localization of the *Drosophila* nuclear sperm proteins by ChIP (Kaiser, Bartkuhn, Renkawitz-Pohl personal communication). However, so far ChIP experiments have failed, likely due to the extreme genome compaction in non-histone based areas of the chromatin on fly sperm, and in part due to the lack of methods to separate the long sperm tail (2000 μm long) from the short nuclei (10 μm).

This information, together with our present knowledge of protamine structure and function, make it clear that the sperm genome is much more complex than what the researchers thought two decades ago. Sperm chromatin composition and chromatin packaging are connected strongly with male infertility problems and the progression of early embryogenesis. Presumably also in mammals, other sperm specific nuclear proteins may exist in order to strengthen the role of protamines. Further investigations are required to clarify the molecular level of sperm nucleus in order to unravel the reasons giving rise to male infertility in *Drosophila* and mammals. Based on our hypothesis, it would be of interest to identify the subset of genes that retain histone packaging, and, on the other hand, the ones which are packaged with sperm specific nuclear proteins, in order to have a better insight on the functional reasons behind this differential packaging.

6.6 Further candidate proteins for sperm chromatin

Based on our hypothesis, we aimed to identify the subset of sperm proteins potentially involved in chromatin and nuclear function. A very recent study from our lab identified >6600 testis proteins, however, some of the sperm nuclear proteins might be under representation due the high compaction of the chromatin (Gärtner et al., in preparation). *Drosophila* sperm nuclear proteomics and its comparison to the existing human sperm proteome would unravel many novel sperm proteins. Furthermore, sperm proteomic dissections are giving direct information about the protein status of the cell as transcription and translation are almost shut off (Amaral et al., 2013). Therefore, in this thesis, we first intended to enrich sperm head for nuclear protein extraction for proteomic purpose (Chapter 5.2).

The isolation of *Drosophila* sperm nuclear proteins was complicated due to extremely long tail and high degree of condensation of the sperm DNA. Since the chromatin is tremendously compacted, mammalian sperm nucleus is resistant to sonication and even washing with ionic detergents (Ward, 2010). For that reason, we tried sonication and observed that although *Drosophila* sperm head and tail are separable via sonication, the tail residues are in diverse length and the morphology is also needle-like shape (Chapter 5.2.1). After separating the head from the tail, the width and shape of sperm head and tail residues were so similar that − excluding their potential difference in density − traditional sucrose density gradient were useless for sub fractionation.

As an alternative, Fluorescence Activated Cell Sorting (FACS), which is the only accessible purification technique to separate cells based on internal staining, intracellular protein expression or expression of transgenic fluorescent protein, could be used to sub fractionate sperm cells (Basu et al., 2010). Indeed, the double transgenic flies expressing RFP in sperm head and GFP in sperm tail would be a perfect sample to sort by FACS. But also here we faced some limitations. First, we never obtained a clear head or tail residues without contaminant as a starting material. Moreover, often diverse length of tail pieces with small tail clouds were observed. Secondly, the shape and the size of the sperm head of *Drosophila* (needle-like shape and approximately 10 µm in length) is very different compared to mammals (disc shaped 5.1 µm by 3.1 µm). Therefore, we are not sure if it is possible to sort cell compartments which are very thin in width. For instance, due to the laminar flow properties of the core stream within the sheath fluid in the FACS machine, we would expect the long axis of the needle-like head and tail sections to align parallel to the direction of flow. Notwithstanding, we cannot estimate any result without any intention.

Despite our unsuccessful attempt of *Drosophila* sperm nuclear protein extraction, instead, we compared the existing developmental testis and sperm proteomics results in order to identify sperm nuclear proteins which had not been detected in previous whole sperm proteome studies (Chapter 5.4). Surprisingly, CG6332 looks like a promising candidate to have a function in sperm. *CG6332* mutants are male sterile. Interestingly, contradictory independent mutagenesis studies were done on mice by two different research groups (Mannan et al., 2003; Yanaka et al., 2000). Yanaka and colleagues observed abnormalities in the spermatogenesis of insertional mutant mice, in contrast, just three years later Mannan and colleagues generated *Theg* knockout mouse models illustrating that Theg is not essential

for mouse spermatogenesis. Therefore, it will be interesting to follow the distribution of CG6332 during spermatogenesis since proteomic data indicate a specific expression for adult testis and it is also expressed in sperm (This work, Gärtner et al., in preparation, Dorus et al., 2006).

7 Supplemental Information

Supplemental Tables

Strain	Fertility
wild type	Fertile (all matings had progeny)
Cad99C^{248A}	Sterile (no matings had progeny)
Cad99C^{248A} rescued with *942-Prtl99C-eGFP*	Relatively fertile (55% of matings had progeny)
Cad99C^{248A} rescued with *386-Prtl99C-eGFP*	Relatively fertile (55% of matings had progeny)
Cad99C^{248A} rescued with *Prtl99C-ΔC-eGFP**	Reduced (42 % of matings had few progeny)
Prtl99C-ΔC	Reduced (50% of matings had progeny)
bam-Gal4>Prtl99C^{RNAi}	Strongly reduced (5% of matings had few progeny)
Prtl99C-ΔC/Cad99C^{248A}	Reduced (27% of matings had progeny)
ProtΔ;Cad99C^{248A}	Sterile (no matings had progeny)

Table S 1 Summary of the male fertility on wild type and various fly strains in which *Prtl99C* is affected. n=20, except * n=14. Few progeny means bottle with only 3-4 offsprings.

Strain	Average nucleus length			Standard deviation	
	Spermatid during ind.	Mature sperm		Spermatid during ind.	Mature sperm
wild type	10.93	10.55		±0.62	±0.65
bam-Gal4>Prtl99C^{RNAi}	13.12	14.26		±1.34	±0.94
Prtl99C-ΔC	12.46	14.09		±0.98	±0.52
Prtl99C-ΔC/Cad99C^{248A}	12.75	13.80		±1.34	±0.64
Cad99C^{248A*}	14.72	-		±1.23	-
ProtΔ	11.74	11.48		±0.58	±0.42
ProtΔ;Cad99C^{248A*}	15.49	-		±1.43	-
Cad99C^{248A} rescued with *386-Prtl99C-eGFP*	12.95	12.99		±0.79	±0.43

Table S 2 Mean length of nuclei of spermatids during individualization (ind.) and mature sperm in wild type and in various fly strains in which *Prtl99C* was affected. Standard deviations are given for each strain. (n = 20).

Figure S1 Human testicular haploid expressed gene protein isoform 1 amino acid alignment with *Drosophila melanogaster* CG6332 protein. The alignment was generated using clustalW. (*), positions which have a single, fully conserved residue; (:), conservation between groups of strongly similar properties; and (.), conservation between groups of weakly similar properties

Target sequences of RNAi constructs

RNAi target sequence against *Prtl99C* (v106856) from the Vienna *Drosophila* Resource Centre

TACGTGGCCTGTGAGATGAAAAGCGATGTCGCCGGAGGACAGCAAAGTTCTTGCCAAAGACAGTCTCCAAG
CGCTCGGCTGAGGGAATCGGAGAGGAGATCGTCCAGATCGAAGACCTTGTGCAGATCAGCAAAGAATCGTC
AGCGAGGGAAGCCGAAACCTCAGCAAAGCAAGCGCAGGCTCAGTCACATGGGCTCGGCAGTGGCATATAT
CCACTTCCTGCGCAAGTTCCAAAGGAAGAATACTGAGTTGCGCACCATCGATCTGCTGAAGACGGCAACT

RNAi target sequence against *CAF1-p75* (v20270) from the Vienna *Drosophila* Resource Centre

GTGCCGTTTGCCATTGTGTCCAACATTCACTATAGCAGGCTTACGGATTTGGCCTGGTCGAGCGACGGCACC
GTCCTGATCGTGTCCAGCACCGATGGCTACTGCTCACTGATTACCTTCGAGCCAACCGAGCTGGGCGACTGC

TATGAAGATATGGAAACAGTGCTGAGCGTTGTTCTAAAATCTTCAGAGAATGCAACGGTGTTGAAAAAGAA
GAGGCAAAAGCTGCGCAAGGTATCGTTGGATGAACCACGGAAACCACTGCAGGAAAAATCGAAACCAAAT
ACAATTAGAAGGGCGTCCGAAGCAGGTATCACAGAGGTAGGGGAAC

RNAi target sequence against *ISWI* (v6208) from the Vienna *Drosophila* Resource Centre

ACACAAACGGCGAGGCAGGAACTTCTTCCGTATATCAATTCGAGGGTGAGGATTGGCGCGAGAAGCAAAAG
CTAAATGCGCTGGGCAACTGGATCGAGCCACCGAAGCGTGAACGCAAAGCCAACTATGCTGTGGATGCCTA
TTTCCGCGAGGCTCTCCGTGTCTCCGAACCCAAGGCACCGAAGGCTCCCCGCCCACCCAAGCAGCCTATCGT
TCAGGACTTTCAGTTC TTCCCACCCC GTCTGTTTGA

RNAi target sequence against *CTCF* (v108857) from the Vienna *Drosophila* Resource Centre

TAAATCGCGACTTGCAGATGTCGCATTGGTACTTCTTCTCGCCGGTGTGGATAACCATGTGTCGCTTCAGCTT
GAACATGTCCTGCGATGCGTAGGTGCAGTGCGGACATTGATATGGTCTCTCGCCCGTATGGCAGGTCATGTG
GCGGCGCAGTTTGGTCAGTTCCACGCTGGCGTATGTGCACTCCGTGCACTTGTGCGGTTTTTCCTTAGTGTGC
TTGTAGCGAGTGTGACGGACCAGCTCGCCGCTGGTGGTGAAGGCGCTTTCGCAGAGCTTGCACTTGTGCGGC
TTATTGCCCATGTGCGTGTTTATGTGGTTTTGCAGGCCCACGTTCGATCGAAAGGACCTCTCGCAGATGGAG
CACTTGAAGGATGGCTCGACGTCATGACTTCGTGAGTGGCGCGTGATCAGAAACTTCTTGCTCGCCGTATAC
GGGCAGTGTGGGCATGAGTACTTATGTCCCGATGCATTCGAATTCTGGCTGGTAGAAGAAGCTGTCTTCAGC
TTCACCTCCTTGTTGCTTAGCACAAAGTCTACGTCCTTCTTGTCGGCATTCTCATCCTCTGTCG
TCGCATTGTCCTCAAATTCGTAGACCTCAGCCTCGT

RNAi target sequence against *CAF1-p180* (BL28918) from the Vienna *Drosophila* Resource Centre

GCAGAGGATTCCAAACCAAAAGAAGTCCCTAAGAAGGAAACAAGCAAAACCGGAGGAAAAGGCAAGAAG
GAGGGAGCAAAACCAGCTGAAAAGAGTAAGAAAGAAGAGAAGGAAGACAGCACAACAAAGTCAAAGAAA
GAGAAAGCAGACTCACCTGCAAATAATCAAAAAGAACAACAAATTGGAGTCAAGAAAAAGACTTCTGAAC
CAGAAGATGCATCGAACTCACACAAATCGGTGACGGCCAAAAAGGATTCCAAGAAAGACGAGGCATCTAC
TCAAGTTAAGTCGGACAACGAATCTCCGGAAGCAGCAGAAATCTCGATGATCCTCTCGACCAGCGAGGCCA
ACAGTTCCAGCAGCGAGCACGAGATGGATGCGGATACGGACACCGCGGCCACCGACAGACCCTCCGCCCAA
AAGGAGACTCGCCTGAACA

Cloning of the *G42592-eGFP, 386-Prtl99C-eGFP* and *Prtl99C-ΔC-eGFP* constructs

To generate the *CG42592-eGFP* construct, the *CG42592* gene together with a 1,548-bp sequence upstream of the translational start codon was PCR amplified using genomic DNA and primers with linked *EcoRI* and *SpeI* restriction sites.

To generate the *386-Prtl99C-eGFP* construct, the *Prtl99C* gene together with a 386-sequence upstream of the translational start codon was PCR amplified using genomic DNA and primers with linked *EcoRI* and *SpeI* restriction sites.

To generate the *Prtl99C-ΔC-eGFP* construct, the first 450-bp of the *Prtl99C* gene together with a 386-bp sequence upstream of the translational start codon was PCR amplified using genomic DNA and primers with linked *KpnI* and *SpeI* restriction sites.

The PCR fragment was inserted into *pChabΔsalΔlacZ-eGFP* in-frame with *eGFP*. Transgenic fly strains were established in w^{1118} background.

8 References

Adams, M.D., Celniker, S.E., Holt, R.A., Evans, C.A., Gocayne, J.D., Amanatides, P.G., Scherer, S.E., Li, P.W., Hoskins, R.A., Galle, R.F., *et al.* (2000). The genome sequence of *Drosophila melanogaster*. Science *287*, 2185-2195.

Amaral, A., Castillo, J., Estanyol, J.M., Ballesca, J.L., Ramalho-Santos, J., and Oliva, R. (2013). Human sperm tail proteome suggests new endogenous metabolic pathways. Molecular & cellular proteomics : MCP *12*, 330-342.

Andrews, J., Bouffard, G.G., Cheadle, C., Lu, J., Becker, K.G., and Oliver, B. (2000). Gene discovery using computational and microarray analysis of transcription in the *Drosophila melanogaster* testis. Genome research *10*, 2030-2043.

Antosch, M., Mortensen, S.A., and Grasser, K.D. (2012). Plant proteins containing high mobility group box DNA-binding domains modulate different nuclear processes. Plant physiology *159*, 875-883.

Ashburner, M., Misra, S., Roote, J., Lewis, S.E., Blazej, R., Davis, T., Doyle, C., Galle, R., George, R., Harris, N., *et al.* (1999). An exploration of the sequence of a 2.9-Mb region of the genome of *Drosophila melanogaster*: the Adh region. Genetics *153*, 179-219.

Ausio, J., Gonzalez-Romero, R., and Woodcock, C.L. (2014). Comparative structure of vertebrate sperm chromatin. Journal of structural biology *188*, 142-155.

Balhorn, M.C., and Balhorn, R. (2011). Protamines. Editorial. Protein and peptide letters *18*, 753-754.

Balhorn, R. (2007). The protamine family of sperm nuclear proteins. Genome biology *8*, 227.

Barckmann, B., Chen, X., Kaiser, S., Jayaramaiah-Raja, S., Rathke, C., Dottermusch-Heidel, C., Fuller, M.T., and Renkawitz-Pohl, R. (2013). Three levels of regulation lead to protamine and Mst77F expression in *Drosophila*. Developmental biology *377*, 33-45.

Basu, S., Campbell, H.M., Dittel, B.N., and Ray, A. (2010). Purification of specific cell population by fluorescence activated cell sorting (FACS). Journal of visualized experiments : JoVE.

Becker, P.B., and Workman, J.L. (2013). Nucleosome remodeling and epigenetics. Cold Spring Harbor perspectives in biology *5*.

Birnboim, H.C., and Doly, J. (1979). A rapid alkaline extraction procedure for screening recombinant plasmid DNA. Nucleic acids research *7*, 1513-1523.

Bischof, J., Maeda, R.K., Hediger, M., Karch, F., and Basler, K. (2007). An optimized transgenesis system for *Drosophila* using germ-line-specific phiC31 integrases. Proceedings of the National Academy of Sciences of the United States of America *104*, 3312-3317.

Blower, M.D., and Karpen, G.H. (2001). The role of *Drosophila* CID in kinetochore formation, cell-cycle progression and heterochromatin interactions. Nature cell biology *3*, 730-739.

Bosco, G., Campbell, P., Leiva-Neto, J.T., and Markow, T.A. (2007). Analysis of *Drosophila* species genome size and satellite DNA content reveals significant differences among strains as well as between species. Genetics *177*, 1277-1290.

Braun, R.E. (2001). Packaging paternal chromosomes with protamine. Nature genetics *28*, 10-12.

Brill, J.A., and Wolfner, M.F. (2012). Overview: Special issue on *Drosophila* spermatogenesis. Spermatogenesis *2*, 127-128.

Caporilli, S., Yu, Y., Jiang, J., and White-Cooper, H. (2013). The RNA export factor, Nxt1, is required for tissue specific transcriptional regulation. PLoS genetics *9*, e1003526.

Carrell, D.T. (2012). Epigenetics of the male gamete. Fertility and sterility *97*, 267-274.

Castillo, J., Amaral, A., and Oliva, R. (2014). Sperm nuclear proteome and its epigenetic potential. Andrology *2*, 326-338.

Catena, R., Escoffier, E., Caron, C., Khochbin, S., Martianov, I., and Davidson, I. (2009). HMGB4, a novel member of the HMGB family, is preferentially expressed in the mouse testis and localizes to the basal pole of elongating spermatids. Biology of reproduction *80*, 358-366.

Chen, D., and McKearin, D.M. (2003). A discrete transcriptional silencer in the bam gene determines asymmetric division of the *Drosophila* germline stem cell. Development *130*, 1159-1170.

Chintapalli, V.R., Wang, J., and Dow, J.A. (2007). Using FlyAtlas to identify better *Drosophila* melanogaster models of human disease. Nature genetics *39*, 715-720.

Chiva, M., Saperas, N., and Ribes, E. (2011). Complex chromatin condensation patterns and nuclear protein transitions during spermiogenesis: examples from mollusks. Tissue & cell *43*, 367-376.

Cho, C., Jung-Ha, H., Willis, W.D., Goulding, E.H., Stein, P., Xu, Z., Schultz, R.M., Hecht, N.B., and Eddy, E.M. (2003). Protamine 2 deficiency leads to sperm DNA damage and embryo death in mice. Biology of reproduction *69*, 211-217.

Cho, C., Willis, W.D., Goulding, E.H., Jung-Ha, H., Choi, Y.C., Hecht, N.B., and Eddy, E.M. (2001). Haploinsufficiency of protamine-1 or -2 causes infertility in mice. Nature genetics *28*, 82-86.

Coletta, A., Pinney, J.W., Solis, D.Y., Marsh, J., Pettifer, S.R., and Attwood, T.K. (2010). Low-complexity regions within protein sequences have position-dependent roles. BMC systems biology *4*, 43.

Cunningham, F., Amode, M.R., Barrell, D., Beal, K., Billis, K., Brent, S., Carvalho-Silva, D., Clapham, P., Coates, G., Fitzgerald, S., *et al.* (2015). Ensembl 2015. Nucleic acids research *43*, D662-669.

Czech, B., Malone, C.D., Zhou, R., Stark, A., Schlingeheyde, C., Dus, M., Perrimon, N., Kellis, M., Wohlschlegel, J.A., Sachidanandam, R., *et al.* (2008). An endogenous small interfering RNA pathway in *Drosophila*. Nature *453*, 798-802.

DeRouchey, J., Hoover, B., and Rau, D.C. (2013). A comparison of DNA compaction by arginine and lysine peptides: a physical basis for arginine rich protamines. Biochemistry *52*, 3000-3009.

Deuring, R., Fanti, L., Armstrong, J.A., Sarte, M., Papoulas, O., Prestel, M., Daubresse, G., Verardo, M., Moseley, S.L., Berloco, M., *et al.* (2000). The ISWI chromatin-remodeling protein is required for gene expression and the maintenance of higher order chromatin structure in vivo. Molecular cell *5*, 355-365.

Dietzl, G., Chen, D., Schnorrer, F., Su, K.C., Barinova, Y., Fellner, M., Gasser, B., Kinsey, K., Oppel, S., Scheiblauer, S., *et al.* (2007). A genome-wide transgenic RNAi library for conditional gene inactivation in *Drosophila*. Nature *448*, 151-156.

Dorus, S., Busby, S.A., Gerike, U., Shabanowitz, J., Hunt, D.F., and Karr, T.L. (2006). Genomic and functional evolution of the *Drosophila melanogaster* sperm proteome. Nature genetics *38*, 1440-1445.

Dottermusch-Heidel, C., Gärtner, S.M., Tegeder, I., Rathke, C., Barckmann, B., Bartkuhn, M., Bhushan, S., Steger, K., Meinhardt, A., and Renkawitz-Pohl, R. (2014). H3K79 methylation: a new conserved mark that accompanies H4 hyperacetylation prior to histone-to-protamine transition in *Drosophila* and rat. Biology open *3*, 444-452.

Doyen, C.M., Chalkley, G.E., Voets, O., Bezstarosti, K., Demmers, J.A., Moshkin, Y.M., and Verrijzer, C.P. (2015). A Testis-Specific Chaperone and the Chromatin Remodeler ISWI Mediate Repackaging of the Paternal Genome. Cell reports *13*, 1310-1318.

Doyen, C.M., Moshkin, Y.M., Chalkley, G.E., Bezstarosti, K., Demmers, J.A., Rathke, C., Renkawitz-Pohl, R., and Verrijzer, C.P. (2013). Subunits of the histone chaperone CAF1 also mediate assembly of protamine-based chromatin. Cell reports *4*, 59-65.

Emelyanov, A.V., Rabbani, J., Mehta, M., Vershilova, E., Keogh, M.C., and Fyodorov, D.V. (2014). *Drosophila* TAP/p32 is a core histone chaperone that cooperates with NAP-1, NLP, and nucleophosmin in sperm chromatin remodeling during fertilization. Genes & development *28*, 2027-2040.

Eren-Ghiani Z., Rathke, C., Theofel I., Renkawitz-Pohl, R. (2015). Prtl99C acts together with protamines and safeguards male fertility in *Drosophila*. Cell Reports *13*, 1–9)

Fabian, L., and Brill, J.A. (2012). *Drosophila* spermiogenesis: Big things come from little packages. Spermatogenesis *2*, 197-212.

Fabrizio, J.J., Hime, G., Lemmon, S.K., and Bazinet, C. (1998). Genetic dissection of sperm individualization in *Drosophila melanogaster*. Development *125*, 1833-1843.

Franco, M.M., Prickett, A.R., and Oakey, R.J. (2014). The role of CCCTC-binding factor (CTCF) in genomic imprinting, development, and reproduction. Biology of reproduction *91*, 125.

Fuller, M.T. (1993). Spermatogenesis. In: The Development of *Drosophila melanogaster*. Cold Spring Harbor Laboratory Press *Bate, M. and Martinez-Arias, A., eds.,* , 71–147

Fuller, M.T. (1998). Genetic control of cell proliferation and differentiation in *Drosophila spermatogenesis*. Seminars in cell & developmental biology *9*, 433-444.

Fuller, M.T., Regan, C.L., Green, L.L., Robertson, B., Deuring, R., and Hays, T.S. (1989). Interacting genes identify interacting proteins involved in microtubule function in *Drosophila*. Cell motility and the cytoskeleton *14*, 128-135.

Gärtner, S. (2014). Chromatin Reorganization in *Drosophila melanogaster* Spermiogenesis: Identification of New Chromatin Components accompanying Histone-to-Protamine Transition. In Faculty of Biology (Philipps - Universität Marburg), pp. 133.

Gärtner, S.M., Rothenbusch, S., Buxa, M.K., Theofel, I., Renkawitz, R., Rathke, C., and Renkawitz-Pohl, R. (2015). The HMG-box-containing proteins tHMG-1 and tHMG-2 interact during the histone-to-protamine transition in *Drosophila spermatogenesis*. European journal of cell biology *94*, 46-59.

Gaucher, J., Boussouar, F., Montellier, E., Curtet, S., Buchou, T., Bertrand, S., Hery, P., Jounier, S., Depaux, A., Vitte, A.L., *et al.* (2012). Bromodomain-dependent stage-specific male genome programming by Brdt. The EMBO journal *31*, 3809-3820.

Gill-Sharma, M.K., Choudhuri, J., and D'Souza, S. (2011). Sperm chromatin protamination: an endocrine perspective. Protein and peptide letters *18*, 786-801.

Gloor, G.B., Preston, C.R., Johnson-Schlitz, D.M., Nassif, N.A., Phillis, R.W., Benz, W.K., Robertson, H.M., and Engels, W.R. (1993). Type I repressors of P element mobility. Genetics *135*, 81-95.

Govin, J., Caron, C., Lestrat, C., Rousseaux, S., and Khochbin, S. (2004). The role of histones in chromatin remodelling during mammalian spermiogenesis. European journal of biochemistry / FEBS *271*, 3459-3469.

Hardy, R.W. (1975). The influence of chromosome content on the size and shape of sperm heads in *Drosophila melanogaster* and the demonstration of chromosome loss during spermiogenesis. Genetics *79*, 231-264.

Herold, M., Bartkuhn, M., and Renkawitz, R. (2012). CTCF: insights into insulator function during development. Development *139*, 1045-1057.

Hime, G.R., Brill, J.A., and Fuller, M.T. (1996). Assembly of ring canals in the male germ line from structural components of the contractile ring. Journal of cell science *109 (Pt 12)*, 2779-2788.

Hirst, J., and Carmichael, J. (2011). A potential role for the clathrin adaptor GGA in *Drosophila* spermatogenesis. BMC cell biology *12*, 22.

Hrdlicka, L., Gibson, M., Kiger, A., Micchelli, C., Schober, M., Schock, F., and Perrimon, N. (2002). Analysis of twenty-four Gal4 lines in *Drosophila melanogaster.* Genesis *34*, 51-57.

Hundertmark,T., Theofel, I., Eren-Ghiani, Z., Miller, D., and Rathke, C. Analysis of chromatin dynamics during *Drosophila* spermatogenesis (Methods in Molecular Biology, submitted manuscript)

Jayaramaiah Raja, S., and Renkawitz-Pohl, R. (2005). Replacement by *Drosophila melanogaster* protamines and Mst77F of histones during chromatin condensation in late spermatids and role of sesame in the removal of these proteins from the male pronucleus. Molecular and cellular biology *25*, 6165-6177.

Jodar, M., and Oliva, R. (2014). Protamine alterations in human spermatozoa. Advances in experimental medicine and biology *791*, 83-102.

Jonchere, V., and Bennett, D. (2013). Validating RNAi phenotypes in *Drosophila* using a synthetic RNAi-resistant transgene. PloS one *8*, e70489.

Kanippayoor, R.L., Alpern, J.H., and Moehring, A.J. (2013). Protamines and spermatogenesis in and : A comparative analysis. Spermatogenesis *3*, e24376.

Kibbe, W.A. (2007). OligoCalc: an online oligonucleotide properties calculator. Nucleic acids research *35*, W43-46.

Kierszenbaum, A.L., and Tres, L.L. (1975). Structural and transcriptional features of the mouse spermatid genome. The Journal of cell biology *65*, 258-270.

Kimura, S. (2013). The Nap family proteins, CG5017/Hanabi and Nap1, are essential for *Drosophila spermiogenesis.* FEBS letters *587*, 922-929.

Kimura, S., and Loppin, B. (2015). Two bromodomain proteins functionally interact to recapitulate an essential BRDT-like function in *Drosophila* spermatocytes. Open biology *5*, 140145.

Klemenz, R., Weber, U., and Gehring, W.J. (1987). The white gene as a marker in a new P-element vector for gene transfer in *Drosophila*. Nucleic acids research *15*, 3947-3959.

Kost, N., Kaiser, S., Ostwal, Y., Riedel, D., Stutzer, A., Nikolov, M., Rathke, C., Renkawitz-Pohl, R., and Fischle, W. (2015). Multimerization of *Drosophila* sperm protein Mst77F causes a unique condensed chromatin structure. Nucleic acids research *43*, 3033-3045.

Kosugi, S., Hasebe, M., Tomita, M., and Yanagawa, H. (2009). Systematic identification of cell cycle-dependent yeast nucleocytoplasmic shuttling proteins by prediction of composite motifs. Proceedings of the National Academy of Sciences of the United States of America *106*, 10171-10176.

Köttgen, M., Hofherr, A., Li, W., Chu, K., Cook, S., Montell, C., and Watnick, T. (2011). *Drosophila* sperm swim backwards in the female reproductive tract and are activated via TRPP2 ion channels. PloS one *6*, e20031.

Krsticevic, F.J., Santos, H.L., Januario, S., Schrago, C.G., and Carvalho, A.B. (2010). Functional copies of the Mst77F gene on the Y chromosome of *Drosophila melanogaster*. Genetics *184*, 295-307.

Laberge, R.M., and Boissonneault, G. (2005). On the nature and origin of DNA strand breaks in elongating spermatids. Biology of reproduction *73*, 289-296.

Leser, K., Awe, S., Barckmann, B., Renkawitz-Pohl, R., and Rathke, C. (2012). The bromodomain-containing protein tBRD-1 is specifically expressed in spermatocytes and is essential for male fertility. Biology open *1*, 597-606.

Letunic, I., Doerks, T., and Bork, P. (2015). SMART: recent updates, new developments and status in 2015. Nucleic acids research *43*, D257-260.

Li, Y., Lalancette, C., Miller, D., and Krawetz, S.A. (2008). Characterization of nucleohistone and nucleoprotamine components in the mature human sperm nucleus. Asian journal of andrology *10*, 535-541.

Luke, L., Tourmente, M., and Roldan, E.R. (2015). Sexual Selection of Protamine 1 in Mammals. Molecular biology and evolution.

Mannan, A.U., Nayernia, K., Mueller, C., Burfeind, P., Adham, I.M., and Engel, W. (2003). Male mice lacking the Theg (testicular haploid expressed gene) protein undergo normal spermatogenesis and are fertile. Biology of reproduction *69*, 788-796.

Markstein, M., Pitsouli, C., Villalta, C., Celniker, S.E., and Perrimon, N. (2008). Exploiting position effects and the gypsy retrovirus insulator to engineer precisely expressed transgenes. Nature genetics *40*, 476-483.

Miller, D., Brinkworth, M., and Iles, D. (2010). Paternal DNA packaging in spermatozoa: more than the sum of its parts? DNA, histones, protamines and epigenetics. Reproduction *139*, 287-301.

Minocherhomji, S., Madon, P.F., and Parikh, F.R. (2010). Epigenetic regulatory mechanisms associated with infertility. Obstetrics and gynecology international *2010*.

Mitchell, A., Chang, H.Y., Daugherty, L., Fraser, M., Hunter, S., Lopez, R., McAnulla, C., McMenamin, C., Nuka, G., Pesseat, S., *et al.* (2015). The InterPro protein families database: the classification resource after 15 years. Nucleic acids research *43*, D213-221.

Morris, C.A., Benson, E., and White-Cooper, H. (2009). Determination of gene expression patterns using in situ hybridization to *Drosophila* testes. Nature protocols *4*, 1807-1819.

Nishikawa, A., Sakamoto, Y., Sakatoku, A., Noguchi, M., Tanaka, D. and Nakamura, S. (2010). Induction of deflagellation by various local anesthetics in Chlamydomonas reinhardtii Dangeard (Chlamydomonadales, Chlorophyceae). Phycological Research *58*, 79–87.

Panchenko, T., Sorensen, T.C., Woodcock, C.L., Kan, Z.Y., Wood, S., Resch, M.G., Luger, K., Englander, S.W., Hansen, J.C., and Black, B.E. (2011). Replacement of histone H3 with CENP-A directs global nucleosome array condensation and loosening of nucleosome superhelical termini. Proceedings of the National Academy of Sciences of the United States of America *108*, 16588-16593.

Park, Y.J., and Luger, K. (2008). Histone chaperones in nucleosome eviction and histone exchange. Current opinion in structural biology *18*, 282-289.

Pircs, K., Nagy, P., Varga, A., Venkei, Z., Erdi, B., Hegedus, K., and Juhasz, G. (2012). Advantages and limitations of different p62-based assays for estimating autophagic activity in *Drosophila*. PloS one *7*, e44214.

Rathke, C. (2007). Chromatinveränderungen während der Spermienentwicklung von *Drosophila melanogaster* - von Histonen zu Protaminen - (Marburg/Germany: Philipps-Universität Marburg), pp. 184.

Rathke, C., Baarends, W.M., Awe, S., and Renkawitz-Pohl, R. (2014). Chromatin dynamics during spermiogenesis. Biochimica et biophysica acta *1839*, 155-168.

Rathke, C., Baarends, W.M., Jayaramaiah-Raja, S., Bartkuhn, M., Renkawitz, R., and Renkawitz-Pohl, R. (2007). Transition from a nucleosome-based to a protamine-based chromatin configuration during spermiogenesis in *Drosophila*. Journal of cell science *120*, 1689-1700.

Rathke, C., Barckmann, B., Burkhard, S., Jayaramaiah-Raja, S., Roote, J., and Renkawitz-Pohl, R. (2010). Distinct functions of Mst77F and protamines in nuclear shaping and chromatin condensation during *Drosophila* spermiogenesis. European journal of cell biology *89*, 326-338.

Renkawitz-Pohl, R., Hollmann, M., Hempel, L. and Schäfer, M. A. (2005). Spermatogenesis. In Comprehensive Insect Physiology, Biochemistry, Pharmacology And Molecular Biology (ed. L. I. Gilbert, K. Iatrou and S. Gill), pp. 157-178. Oxford: Elsevier Ltd.

Riparbelli, M.G., Cabrera, O.A., Callaini, G., and Megraw, T.L. (2013). Unique properties of *Drosophila* spermatocyte primary cilia. Biology open *2*, 1137-1147.

Ronfani, L., Ferraguti, M., Croci, L., Ovitt, C.E., Scholer, H.R., Consalez, G.G., and Bianchi, M.E. (2001). Reduced fertility and spermatogenesis defects in mice lacking chromosomal protein Hmgb2. Development *128*, 1265-1273.

Rousseaux, S., and Khochbin, S. (2011). Epigenetics and Human Reproduction. Springer Berlin Heidelberg (Online ISBN 978-3-642-14773-9)

Rousseaux, S., and Khochbin, S. (2015). Histone Acylation beyond Acetylation: Terra Incognita in Chromatin Biology. Cell journal *17*, 1-6.

Russell, S.R., and Kaiser, K. (1993). *Drosophila melanogaster* male germ line-specific transcripts with autosomal and Y-linked genes. Genetics *134*, 293-308.

Russell, S.R.H., Kaiser, K (1993). mst35b, a male germline specific gene. Paper presented at: Europ Dros Res Conf 13.

Saiki, R.K., Gelfand, D.H., Stoffel, S., Scharf, S.J., Higuchi, R., Horn, G.T., Mullis, K.B., and Erlich, H.A. (1988). Primer-directed enzymatic amplification of DNA with a thermostable DNA polymerase. Science *239*, 487-491.

Sambrook, J.F., E.F.; Maniatis, T. (1989). Molecular cloning: a laboratory manual. (Cold Spring Harbor: Cold Spring Harbor Laboratory Press).

Schlichting, K., Demontis, F., and Dahmann, C. (2005). Cadherin Cad99C is regulated by Hedgehog signaling in *Drosophila*. Developmental biology *279*, 142-154.

Schlichting, K., Wilsch-Brauninger, M., Demontis, F., and Dahmann, C. (2006). Cadherin Cad99C is required for normal microvilli morphology in *Drosophila* follicle cells. Journal of cell science *119*, 1184-1195.

Scott Pitnick, G.S.S., Therese A. Markow (1995). How long is a giant sperm? Nature *375*.

Shang, E., Nickerson, H.D., Wen, D., Wang, X., and Wolgemuth, D.J. (2007). The first bromodomain of Brdt, a testis-specific member of the BET sub-family of double-bromodomain-containing proteins, is essential for male germ cell differentiation. Development *134*, 3507-3515.

Southall, T.D., and Brand, A.H. (2008). Generation of Driver and Reporter Constructs for the GAL4 Expression System in *Drosophila*. CSH protocols *2008*, pdb prot5029.

Spradling, A.C., and Rubin, G.M. (1982). Transposition of cloned P elements into *Drosophila* germ line chromosomes. Science *218*, 341-347.

St Pierre, S.E., Ponting, L., Stefancsik, R., McQuilton, P., and FlyBase, C. (2014). FlyBase 102--advanced approaches to interrogating FlyBase. Nucleic acids research *42*, D780-788.

Stros, M., Launholt, D., and Grasser, K.D. (2007). The HMG-box: a versatile protein domain occurring in a wide variety of DNA-binding proteins. Cellular and molecular life sciences : CMLS *64*, 2590-2606.

Takemori, N., and Yamamoto, M.T. (2009). Proteome mapping of the *Drosophila melanogaster* male reproductive system. Proteomics *9*, 2484-2493.

Theofel, I., Bartkuhn, M., Hundertmark, T., Boettger, T., Gärtner, S.M., Leser, K., Awe, S., Schipper, M., Renkawitz-Pohl, R., and Rathke, C. (2014). tBRD-1 selectively controls gene activity in the *Drosophila* testis and interacts with two new members of the bromodomain and extra-terminal (BET) family. PloS one *9*, e108267.

Thummel, C.S., Boulet, A.M., and Lipshitz, H.D. (1988). Vectors for *Drosophila* P-element-mediated transformation and tissue culture transfection. Gene *74*, 445-456.

Tirmarche, S., Kimura, S., Sapey-Triomphe, L., Sullivan, W., Landmann, F., and Loppin, B. (2014). *Drosophila* protamine-like Mst35Ba and Mst35Bb are required for proper sperm nuclear morphology but are dispensable for male fertility. G3 *4*, 2241-2245.

Tokuyasu, K.T. (1974). Dynamics of spermiogenesis in *Drosophila melanogaster*. IV. Nuclear transformation. Journal of ultrastructure research *48*, 284-303.

Toto, M., D'Angelo, G., and Corona, D.F. (2014). Regulation of ISWI chromatin remodelling activity. Chromosoma *123*, 91-102.

UniProt, C. (2015). UniProt: a hub for protein information. Nucleic acids research *43*, D204-212.

Utsuno, H., Miyamoto, T., Oka, K., and Shiozawa, T. (2014). Morphological alterations in protamine-deficient spermatozoa. Human reproduction *29*, 2374-2381.

Vazquez, J., Belmont, A.S., and Sedat, J.W. (2002). The dynamics of homologous chromosome pairing during male *Drosophila* meiosis. Current biology : CB *12*, 1473-1483.

Vibranovski, M.D., Lopes, H.F., Karr, T.L., and Long, M. (2009). Stage-specific expression profiling of *Drosophila* spermatogenesis suggests that meiotic sex chromosome inactivation drives genomic relocation of testis-expressed genes. PLoS genetics *5*, e1000731.

Ward, W.S. (2010). Function of sperm chromatin structural elements in fertilization and development. Molecular human reproduction *16*, 30-36.

Wasbrough, E.R., Dorus, S., Hester, S., Howard-Murkin, J., Lilley, K., Wilkin, E., Polpitiya, A., Petritis, K., and Karr, T.L. (2010). The *Drosophila melanogaster* sperm proteome-II (DmSP-II). Journal of proteomics *73*, 2171-2185.

Wouters-Tyrou, D., Martinage, A., Chevaillier, P., and Sautiere, P. (1998). Nuclear basic proteins in spermiogenesis. Biochimie *80*, 117-128.

Yamamoto, M.T., and Takemori, N. (2010). Proteome profiling reveals tissue-specific protein expression in the male reproductive system of *Drosophila melanogaster*. Fly *4*, 36-39.

Yanaka, N., Kobayashi, K., Wakimoto, K., Yamada, E., Imahie, H., Imai, Y., and Mori, C. (2000). Insertional mutation of the murine kisimo locus caused a defect in spermatogenesis. The Journal of biological chemistry *275*, 14791-14794.

Yasuno, Y., and Yamamoto, M.T. (2014). Electron microscopic observation of the sagittal structure of *Drosophila* mature sperm. Microscopy research and technique *77*, 661-666.

Yu, Y.E., Zhang, Y., Unni, E., Shirley, C.R., Deng, J.M., Russell, L.D., Weil, M.M., Behringer, R.R., and Meistrich, M.L. (2000). Abnormal spermatogenesis and reduced fertility in transition nuclear protein 1-deficient mice. Proceedings of the National Academy of Sciences of the United States of America *97*, 4683-4688.

Zhao, M., Shirley, C.R., Hayashi, S., Marcon, L., Mohapatra, B., Suganuma, R., Behringer, R.R., Boissonneault, G., Yanagimachi, R., and Meistrich, M.L. (2004). Transition nuclear proteins are required for normal chromatin condensation and functional sperm development. Genesis *38*, 200-213.

Zini, A., and Agarwal, A. (2011). Sperm Chromatin: Biological and Clinical Applications in Male Infertility and Assisted Reproduction (Springer New York).

Zoller, R., and Schulz, C. (2012). The *Drosophila* cyst stem cell lineage: Partners behind the scenes? Spermatogenesis *2*, 145-157.

9 Abbreviations

aa	amino acid
AB	Antibody
Amp	Ampicillin
APS	Ammonium persulfate
bp	base pairs
BSA	Bovine serum albumin
°C	Celsius degree
cDNA	complementary DNA
ChIP	Chromatin Immunoprecipitation
ChIP-Seq	Chromatin Immunoprecipitation follow by Sequencing
c-LCR	central low complexity region
cm	centimeter
CO_2	Carbon dioxide
CyO	*Curly of the Oster*
ddH_2O	Aqua double
DIG	Digoxigenin
dj	Don juan
DMEM	Dulbecco's Modified Eagle Medium
DMSO	Dimethyl sulfoxide
DNA	Deoxyribonucleic acid
DNase	Deoxyribonuclease
dNTP	Deoxyribonucleotide Phosphates
DTT	Dithiothreitol
ECL	Enhanced chemiluminescence
EDTA	Ethylenediaminetetraacetic acid
e-GFP	enhanced green fluorescent protein
et al	et alii (and others)
FRT-FLP	Flippase recognition target (FRT), the recombinase (Flp)
F-PBS	Formaldehyde in PBS
g	gram
h	hour
HMG-box	High Mobility Group box
HS Buffer	Hybridization Solution Buffer

IC	Individualization complex
IF	Immunofluoresence
IPTG	Isopropyl β-D-1-thiogalactopyranoside
KAc	Potassium acetate
KCl	Potassium chloride
Kan	Kanamycin
kb	kilobase
kDa	kilo Dalton
kg	kilogram
l	liter
LB	Luria-Bertani
Levamisole	L(-)2,3,5,6-Tetrahydro-6-phenyl imidazole[2,1-6]- thiazole
M	Molar
µg	Microgram
$MgCl_2$	Magnesium chloride
min	Minute
ml	Milliliter
mm	Millimeter
mM	Millimolar
MOPS	3-morpholinopropane-1-sulfonic acid
mRNA	messenger RNA
mt	mitochondrial
NaCl	Sodium chloride
Na_2HPO_4	Disodium Phosphate
NaH_2PO_4	Monosodium phosphate
NBT	Nitrotetrazolium Blue chloride
NCBI	National Center for Biotechnology Information
NEB	New England Biolabs
NLS	Nuclear Localization Signal
nm	nanometer
OD	Optical Density
ORF	Open Reading Frame
PBS	Phosphate-buffered saline
PCR	Polymerase Chain Reaction
pg	Pico gram
pH	Power of hydrogen

pI	Isoelectric point
POD	Horse-radish peroxidase
Prot	Protamine
RNA	Ribonucleic acid
RNase	Ribonuclease
RNAi	RNA interference
Rpl32	Ribosomal protein *gene* L32
rpm	Revolutions per minute
RT	Room Temperature
RT-PCR	Reverse transcription polymerase chain reaction
SB	Squishing buffer
SDS	Sodium dodecyl sulfate
s	second
SMART	Simple Modular Architecture Research Tool
Sp	*Sternopleura*
TAE	Tris-Acetate/EDTA
TBS	Tris-buffered saline
TBSTT	Tris-buffered saline with Tween-20 and Triton X-100
TEMED	Tetramethylethylenediamine
Tris	tris(hydroxymethyl)aminomethane
Triton X-100	t-octylphenoxypolyethoxyethanol
Tween-20	Polyoxyethylene (20) sorbitan monolaurate
U	Unit
Ubx	*Ultrabithorax*
UTR	untranslated region
UV	Ultraviolet light
V	Volume
v/v	volume per volume
WB	Western blot
w/v	weight per volume
X-Gal	5-bromo-4-chloro-3-indolyl-β-D-galactopyranoside

10 Curriculum vitae

Personal Information	Zeynep Eren Ghiani 27/06/1988 Gönen/Turkey Married, no children

Education

Since Sept 2012	Doctorate in Biology Philipps-Universität Marburg, Germany Department of Developmental Biology Prof. Dr. Renate Renkawitz-Pohl Lab
Oct 2011-June 2012	Master in Bioengineering Miguel Hernández University of Elche, Spain Unit of Genetics, Institute of Bioengineering Prof. Dr. María Rosa Ponce Molet Lab Grade: 9.69/10
Sep 2006-Jan 2011	Bachelor in Biochemistry Ege University, Turkey Faculty of Science Department of Biochemistry Mentor: Prof. Dr. Figen Zihnioğlu Grade: 3.33/4

Publications

- Hundertmark,T., Theofel, I., Eren-Ghiani, Z., Miller, D., and Rathke, C. Analysis of chromatin dynamics during *Drosophila* spermatogenesis (Methods in Molecular Biology, submitted manuscript)

- Eren-Ghiani Z., Rathke, C., Theofel I., Renkawitz-Pohl, R. Prtl99C acts together with protamines and safeguards male fertility in *Drosophila.* (2015, Cell Reports 13, 1–9)

- Canbay E, Habip A, Kara G, Eren Z., Akyilmaz E. A microbial biosensor based on *Lactobacillus delbruecki sp*. bacterial cells for simultaneous determination of lactic and pyruvic acid. (2015, Food Chemistry)

Scientific Communications during PhD training

- Eren-Ghiani, Z., Renkawitz-Pohl, R. (2015) Synthesis, its control and function of sperm proteins in *Drosophila.* "Frontiers in Male Infertility Research" : Open sessions of the Reprotrain Final Management Meeting (Oral Presentation)

- Eren-Ghiani, Z., Rathke, C., Theofel I., Renkawitz-Pohl, R. (2015). Protamine-like (Prtl) protein is essential for fertility and compacts the paternal genome in *Drosophila melanogaster* (Poster)

- Secondment in Dr. Willy Baarends Lab (Erasmus MC, Rotterdam, May 2015) working on the identification of the Paf-1 complex members in mouse and human testis.

- Eren, Z., Rathke, C., Renkawitz-Pohl, R. (2014) Identification of new sperm proteins in *Drosophila* to unravel male infertility. Marie Skłodowska-Curie conference: ESOF 2014 "Transferable skills: MSCA added value for your CV". (Poster)

- Eren, Z., Rathke, C., Renkawitz-Pohl, R. (2013) Ptl-1, a newly identified chromatin component in *Drosophila melanogaster*. The Florence-Utah International Symposium on Genetics of Male Infertility: From Research to Clinic. (Oral Presentation)

Scientific workshops and conferences attended during PhD training

- 3rd Chromatin Symposium 2015, Changes in Differentiation and Malignancies, Marburg/Germany 2015
- 3rd REPRO-TRAIN Workshop (Biomedical App. and Transfer of Knowledge Opportunities organized by "Oryzon" and "Medipex"). Barcelona 2015
- Marie Skłodowska-Curie conference: ESOF 2014 "Transferable skills: MSCA added value for your CV", Copenhagen/Denmark 2014
- 2nd REPRO-TRAIN Workshop (Model organism in studying male infertility- from fly to human). Marburg 2014
- 4th Winter School of the Collaborative Research Centre TRR81, Austria 2014
- 5th Florence-Utah Symposium on Genetics of Male Infertility, Italy 2013
- 2nd Chromatin Symposium 2013-Changes in Differentiation and Malignancies. Netherlands 2013
- 1st REPRO-TRAIN Workshop (Proteomics, Epigenetics, Transcriptomics and Sperm Phenotypic Assessment). Barcelona 2013
- International Joint Meeting of the German Society for Cell Biology (DGZ) and the German Society for Developmental Biology (GfE), Germany 2013
- Key mechanisms in the regulation of the testis function Symposium, Germany 2013

Soft-skills workshops attended during PhD training

- Speak up - rhetoric basics 2015
- Writing grant applications 2014
- Writing Scientific Publications in Life and Natural Sciences 2014

- Project Management Basics 2013
- Communication at Congress 2013

More than Science…

- Roche Continents 2015- Selected as one of the 100 top-talented student
- Mentee in Sci-Mento Mentoring network for talented female scientists 2013-2015
- Representative of ESR/ER Feedback Committee (EFC) and member of the Supervisory Board of Marie-Curie REPROTRAIN Consortium 2012-2015

11 Acknowledgements

I wish to express my utmost gratitude to my mentor, Prof. Dr. Renate Renkawitz-Pohl, for being a wonderful supervisor, scientist and a role model for me. I am forever thankful for her constant support and encouragement, and for allowing me to perform my PhD in her lab. I would like to extend my sincerest thanks to Dr. Christina Rathke for her supervision, continuous support and for her pre-work of this project.

I thank to Prof.Dr. Alexander Brehm, Prof.Dr. Hans-Ulrich Mösch and Prof.Dr. Monika Hassel for their time and for being a member of my dissertation committee.

My special thanks to Nicola for being a part of my life in Germany and for all kind of bureaucratic/private supports. Thanks to Silvia and Ina for proof-reading this work and for translating my summary to German, to Lisa and Tim for being very friendly and for helpful discussions on our Friday seminars, moreover thanks to Tine, Sophie and Steffi for introducing me the basics in *Drosophila* genetics. Overall, I want to give many thanks to all members of Renkawitz-Pohl, Önel and Rathke Labs for creating a helpful and positive working environment. Katja, thank you very much for your help with Photoshop, Illustrator and for supporting my bureaucratic issues. I thank Christiane, Ruth for injecting my transformation constructs, furthermore to Lubjinka, Inge, Angela, and Isolde for their amiable attitude and technical support to this work. I am grateful to Prof. Dr. C. Dahmann (Dresden) for Cad99C mutants, and to Dr. D. Miller (Leeds) for the decondensation protocol. My deep thanks to REPRO-TRAIN Marie Curie Initial Training Network (PITN-2011-289880) for financing this project and to all REPRO-TRAIN members for being a wonderful research community. I also thank an organization: Sci-Mento, for supporting young women scientists and thanks to Prof. Dr. Reinhard Jahn for being my mentor. Most importantly thanks to my mentee group Annina, Sarah, Suse and Tanja for their constant support.

Gisela danke ich für ihre Unterstützung während dieser Zeit. Ich habe das Glück, eine Lehrerin wie dich zu haben.

I would like to finish with my beautiful country, Turkey where the most basic source of my life energy resides: my family. Siz olmadan bunu asla başaramazdım. Sizlere minnettarım! And many thanks to my other part of family who are in Italy. Grazie mille a mia famiglia Sarda per sempre sostenermi. Por último gracias a ti, mi corazón. ¡Gracias por siempre darme las fuerzas y por apoyarme en cualquier momento que te necesitaba!

12 Declaration

I, MSc Zeynep Eren Ghiani, certify that the work performed in this Ph.D. thesis, entitled "**More than protamines: Identification of further sperm proteins from which Prtl99C is essential for male fertility and full chromatin compaction in *Drosophila melanogaster***" is my own work, carried out by me under the supervision of Prof. Dr. Renate Renkawitz-Pohl, Department of Developmental Biology, Philipps-Universität Marburg, in the period between September 2012-December 2015.

I declare that I have faithfully acknowledged, referred to the authors wherever their works have been cited in the text and the body of the thesis.

Marburg

.../12/2015

_____

Zeynep Eren Ghiani